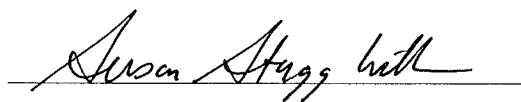


Investigation of Pulsed Electric Field (PEF) as an Intensification Pretreatment for Solvent Lipid Extraction from Microalgae, utilizing Ethyl Acetate as a Greener Substitute to Chloroform-based Extraction

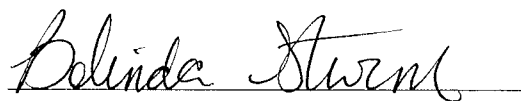
By

Mauricio D. Antezana Zbinden

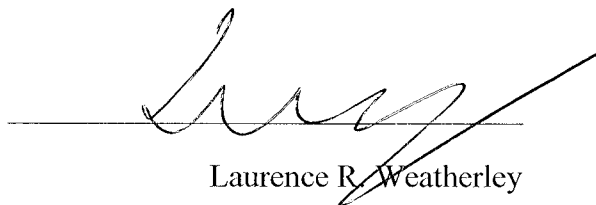
Submitted to the graduate degree program in Chemical & Petroleum Engineering and the Graduate Faculty of the University of Kansas in partial fulfillment of the requirements for the degree of Master of Science.



Co-chairperson: Susan Stagg-Williams



Co-chairperson: Belinda S.M. Sturm



Laurence R. Weatherley

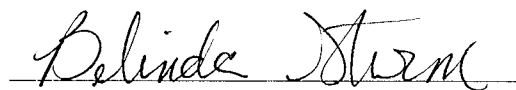
Date Defended: February, 14th 2011

The Thesis Committee for **Mauricio D. Antezana Zbinden**
certifies that this is the approved version of the following thesis:

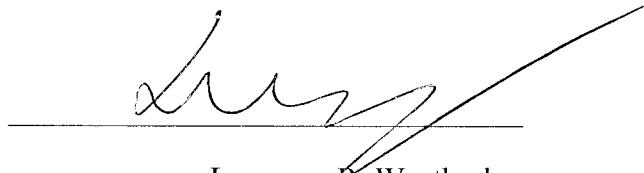
**Investigation of Pulsed Electric Field (PEF) as an Intensification Pretreatment for
Solvent Lipid Extraction from Microalgae, utilizing Ethyl Acetate as a Greener
Substitute to Chloroform-based Extraction**



Co-chairperson: Susan Stagg-Williams



Co-chairperson: Belinda S.M. Sturm



Laurence R. Weatherley

Date approved: February, 15th 2011

Investigation of Pulsed Electric Field (PEF) as an Intensification Pretreatment for Solvent Lipid Extraction from Microalgae, utilizing Ethyl Acetate as a Greener Substitute to Chloroform-based Extraction

Abstract

By

Mauricio D. Antezana Zbinden

As a crucial alternative to petroleum liquid fuels and first generation biodiesel, microalgae represent the most promising renewable source of lipids, thought to be capable of meeting global transportation fuel needs. The most promising characteristics of this alternative energy source are its CO₂ neutrality, high biomass growth, high lipid yield, and noncompetitive stance toward food supply.

To date, development of economically feasible lipid solvent extraction processes of industrial scale face two significant challenges: green solvent selection with efficient extractive characteristics and requirement of cell disruption pretreatment. In this contribution, the utilization of ethyl acetate-based solvents is suggested as a green alternative. Moreover, the novel utilization of Pulsed Electric Field (PEF) as a membrane permeating technique for intensification of the lipid extraction is analyzed.

When compared to inherently toxic chloroform-based solvent (Bligh & Dyer method), this work characterizes ethyl acetate as a less efficient and slower solvent in extracting lipids from *Ankistrodesmus falcatus* wet biomass. A possible explanation to

these inefficiencies was hypothesized to be ethyl acetate's poor membrane disintegration capabilities.

In regards to lipid extraction intensification, the utilization of PEF as a membrane disrupting pretreatment was investigated, focusing in the inefficiencies presented by the ethyl acetate-based system. The novel application of PEF to *Ankistrodesmus falcatus* wet biomass suspension resulted in mixed conclusions. Although no increase in total lipid extraction was achieved, a significant enhancement in the rate of lipid recovery was demonstrated. This crucial intensification shows the PEF application is a valid enhancement treatment that warrants further investigation.

To My Parents and Brothers

TABLE OF CONTENTS

TABLES.....	ix
FIGURES	x
ACKNOWLEDGEMENTS	xiv
INTRODUCTION	1
<i>1.1 Microalgae as a renewable feedstock for biofuel production</i>	<i>1</i>
<i>1.2 Ankistrodesmus falcatus strain – Lipid profile and physical characteristics</i>	<i>4</i>
<i>1.3 Block Flow Diagram of algae processing for fuel production</i>	<i>13</i>
<i>1.4 Solvent extraction:</i>	<i>15</i>
<i>1.5 Cell disruption pretreatments to intensify solvent extraction</i>	<i>18</i>
<i>1.6 Electroporation as a pretreatment technique</i>	<i>21</i>
PEF as a technique to intensify algal lipid extraction	25
<i>1.7 Summary of goals</i>	<i>26</i>
References Cited in CHAPTER 1	27
CHAPTER 2	32
EXPERIMENTAL SETUP, METHODS, AND PROCEDURES	32
2.1 EXPERIMENTAL SETUP	32
2.1.1 Reactor Setup for Algae Growth	32
2.1.2 Feed Preparation & Reactor Maintenance	34
2.1.3 Pulsed Electric Field (PEF): Circuit and Pretreatment Chamber	37
2.2 EXPERIMENTAL METHODS & PROCEDURES	40
2.2.1 Algal Growth	41
2.2.2 Algal Harvesting	41
2.2.3 Algal Dewatering	41
2.2.4 Algae Pretreatment with PEF	41

<u><i>Pulsed Electric Field as a pretreatment</i></u>	42
<u>PEF without Cooling:</u>	44
<u>PEF with Cooling:</u>	45
2.2.5 Solvent Extraction & Solvent-Product Separation	46
<u><i>Lipid Extraction Procedure with Chloroform</i></u>	46
<u><i>Lipid Extraction Procedure with Ethyl Acetate</i></u>	47
<i>Algal Lipids Rate of Extraction – 24hr Kinetics of Extraction</i>	48
<i>Lipid Extraction at $t = 0, t_o$</i>	48
2.2.6 Chemical Transformation of Algal Lipids into Fatty Acid Methyl Esters (FAMES)	49
2.2.7 Product Quantification	50
2.3 ANALYTICAL PROCEDURES	50
2.3.1 Gas Chromatography – Mass Spectrometry	50
<u>Apparatus calibration – Determination of Response Factors (RF)</u>	52
<u>Sample Calculation:</u>	53
<u>GCMS Hardware and Temperature Program:</u>	54
2.4 MICROSCOPIC INVESTIGATION	54
2.4.1 Determination of Ankistrodesmus Auto-Fluorescence	55
2.4.3 Algae Staining Procedure Calcein AM and Propidium Iodide (PI) Staining of Algae - Procedure	62
<u>Exemplification of desired results</u>	63
2.4.4 Determination of Population Viability after PEF Treatment	65
<u>References Cited in CHAPTER 2</u>	65
CHAPTER 3	66
RESULTS & DISCUSSION	66
3.1 Comparison of solvent extraction efficiency and kinetics with chloroform-based and ethyl acetate-based solvent systems	66

<u>Total Algal Lipids Extraction Efficiency</u>	66
<u>Kinetics of Extraction</u>	75
3.2 PEF Application to <i>Ankistrodesmus falcatus</i>: Increase in Membrane Permeability validated with Fluorescent Microscopy	80
3.3 Application of PEF as an intensification treatment for solvent lipid extraction	86
<u>References Cited in CHAPTER 3</u>	91
CHAPTER 4	93
CONCLUSIONS & RECOMMENDATIONS FOR FUTURE WORK	93
4.1 Conclusions	93
4.2 Recommendations for future Work	95
Appendix A	98
A.1 Solvent Extraction & Solvent-Product Separation	98
<u>Lipid Extraction Procedure with Chloroform</u>	98
<u>Lipid Extraction Procedure with Ethyl Acetate</u>	99
A.2 Chemical Transformation of Algal Lipids into Fatty Acid Methyl Esters (FAME)	100
A.3 Algae Staining Procedure Calcein AM and Propidium Iodide (PI) Staining of Algae - Procedure	101

TABLES

Table 1.1: Extracted from Chisti et al.⁴. Comparison of different renewable feedstocks for biodiesel production. Microalgae theoretically represent a superior feedstock with excellent oil lipid yield, translating to significantly smaller land requirements.....	2
Table 1.2: Chemical composition of potential microalgae strains for liquid fuel production. This report ¹¹ describes <i>Ankistrodesmus falcatus</i> as a promising microalga for high lipid production.	6
Table 1.3: Electroporation phenomenon has found many possible industrial applications, where signification research efforts are being spent. However, utilization of PEF as algal cell disruption for lipid solvent extraction intensification is a novel application.	24
Table 2.1: List of main chemical components that make up the algal media, which delivered the necessary nutrients and trace metals.	36
Table 2.2: List of main FAMES being monitored by this procedure in order to determine the total lipid extraction of the solvents in question.	51
Table 2.3: Average Response Factors calculated from GC-MS calibration, utilized to determine each FAME concentration.	52
Table 2.4: Example of GC-MS results obtained from a particular sample, following by the calculated concentrations of each FAME.	53
Table 2.5: Excitation and Emission regions proper of <i>Ankistrodesmus</i>' auto-fluorescence, PI molecular stain, and Calcein molecular stain.....	61
Table 2.6: Loading of Calcein AM and PI into <i>Ankistrodesmus</i> was effectively achieved by following this parameters.....	62
Table 3.1: B&D (CHCl₃/MeOH/H₂O 1:2:0.8 v/v/v) is the most widely cited lipid extraction method. Due to chloroform's health and environmental concerns, multiple solvent mixtures have been investigated as alternatives. Most of the known alternatives do not perform as efficiently as chloroform-based solvent.	68
Table 3.2: Maximum solubility of selected lipids in organic solvents (mg/mL). TAG concentrations are reported in an attempt to understand if solubility limits have been reached, possibly explaining the observed extraction inefficiencies of the EtOAc-based system.	69
Table 3.3: Chemical properties of solvents, solvent mixtures, and TAG. Original obtained from Sheng et al. ⁴	71

FIGURES

Figure 1.1: Lipid productivity ¹², describing <i>Ankistrodesmus falcatus</i> as a promising algal strain. Dark grey bars represent the average lipid productivity found in literature, while light grey bars indicate the calculated values for biomass productivity.....	7
Figure 1.2: Effects of nutrient limitation on biochemical constituents of <i>Ankistrodesmus falcatus</i>. <i>Ankistrodesmus</i> produces triglycerides as the main type of lipids. However, this figure shows that it can also produce significant amount of phospholipids, which are undesirable compounds to the presence of phosphorous. Phosphorous will translate into technological difficulties on the catalytical transformation during the downstream processing. ¹³	8
Figure 1.3: Microscopic image of <i>Ankistrodesmus falcatus</i>.....	9
Figure 1.7: Results of an environmental, health, and safety (EHS) assessment for 26 common solvents developed by Koller et al.³¹ . Ethyl acetate obtained an index of 2.9, while methanol and chloroform obtained an index of 4.1 and 4.0 (nine is the max value, indicating extremely poor EHS properties. Ethyl acetate represents an excellent EHS candidate to perform research on algal lipid extraction.....	17
Figure 1.10: Graph obtained from Toepfl et al.⁴², illustrating the permeabilization of cells after exposure to electric field and actual applications with typical electric field strength and energy input requirements.....	23
Figure 1.11: Graph obtained from Toepfl et al., comparing the energy required for cell disintegration of multicellular tissue (potato tissue) with different techniques. PEF requires the shortest time as well as the lowest energy to pre-treat the cells. This important characteristics suggest that PEF could be an excellent candidate for algal cell disruption prior to lipid extraction ⁴².....	26
Figure 2.1: Conceptual diagram of the 4L chemostat utilized to cultivate the algal biomass.	32
Figure 2.2: Actual image of <i>Ankistrodesmus</i> chemostat operated to obtain the algal biomass.	34
Figure 2.4: Electrical diagram describing the main components of the Pulsed Electric Field apparatus; HF Generator, Marx Generator, and Electroporation Chamber.	39
Figure 2.10: <i>Ankistrodesmus</i> has two auto-fluorescence regions at 470 nm and 680 nm, which corresponds to the blue and red fluorescence of the visible light spectrum, respectively. (A) illustrates <i>Ankistrodesmus</i> red fluorescence, (B)	

blue fluorescence, (C) illustrates a transmission image of this alga, and (D) illustrates an image of all channels combined.....	56
Figure 2.11: Schematic diagram explaining the fundamental component of an epifluorescence microscope.....	57
Figure 2.12: Montage of images emitting a signal at higher wavelengths. The excitation wavelength utilized for this montage was of 477 nm. This montage illustrates the regions of auto-fluorescence for <i>Ankistrodesmus</i> : images 1-2 (470-490 nm emission) and 17-21 (660-700 nm emission).	58
Figure 2.13: The systematic collection of emission wavelength signals associated with multiple excitation wavelengths (458 nm, 477 nm, 488 nm, 514 nm, 543 nm, and 633 nm) produces the above spectrum, proper of <i>Ankistrodesmus</i> algae strain. These spectrums indicate the presence of two (2) auto-fluorescence regions. The first region emits its fluorescence approximately 475-500 nm (light blue region), while the second region emits its energy approximately in the 675-700 nm (red region).....	60
Figure 2.14: Multiple images of two healthy algal cells, describing the desired results of Calcein AM and PI when exposed to microorganisms, whose membranes have not been compromised. (A) Calcein channel, (B) transmission image, (C) PI channel, (D) auto-fluorescence channel, and (E) a superposition of all previously mentioned channels.....	63
Figure 2.15: Multiple images of a single healthy algal cell, describing the desired results of Calcein AM and PI when exposed to a microorganism, whose membrane have been compromised. (A) Calcein channel, (B) transmission image, (C) PI channel, (D) auto-fluorescence channel, and (E) a superposition of all previously mentioned channels.....	64
Figure 3.1: The utilization of EtOAc as a green solvent to extract algal lipids from <i>Ankistrodesmus falcatus</i> after 24-hr contact proved to perform 83-88% as efficient when compared to CHCl ₃ . Results corresponds to average of triplicate samples \pm 90% Confidence Interval (CI).....	67
Figure 3.2: Original image obtained from Sheng et al. ⁴ . TEM image of Cyanobacteria <i>Synechocystis</i> cells before, and after, solvent contact in order to compare the different effects of these solvents to the microorganism's structure. Comparison between an intact healthy cell with no solvent contact (a), cell residual after CHCl ₃ -Methanol extraction (b), and isopropanol extraction (c). <u>Black arrows</u> indicate the cytoplasm membrane. <u>White arrows</u> show disruption and loss of thylakoid membrane. <u>OM</u> : Outer membrane; <u>PD</u> : Peptidoglycan layer; <u>PM</u> : plasma membrane; <u>T</u> : thylakoid membranes; <u>C</u> : carboxysome.....	75

- Figure 3.3: 24-hr kinetics study analyzing the extraction rate of the chloroform-modified B&D method, where CHCl_3 acts as the main solvent. This technique showed no time dependency at recovering the algal lipids from the wet-biomass. Figure 3.4 shows a simplified experiment, where only the first 6hrs were investigated..... 76**
- Figure 3.4: 6-hr kinetics study analyzing the extraction rate of the “chloroform-modified” B&D method, where CHCl_3 acts as the main solvent. This experiment, in conjunction with Figure 3.3 confirms that this system shows no time dependency at recovering the algal lipids from wet-biomass. 77**
- Figure 3.5: 24-hr kinetics study analyzing the extraction rate of the ethyl acetate-modified B&D method, where EtOAc acts as the main solvent. This technique showed that a minimum of 4 hours are required to recover the algal lipids from the wet-biomass. 78**
- Figure 3.6: Epifluorescence microscopy images of *Ankistrodesmus falcatus* population prior to any pretreatment (Negative Control) indicate the healthy state of most of the algal cells. Calcein fluorescing cells (green channel) signify that their cytoplasmic membranes are intact. On the other hand, PI fluorescing cells (red channel) indicate that these cells are dead. The red fluorescing strictly indicates that the cytoplasmic membranes of these cells have been permeated, allowing bulk fluid to penetrate into the cells. 81**
- Figure 3.7: An experimental artifact of PEF treatment in a batch system is a temperature increase of the treated media. This *Ankistrodesmus* population has only been exposed to the temperature swing associated with PEF pretreatment (no electric field was applied). This image indicates that the temperature stresses have not induced any cytoplasmic membrane permeation. This algae population exposed to temperature stresses is as healthy as the negative control population shown on Figure 3.6. 83**
- Figure 3.8: This *Ankistrodesmus* population was exposed to PEF treatment. The epifluorescence image clearly indicates that the vast majority of the algal population has had their cytoplasmic membranes irreversibly permeabilized due to the electrical pulses. The PI fluorescing cells (red channel) have seen bulk media fluid freely penetrate inside the cells..... 84**
- Figure 3.9: Cell viability of the previously shown images (Figure 3.6, Figure 3.7, and Figure 3.8) was determined by eye-count. The PEF pretreatment resulted into an extremely effective technique to permeate the algal membranes, allowing fluid to rush inside the cell. These results clearly show that the electric field associated with our PEF treatment is the reason behind membrane permeation; not temperature stresses..... 85**

Figure 3.10: Application of PEF to a fraction of the wet biomass attempted to intensify the extraction. The small electroporation pretreatment did not show any indication of lipid recovery intensification.	87
Figure 3.11: This time, the entire volume of wet algal biomass was exposed to the PEF treatment prior to solvent extraction (Full PreTreatment). Even though the total lipid extraction did not show indications of recovery improvement, the rate of extraction of the fully pretreated system did indicate faster recovery at time $t = 0$ (t_0).	88
Figure 3.12: Research efforts were focused at investigating the apparent extraction intensification observed at time t_0 due to PEF pretreatment. All these results were obtained at t_0. Wet biomass contacted the solvents at the same elevated temperatures (35°C) observed after electroporation to obtain temperature consistency. Ethyl acetate extractions with prior PEF pretreatment (green column) did indicate significant extraction rate intensification, when compared to the ethyl acetate control (blue column). Chloroform extraction was plotted for total extraction reference. Results correspond to average of triplicate \pm 90% confidence interval.	90
Figure 3.13: Was the temperature increase associated with the electrical pretreatment the reason behind the observed extraction intensification? For this set of results the all wet biomass contacted the solvents at ambient temperature. Wet biomass exposed to PEF pretreatment did indicate consistent extraction intensification at t_0. Chloroform extraction was plotted for total extraction reference. Results correspond to average of triplicate \pm 90% confidence interval.	91

ACKNOWLEDGEMENTS

Dr. Susan M. Stagg-Williams, my advisor, for your invaluable guidance and support throughout my experience of graduate education.

Dr. Belinda S.M. Sturm, my advisor, for introducing me to the field of microbiology and its application. Also, for your patience, guidance, mentoring, and time for listening at the time of making important decisions.

Dr. Laurence Weatherley, for being part of my committee and introducing me to the experience of research initially.

The United States Department of Transportation Research Innovative Technology Administration (DTOS59-06-G-0047), for supporting this research. Also, the Transportation Research Institute at The University of Kansas, for providing travel funds to conferences and the advancement of this research.

Microscopy and Analytical Imaging Laboratory at The University of Kansas, for supporting this research. Dr. David Moore and Heather Shinogle, for introducing me to the world of microscopy, the countless hours of fluorescing imaging, and for being incredible companions in my quest for “killing algae.”

Wes Ellison, for providing invaluable assistance, suggestions, patience, and most importantly for constructing several generations of electrical circuits, part of my experimental apparatus. Also, Dr. Ray Carter, for proving important and valuable support running the GC-MS analytical method.

Chemical & Petroleum Engineering Faculty and Staff at the University of Kansas, for sharing their knowledge and passion for their subjects of interest. Especially Alan Walker and Carol Miner, for providing their technical support and company.

All my fellow laboratory graduate students, for all their companionship and invaluable discussions, which at the time might have seemed pointless: Andrew Duncan, Ryan Coiner, and Lindsey Witthaus

Undergraduate students for providing amusing company and invaluable help: Cristiana Sandigo and Dan Klapper.

To my many friends who made this graduate education experience unforgettable: Marcos Barbeitos, Arely Torres, Marta De Carli, Lindsey Witthaus, Lori Fuqua, Andrew Duncan.

To my parents and brothers, for providing unending support, spiritual strength, invaluable advice, and for always being there in one way or another. You will always make my world better, and I will always be counting down the days to go home and share life with you.

CHAPTER 1

INTRODUCTION

1.1 Microalgae as a renewable feedstock for biofuel production

Continued utilization of liquid fuels derived from petroleum is now widely recognized as an unsustainable source of energy. The depleting availability of petroleum and the contribution of petroleum-derived fuels to the accumulation of greenhouse gases in the environment have prompted an active search of renewable feedstocks for liquid fuel production. Biologically-derived fuels have increasingly been mentioned as an important alternative source of energy ². Photosynthetic plants, including rapeseed, corn, sunflower, soybean, coconut, and others, produce and store lipid oils in the form of triacylglycerols (TAGs), which can be chemically transformed into biodiesel fuels through transesterification reactions ⁴. Biodiesel, derived from oil crops, represents a renewable and carbon neutral alternative to petroleum fuels. However, the significant economic and environmental impact of using agricultural crops, especially food crops, as a feedstock for bio-fuels has raised crucial sustainability issues. The most recent and noticeable example took place in 2007-2008, when worldwide food prices experienced significant increases, and ethanol and other bio-fuels were blamed as significant contributors ⁵.

Microalgae represent another potential alternative feedstock for fuel production, perhaps the most promising renewable source of oil, capable of meeting global transportation fuel needs ⁶. The characteristics that make microalgae such an attractive alternative are (i) similar to photosynthetic plants, it requires carbon dioxide to perform basic metabolism, therefore it is considered CO₂ neutral; (ii) when compared to

other bio-sources for fuels, microalgae's growth rate is significantly higher; and finally (iii) microalgae does not compete against human food supply or water usage like other bio-sources do. Chisti et al.⁴ presents in

Table 1.1 an eye-opening comparison between microalgae and other terrestrial plants, which underlines algae's superiority as an lipid oil producer, and therefore as an alternative feedstock for fuel production.

Table 1.1: Extracted from Chisti et al.⁴. Comparison of different renewable feedstocks for biodiesel production. Microalgae theoretically represent a superior feedstock with excellent oil lipid yield, translating to significantly smaller land requirements.

Crop	Oil yield [L/ha]	Land area needed [M ha] ^a	Percent of existing US cropping area ^a
Corn	172	1540	846
Soybean	446	594	326
Canola	1190	223	122
Jatropha	1892	140	77
Coconut	2689	99	54
Oil palm	5950	45	24
Microalgae ^b	136,900	2	1.1
Microalgae ^c	58,700	4.5	2.5

^a For meeting 50% of all transport fuel needs of the U.S.

^b 70% oil (by wt) in biomass

^c 30% oil (by wt) in biomass

The development of fuels from microalgae is still in its early stages to become a sound and competitive technology. Despite being initially conceived in the late 1980's, no industrial scale process capable of deriving any liquid fuel from algal feedstock has been built to date, with the main barrier for algal fuel production being the high final cost⁷. The production of fuels from algae is divided into different stages: (a) algae growth, (b) harvesting of algae, (c) lipid extraction, (d) and catalytic conversion. Important technological breakthroughs are still needed in all areas in order to make this alternative feedstock economically competitive, especially since any fuel derived from it

must be of comparable cost with petroleum-derived fuels already available. For example, the process area of lipid extraction has already been identified as energy intensive, due to solvent evaporations and other pretreatments. It has been estimated that 40-60% of the product cost is associated with this extraction-separation phase ⁷, thus any process intensification obtained on this front translates to significant improvements. The challenge of efficient lipid extraction represents the main focus of this Master's thesis work. To date, the development of an economically feasible lipid solvent extraction process of industrial scale faces two significant challenges in the environmental and technological areas; solvent toxicity and requirement of cell disruption pretreatment.

Algal lipid recovery of laboratory scale is conventionally performed with solvent extraction. The Bligh & Dyer (B&D) method, which utilizes a chloroform-methanol-water mixture, is the procedure of choice due to high extraction efficiency. However, this procedure has critical limitations as a scalable process, due to chloroform's high toxicity⁸. Thus, the identification of an equally efficient solvent with green characteristics is critical.

Due to the structural complexity associated with microalgae, effective lipid solvent recovery has shown to be dependent on prior cell disruption treatment. Any algal pretreatment will be required to have minimal energy utilization if algal biomass is to become a competitive alternative energy source.

The following sections will present *Ankistrodesmus falcatus* as an excellent lipid producer and source of biomass for biofuel productions. Then, ethyl acetate (EtOAc) will be suggested as a green alternative to chloroform (CHCl_3) solvent. Finally, electroporation phenomena obtained from pulsed electric field (PEF) will be introduced

as a scalable algal cell disruption pretreatment that intensifies lipid recovery during solvent extraction.

1.2 Ankistrodesmus falcatus strain – Lipid profile and physical characteristics

Microalgae are photosynthetic organisms growing found in both marine and freshwater aquatic environments. Similar to wood, corn, sugarcane, and other plants, algae use photosynthesis to convert sunlight energy into chemical energy, which is stored in the form of proteins, carbohydrates, and lipids. Algae primarily require three components to grow: sunlight, carbon dioxide, and water. Microbiologists have categorized microalgae into a variety of classes, mainly distinguished by basic cellular structure, pigmentation, and life cycle ⁹. The three most important classes of microalgae based on their abundance are diatoms (*Bacillariophyceae*), green algae (*Chlorophyceae*), and the golden algae (*Chrysophyceae*). The combined three classes of microalgae correspond to an overwhelming number of strains as potential feedstocks, and thus a screening process to determine the best suitable strains for biofuel production is required. The screening process certainly needs to look at what types of fuel products are available from each biomass. This section will provide a brief overview of the type of products for fuel production desired from microalgae, and a brief historical review of the development of the screening process. Meanwhile, *Ankistrodesmus falcatus* will be presented as an important candidate for biodiesel production.

Determination of total amount and type of chemical energy that the multiple microalgae strains could produce and store is an important aspect for the selection of specific microorganism. All main biochemical fractions of microalgae (lipids,

carbohydrates, and proteins) can be transformed into fuels. The highest energy content is obtained from lipids. The lipids of some species are hydrocarbons, similar to those found in crude oil, while those of other species resemble seed oils, which can be converted to synthetic diesel (biodiesel) by transesterification. Carbohydrates and proteins are commonly converted into alcohols by a fermentation process.

In order to identify the most promising strains of algae for biofuel production, the US Department of Energy established the Solar Energy Research Institute (SERI) Microalgae Culture Collection in 1984. SERI is currently known as the National Renewable Energy Laboratory (NREL). By organized screening programs, this collection was able to gather microalgae strains that (i) had a high potential as a fuel feedstock (lipid and carbohydrate producers), and (ii) had been partially characterized for culture requirements and chemical composition. Some of the criteria that guided the selection of strains for the collection, in descending order of importance, are as follows ¹⁰:

- Energy yield (growth rate x energy content)
- Type of fuel products available from biomass (hydrocarbon, diesel, alcohol, methanol)
- Environmental tolerance range (temperature, salinity, pH)
- Performance in mass culture (highly competitive, predator resistant)
- Media supplementation requirements (trace minerals and vitamins addition)

Ankistrodesmus falcatus, member of the green algal classification, was included in the Microalgae Culture Collection ¹⁰ and is known to be an excellent lipid producer and potential feedstock for biodiesel production. Table 1.2 shows the chemical composition of early promising microalgae including high producers of hydrocarbons, carbohydrates, proteins, and lipids. *Ankistrodesmus falcatus* is part of this early screening

process performed by SERI ¹¹. Under nitrogen limitation, this report shows that *Ankistrodesmus* can produce around 43% lipids from ash-free dry weight.

Table 1.2: Chemical composition of potential microalgae strains for liquid fuel production. This report ¹¹ describes *Ankistrodesmus falcatus* as a promising microalga for high lipid production. Percentage of macromolecules content per ash-free dry weight.

Name	Stress	Main Product ^a	Protein ^a	Carbo-hydrate ^a	Lipid ^a	Glycerol ^a
<i>Botryococcus</i>	+++	Hydrocarbon	0.206	0.143	0.542	0.001
<i>Ankistrodesmus</i>	+	Lipid	0.151	0.193	0.426	0.000
<i>Isochrysis</i>	+++	Lipid	0.233	0.205	0.260	0.001
<i>Nannochloropsis</i>	+	Lipid	0.230	0.070	0.540	0.000
<i>D. salina</i>	++	Glycerol	0.125	0.555	0.092	0.047
<i>Chlamydomonas</i>	-	Carbohydrate	0.170	0.590	0.230	0.000
<i>Cyclotella cryptica</i>	+	Carbohydrate	0.130	0.670	0.180	0.000
<i>Spirulina platensis</i>	-	Protein	0.500	0.088	0.166	0.000
<i>Chlorella (Thomas)</i>	-	Protein	0.469	0.097	0.207	0.000
<i>Nannochloropsis</i>	-	Protein	0.558	0.156	0.286	0.000
<i>D. Salina</i>	++	Glycerol	0.359	0.125	0.185	0.277

- No stress
- + Nitrogen stress
- ++ Osmotic stress
- +++ Nitrogen and osmotic stress

A more recent literature survey presented in 2009 by Griffiths et al.¹² confirmed the promise of *Ankistrodesmus falcatus* as an important microalgae strain for bio-fuel production. This author performed a literature survey among 55 most promising algal strains, focusing on lipid productivity. Defined as the product between biomass productivity and lipid content, lipid productivity provides an indicator of oil produced on the basis of volume and time. Figure 1.1 presents this lipid productivity comparison, positioning *Ankistrodesmus falcatus* as a highly efficient lipid producer. Despite the author's acknowledgement that literature data is far from standardized, the collected information provides an important framework for species selection, and it supports the

decision to use *Ankistrodesmus falcatus* as an algal strain for biofuel production experiments.

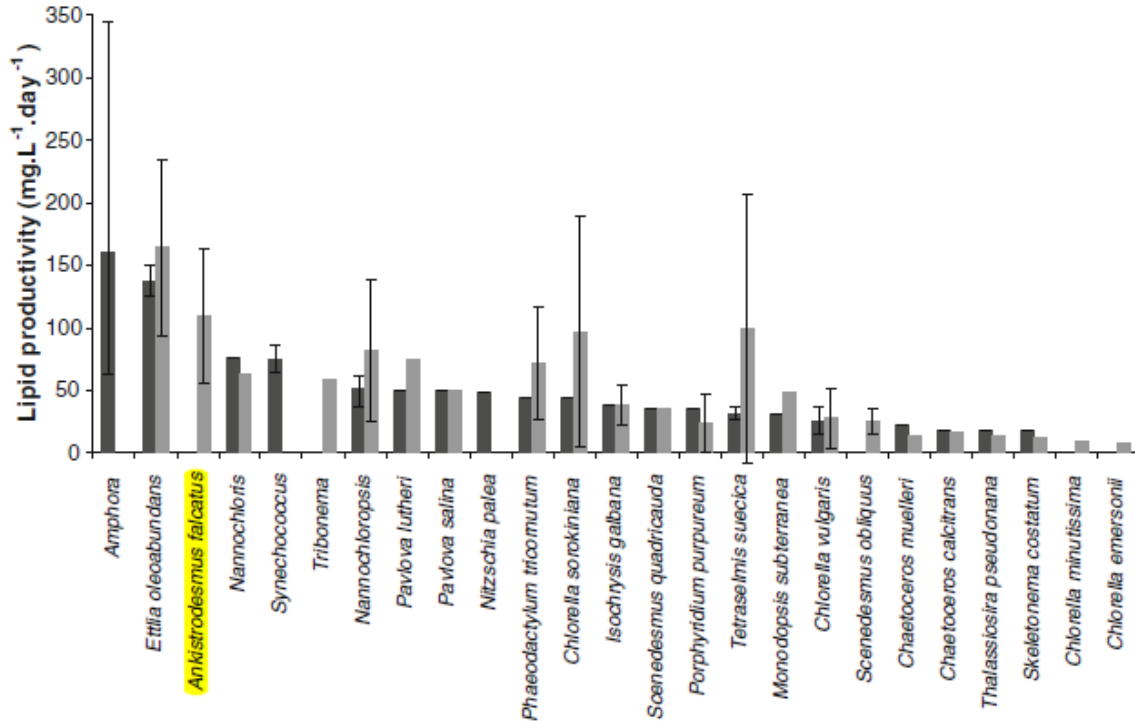


Figure 1.1: Lipid productivity ¹², describing *Ankistrodesmus falcatus* as a promising algal strain. Dark grey bars represent the average lipid productivity found in literature, while light grey bars indicate the calculated values for biomass productivity.

Finally, there have been a significant number of discussions regarding the ideal types of lipids that are to be generated by microalgae, or extracted by the downstream processing for eventual chemical transformation. The commercial development of microalgae as a feedstock for bio-fuel production will be most successful if the oils extracted are compatible with already-developed chemical transformation processes working in refineries. It is well documented that downstream processing technology of crude oil involving catalysis are very susceptible to the presence of impurities like sulfur and phosphorous. Since phospholipids are essential molecules to cellular membranes, and

therefore ubiquitous to all strains, it is critical for lipid extraction to target intercellular neutral lipids, rather than membrane-bound phospholipids. Kilham et al.¹³ present in Figure 1.2 the composition of major lipid classes for *Ankistrodesmus falcatus* grown under different nutrient limitations of nitrogen and phosphorus. This information provides a point of reference regarding the distribution of neutral and phospholipids produced by this strain. Under the different growth conditions, *Ankistrodesmus* produces total lipids with a composition of 50-65% neutral lipids and 25% phospholipids. If lipid extraction yields both neutral and phospholipids, downstream processing or catalysis would need to remove phosphorous.

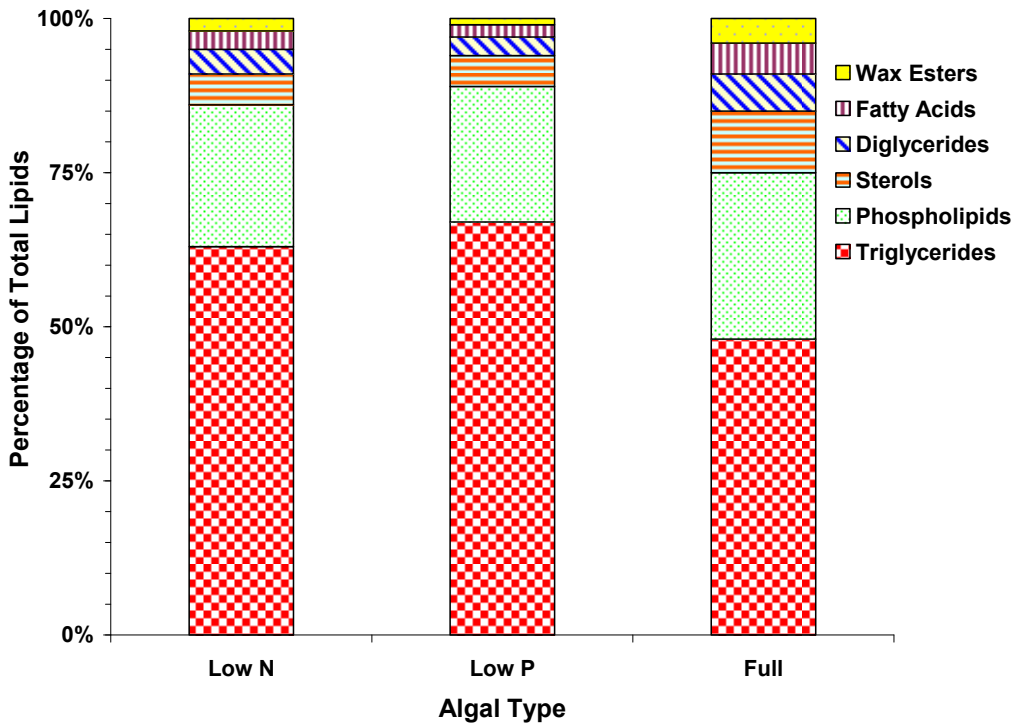


Figure 1.2: Effects of nutrient limitation on biochemical constituents of *Ankistrodesmus falcatus*. *Ankistrodesmus* produces triglycerides as the main type of lipids. However, this figure shows that it can also produce significant amount of phospholipids, which are undesirable compounds to the presence of phosphorous. Phosphorous will translate into technological difficulties on the catalytical transformation during the downstream processing.¹³

Physiologically, *Ankistrodesmus falcatus* is a unicellular, uninucleate green alga. It is a photoautotrophic microorganism that utilizes the energy from the sun to produce its own energy (ATP) as well as relying on CO₂ as a carbon source¹. Nevertheless, if needed, it can also grow heterotrophically. *Ankistrodesmus* has a needle-like shape, with gradually tapering ends. Usually it is about 3 µm in diameter at the broadest point, and it averages about 40 µm in length. Figure 1.3 shows a brightfield microscopic image of this strain under 40 x magnifications.

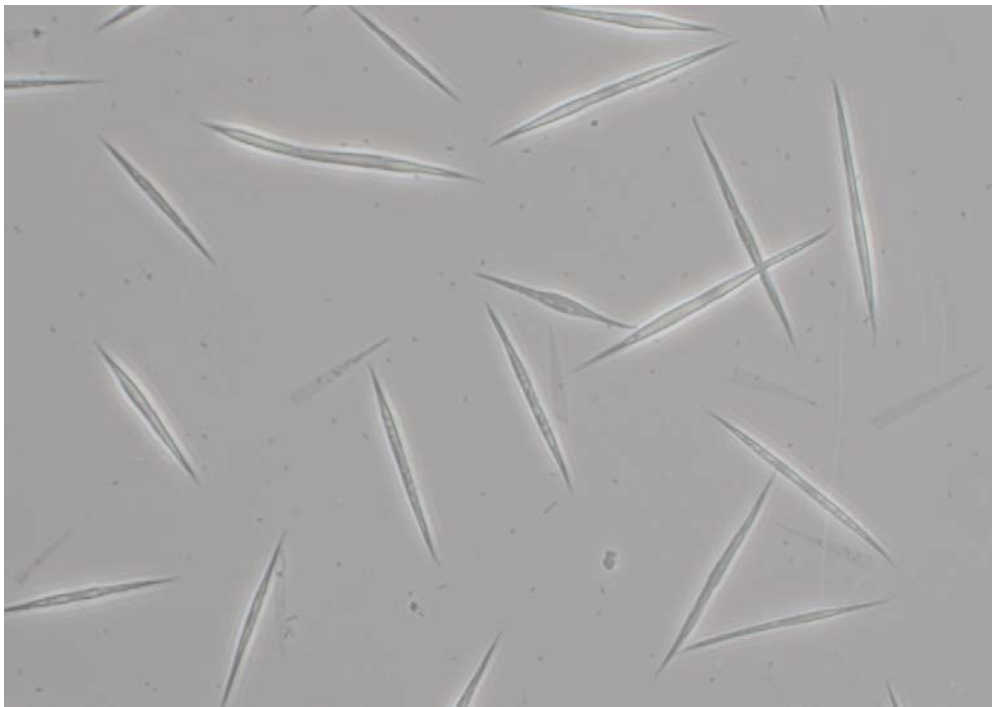


Figure 1.3: Microscopic image of *Ankistrodesmus falcatus*.

In terms of its outer anatomy, *Ankistrodesmus falcatus* possesses a cell wall and cell membrane. Eukaryotes' cell walls provide the structural strength to the microorganisms. They are relatively permeable and are located outside the cell membrane itself. Utilizing electron microscopy imaging, Sponsler et al.¹⁴ estimated the wall-thickness of *Ankistrodesmus* at about 1,000 Å (0.1 µm). Cell walls are defined as rigid,

homogeneous and often, multilayered structures. Even though their biochemical compositions do significantly change from one strain of algae to another, a major component of all algal cell walls, *Ankistrodesmus* included, is the Peptidoglycan layer¹⁵.

With regards to the algal cell membrane, it is structurally considered to be a phospholipid bilayer. It usually is about 80 Å (0.008 µm) wide, and it is considered to have fluid-like consistencies. Functionally, the cell membrane has three major duties¹: (i) it is the site of key enzymes for critical biological processes, e.g. electron transport, (ii) it functions in energy conservation by generating a proton motive force, and (iii) it works as a highly selective membrane, allowing the traffic of only certain compounds in order to concentrate specific metabolites and excrete waste materials. The membrane's selective permeability creates a physical barrier for efficient extraction of high-energy intracellular compounds stored by *Ankistrodesmus*, and we will attempt to reduce the membrane selectivity by significantly increasing its permeability.

It has been well documented that microalgae can obtain a significant increase of lipid production and fixation by growing under nitrogen limitations^{12, 16}, *Ankistrodesmus falcatus* not being the exception⁷. Transmission electron microscopy (TEM) research performed by Solomon et al.¹⁷ provided critical insight of where *Ankistrodesmus falcatus* stores the lipid bodies in its interior. Figure 1.5 and Figure 1.6 illustrate the internal structure of these microorganisms grown in N-replete, and N-deplete mediums, respectively. N-deprivation (Figure 1.6) resulted in the distinct accumulation of lipids, which appeared as droplets within the cytoplasm. The comparison of these two images provides an excellent visualization of where the targeted compounds for extraction are located in an *Ankistrodesmus-falcatus* cell.

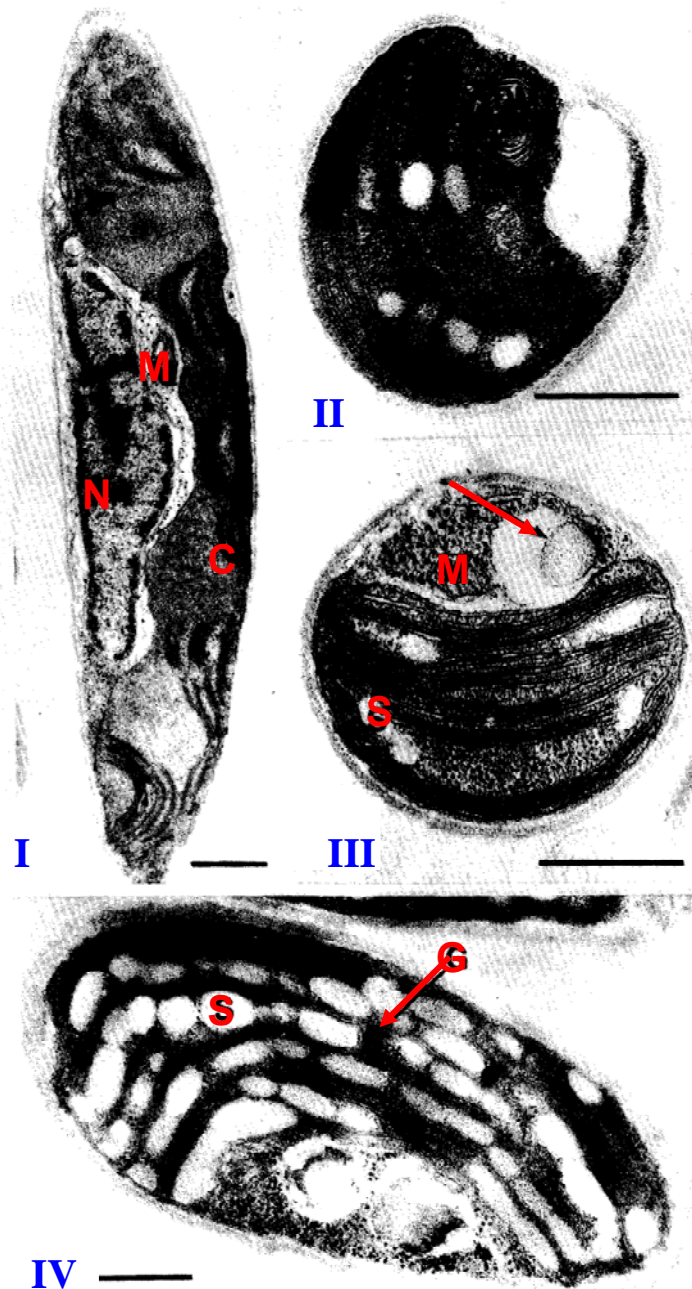


Figure 1.4: Nitrogen-sufficient cells of *Ankistrodesmus falcatus*. Scale bars = 0.5 μm . (I) A longitudinal media section of a portion of the cell shows one long parietal chloroplast [C] and the nucleus [N], with a mitochondrion [M] between them. (II) Cross-section view of a cell. (III) A mitochondrion [M] and possibly a microbody [arrow] are located near the chloroplast. The starch granules [S] can also be seen. (IV) In oblique view, numerous starch granules [S] can be seen packing the chloroplast. [G] = Dense granule

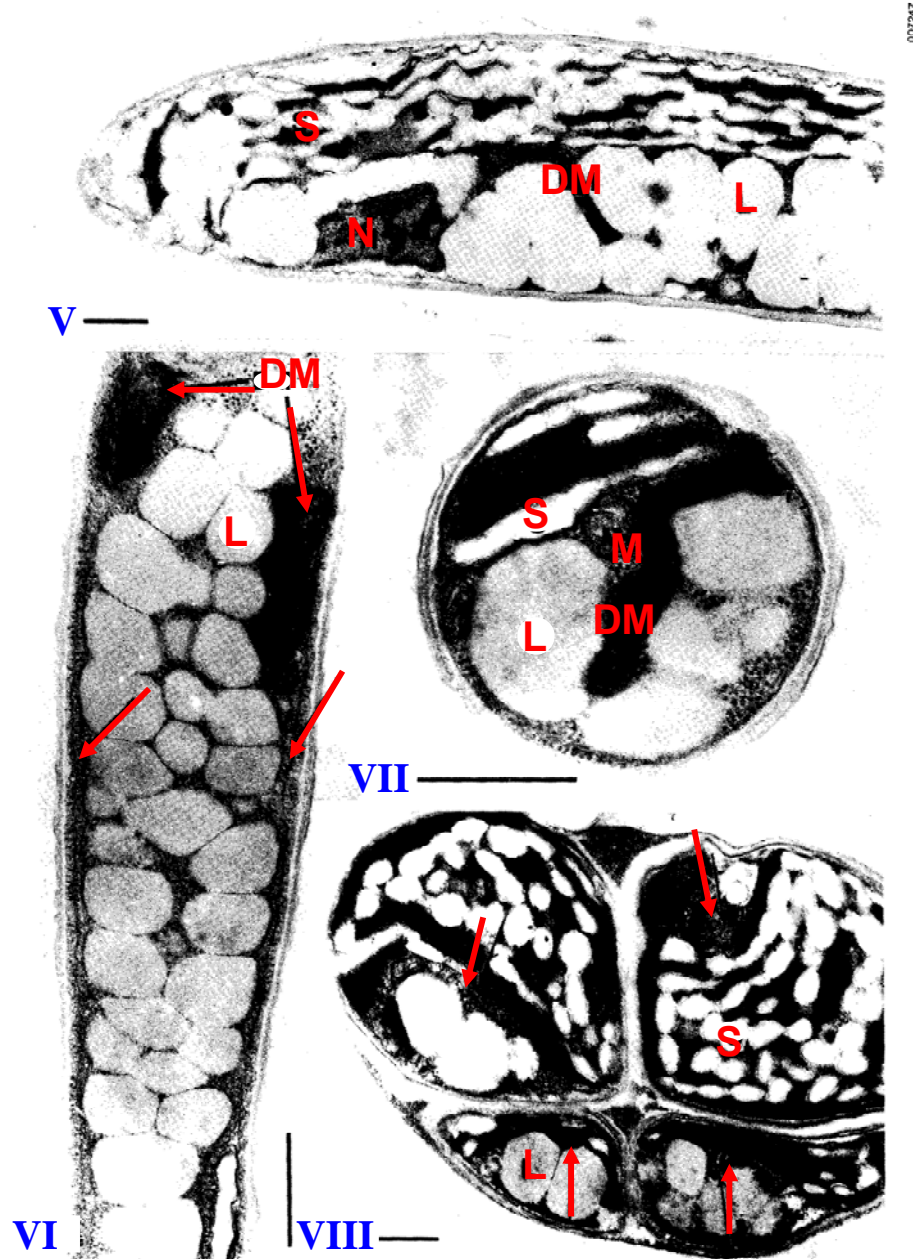


Figure 1.5: Nitrogen-stressed cells of *Ankistrodesmus falcatus*. These TEM images illustrate a significant amount of lipids present, as well as their relative position in the cytoplasm. (V) In this oblique section, food storage bodies occupy a large proportion of the cell volume. Starch granules [S] fill the chloroplast, and lipid droplets [L] occupy most of the cytoplasmic region. The nucleus [N] and double membrane structure [DM] are also present. (VI) Tightly packed lipids fill the cytoplasmic portion of the cell. Two double membrane structures [DM] lie nearby, and a double layer of membrane [arrows] lines the volume occupied by the lipid droplets. (VII) This cross-sectional view shows the relationship between the chloroplast [C] with starch granules [S] and the cytoplasmic region, which contains the lipids [L]. (VIII) Cross section through four autospores retained within the mother cell wall.

1.3 Block Flow Diagram of algae processing for fuel production

The production of fuels from algae is divided into different stages: (i) algae growth, (ii) harvesting of algae, (iii) lipid extraction, (iv) and catalytic conversion. Below is a brief overview of each stage and the different approaches being investigated in the literature.

Algae Growth: Production of algal biomass can be carried out in fully contained photobioreactors or in open channels and ponds⁴. Besides the type of reactor, there exist crucial considerations that need to be addressed including algal strain selection, nutrient additions, and control of multiple variables such as residence time, media pH, and light intensity to maximize production of targeted intercellular compounds.

Harvesting of Algae: This step requires the application of fundamentals of solid-liquid separations¹⁸. Some of the options for this processing step include flocculation, centrifugation, and filtration¹⁹.

Lipid Extraction: Regarding the extraction of intracellular compounds stored by algae, solvent extraction has received significant attention. There has been a significant effort in reporting the efficiency of multiple solvents, including traditional solvents like straight-chain hydrocarbons²⁰, chloroform²⁰, and novel solvents like supercritical fluids²¹.

One critical factor that has been proven is the necessity of cell disruption treatment prior to solvent extraction to enhance lipid recovery²². This cell-disruption pretreatment represents our main area of research focus.

Catalytic Transformation: The utilization of a new and more complex algal oil feedstock, instead of petroleum, requires the development of new chemical transformation processes.

As expected, there is plenty of research that does not fit the general process to algal fuel production suggested above. For example, thermal liquefaction^{23, 24} involves direct conversion of the microalgae biomass to algal oil by heating to high temperatures. Key advantages of this process would be the elimination of biomass concentration, cell disruption, and maybe solvent extraction, since it can be performed with high water content. However, it is a new concept with plenty of questions to be answered.

A possible commercial operation of biodiesel production from algal biomass is suggested to follow the general block flow diagram described in Figure 1.7, utilizing solvent extraction to recover the algal lipids, with a prior cell disruption to improve this recovery.

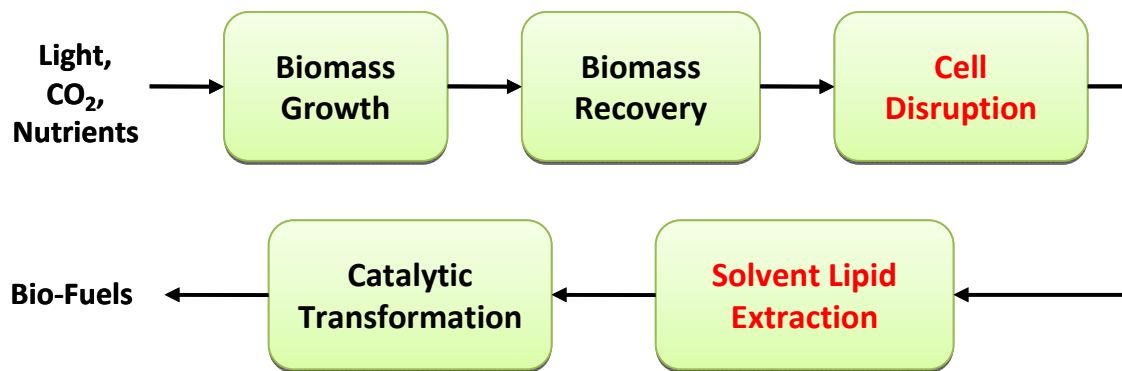


Figure 1.6: Block Flow Diagram for the production of algal fuels. Our research was focused on the cell-disruption and solvent lipid extraction areas.

1.4 Solvent extraction:

The B&D method ²⁵ is the most common technique for lipid extraction in laboratory settings. Soxhlet extraction is another popular method ²²; however, algal lipid extraction with B&D has been utilized so extensively, it has become a point of reference in terms of extraction efficiency.

Lipids are classified into two groups: the non-polar or neutral (triglycerides, diglycerides, monoglycerides, and sterols) and the more polar lipids (free fatty acids, phospholipids) ²⁶. Following the common rule of like-dissolves-like, the neutral lipids dissolve well in apolar organic solvents, but the polar lipids, especially phospholipids, only dissolve in relatively polar solvents. A solvent mixture, sufficiently polar to remove the lipids from their association with cell membranes, but sufficiently non-polar to dissolve the neutral lipids, is therefore required to efficiently extract lipids from microalgae. This is exactly the case of the B&D method, which initially consists of a monophasic mixture of chloroform (CHCl_3), methanol (MeOH), and water (H_2O). At this stage the 1-phase liquid system provides excellent contact between algae and solvent. The homogenate system is later diluted (by adding H_2O and CHCl_3) to create a biphasic liquid system, purifying the lipids in the chloroform layer, and leaving the nonlipids in the aqueous layer ²⁷. In addition to the original B&D method, modified B&D methods utilizing more industrial-scale solvents like isopropanol and hexane have been reported²⁸.

The crucial drawback for the B&D method is that it is not scalable to industrial magnitudes due to chloroform's toxicity; it is believed to be a carcinogen ²⁹. The development of algal fuel technology will be of large proportions and scale, utilizing significant volumes of solvents. Therefore, solvents will play a critical role in the

environmental performance of the overall process, and they will impact cost, safety, and worker health, making the selection and utilization of green solvents imperative. Currently, hexane, which is a “Not-Preferred” FDA (Food & Drug Administration) solvent ²⁹, is used in the extraction of a wide range of natural products and vegetable oils in the USA, and it is an active candidate being considered to extract algal lipid for this industrial process. However, following the principles of green chemistry, which ask us for “utilization of safer solvents and auxiliaries” ³⁰, we have explored the utilization of a greener solvent to modify the B&D method. We suggest the utilization of ethyl acetate (EtOAc) as the nonpolar solvent to modify the traditional B&D method.

In order to choose “safer solvents and auxiliaries”, it is critical to evaluate the Environmental, Health, and Safety (EHS) properties of each candidate solvent. The EHS properties of a solvent include its ozone depletion potential, biodegradability, toxicity, and flammability ³¹. Capello et al.⁸ developed a chemical assessment method based on EHS criteria. In this method, each solvent was assessed based on its performance in nine categories: (1) release potential, (2) fire/explosion, (3) reaction/decomposition, (4) acute toxicity, (5) irritation, (6) chronic toxicity, (7) persistency, (8) air hazard, and (9) water hazard. Figure 1.7, extracted from Capello et al.⁸, illustrates the results obtained for 26 organic solvents commonly used in the chemical industry, which supports our reasoning of using EtOAc as a solvent for algal lipid extraction (the lower the solvent EHS score, the better the solvent). EtOAc obtained an EHS indicator score of 2.9 point, while hexane obtained a value of 4.1. In addition to Figure 1.7, Koller et al.³¹ elaborated an Excel-based tool, available in the web, which is capable of generating these results. Utilizing

this tool, and in order to put things into perspective, it was calculated that chloroform obtained a value of 4.0.

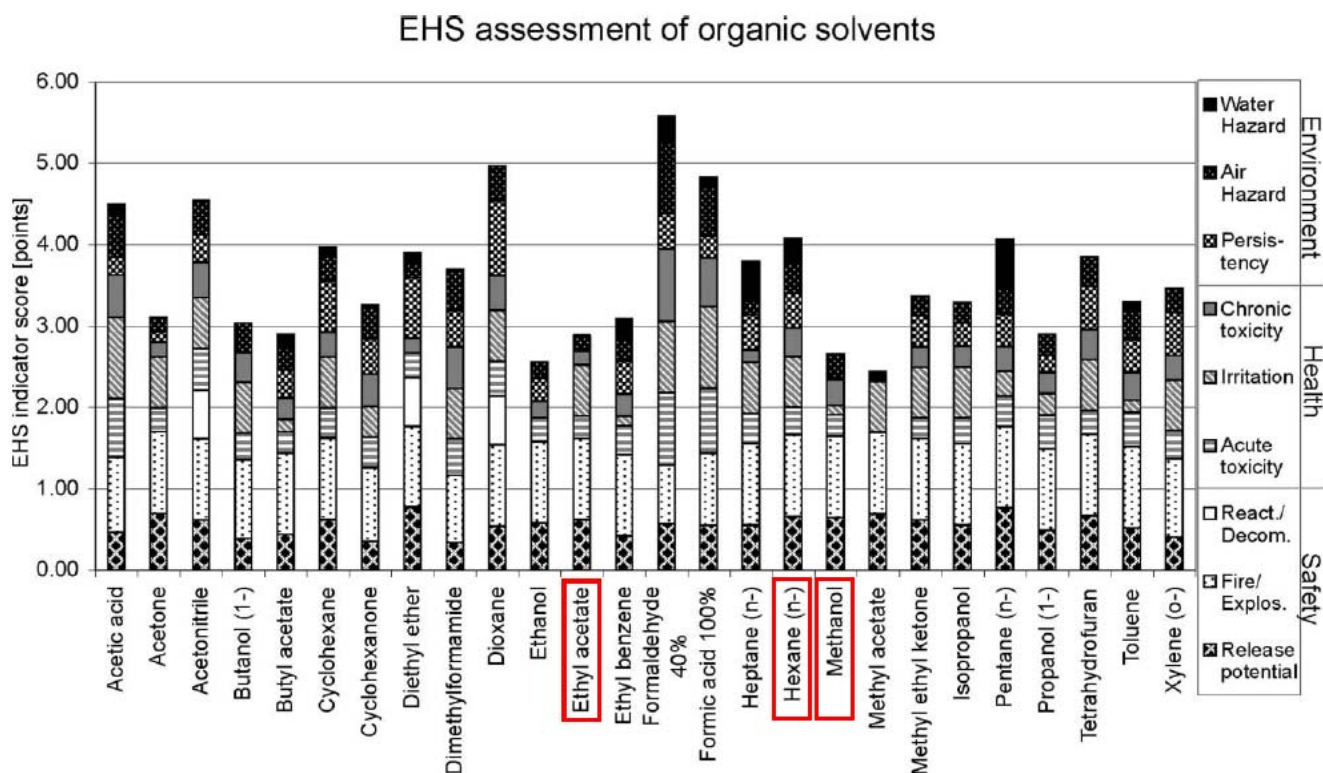


Figure 1.7: Results of an environmental, health, and safety (EHS) assessment for 26 common solvents developed by Koller et al.³¹. Ethyl acetate obtained an index of 2.9, while methanol and chloroform obtained an index of 4.1 and 4.0 (nine is the max value, indicating extremely poor EHS properties). Ethyl acetate represents an excellent EHS candidate to perform research on algal lipid extraction.

An EtOAc-modified B&D method (EtOAc/MeOH/H₂O, 2:1:0.8, v/v/v) is suggested as a replacement to the traditional chloroform-based system. This solvent-mixture is considered as a green alternative, which still enjoys the practical monophasic-biphasic approach of separation and purification.

1.5 Cell disruption pretreatments to intensify solvent extraction

The much desired lipids and other high value byproducts from algal microorganisms are mostly intercellular. They are produced within the microbial organisms and kept inside the cytoplasm. This lack of excretion of targeted algal compounds forces the utilization of an extraction step. In the case of solvent extraction, a prior cell disruption pre-treatment, such as ultrasound and mechanical disruption, has proven to be beneficial for better extraction obtaining up to 2-fold process intensification^{22, 32}.

Microorganisms, including algae, are more robust than is generally believed. Microorganisms' resistance to disruption has been discussed by Wimpenny³³. He points out that the internal pressure due to osmosis inside an organism as *Sarcina lutea* is about 20 atmospheres, and that the cell wall and membrane responsible for holding this structure are about as strong, weight for weight, as reinforced concrete. A large variety of disruption methods have been developed to disintegrate these strong cellular walls and membranes and liberate the cell contents. Figure 1.9, obtained from Chisti et al.³, summarizes the most common methods used for disruption of microbial cells, applied in different industries.

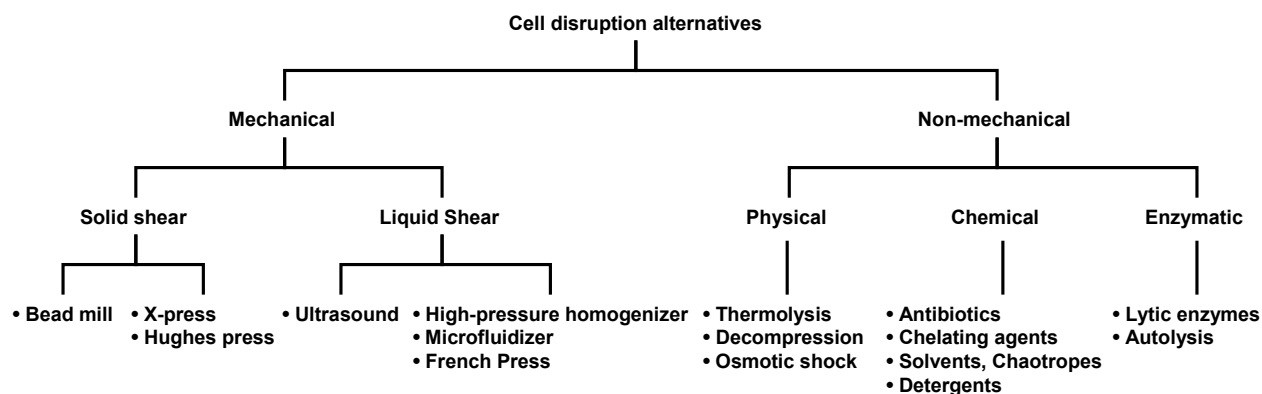


Figure 1.8: Methods of microbial cell disruption (adapted from Chisti et al.³)

One of the most common disruption methods is the bead mill. This method can achieve efficient cell disruption at both laboratory and industrial scale³⁴. The mechanism behind this effective pretreatment is the bead-cell collision resulting in strong cell rupturing. Another common method of cell rupturing is sonication or ultrasound. This is the most widely-used disruption method in laboratories settings³⁵. It creates a mechanism of cell disruption due to the shear stress associated with the cavitation phenomena. Even though it is a popular laboratory tool, it is largely inefficient for pilot scale or industrial use³⁵. The high pressure homogenizer³⁴ is another effective pre-treatment. It achieves cell disruption by passing the cell suspension at very high pressures through an adjustable orifice discharge valve. However, this elevated operating pressure makes this technique a non-attractive option for industrial scale. The non-mechanical methods achieving physical disruption at industrial scale are limited. One simple and promising method is osmotic shock. This method consists in diluting an equilibrated cell suspension into a high osmotic pressure system, causing cells disruption due to the abrupt change in external pressure. Finally, enzymatic disruption has proven to be advantageous by being very specific, attacking the Peptidoglycan structure of the cell wall³⁴. However, it is very

unlikely that this technique can achieve industrial scale processing due to its slow acting treatment.

Some cell disrupting pretreatments shown in Figure 1.9 have successfully enhanced the lipid solvent extraction from microalgae. Such is the case with ultrasound sonication, where Ranjan et al.²² compared the effect of this pretreatment in conjunction with the B&D method and observed an approximate 200% improvement in lipid extraction. The author attributes the extraction improvement to the cell disruption created by the bubbles' implosion, which increased the solvent-lipid contact. He points out that, without the cell disruption, the extraction was governed by mass transfer with poor lipid-solvent contact, as well as the solvent power to dissolve the microorganism organelles.

Autoclaving, bead-beating, microwaves, and osmotic shock are other cell disruption techniques described in literature to improve algal lipid extraction when contacted with a slightly modified B&D method. The extraction improvement highly depended on the strain of algae used³². In their specific study, Lee et. al. demonstrated that microwave was the most effective method for lipid extraction intensification.

The selection of cell disruption pretreatment will strictly depend on the associated intensification of the method in conjunction with the energy requirements. Thus, the novel utilization of pulsed electric field (PEF) technology is suggested as a promising option of cell disruption for lipid extraction. This technique relies on the application of short pulses of strong electric field, with minimum energy requirements and short exposures.

1.6 Electroporation as a pretreatment technique

Electroporation or electroporabilization is a membrane phenomenon in which cell suspensions are exposed to high electric fields for brief periods of time. When electroporation is applied, the treated cells experience an increase in membrane permeability, which provides greater access into (or out of) the cell cytoplasm. The mechanisms of microbial or cell electroporation are not completely elucidated, but it has been postulated that lipids rearrange within the bilayer due to electrostatic interactions, forming pores that causes this permeabilization to increase ³⁶.

The very early applications of electroporation (although the term was not defined at that time) date back to the 1910s when it was reported that electrically-treated milk was being supplied to the city of Liverpool as early as 1915. It was suggested that the accompanying heat generated during the process was not the main factor in the destruction of bacteria but the “electric current is an important destroying agent” ³⁷. In the 1950’s, very early observations suggested that some type of “electrical breakdown” might occur in electrically-stimulated membranes ³⁸, and in 1960 the use of high-voltage pulses for the destruction of microorganisms was suggested by Gossling et al. ³⁹. In the course of subsequent studies, it was shown that the site of the electrical field interaction is the lipid portion of the cell membrane. This insight created great interest in modeling lipid systems to discern the molecular mechanism of electroporation. To date, it is known that the cell membrane of most eukaryotes, algae included, is made up of phospholipids that form a non-planar lipid bilayer along with membrane proteins. Cell membranes of most cells carry a fixed negative charge and are made up of charged ions and proteins ⁴⁰. A

transmembrane potential (TMP) exists across the cell membrane, because of ionic gradients on the inside and outside of the membrane. Application of an external electric field above TMP induces a noticeable polarity of the cell, creates a charge separation, and produces a dipole moment that is parallel to the external field. In the presence of external electric fields with short-duration pulses, pore formation is observed. The reason behind the pore formation is the lipid's head rearrangement in the bilayer of the cell membrane. Figure 1.10 presents a conceptual illustration of the effects of pulsed electric field (PEF), inducing the electroporation phenomena on a bilayer lipid membrane.

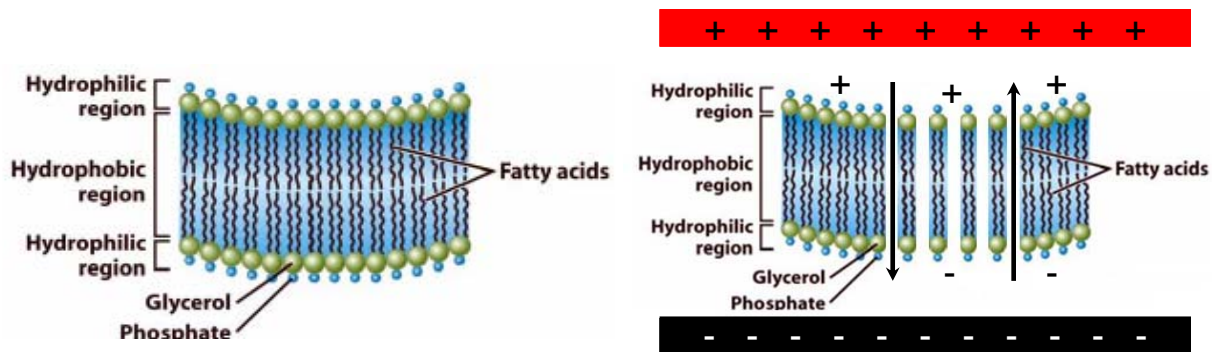


Figure 1.9: Conceptual illustration of the effects of pulsed electric field (PEF) inducing the electroporation phenomena on a bilayer lipid membrane. Original obtained from Madigan et al. ¹.

When the applied electric field is below a critical value, the pore formation has been reported to be reversible. This pore formation occurs in the part of the cell where the dipole moment is induced, and it is associated with an increase in conductivity of the solution. Resealing of the membrane, once the electric field is removed, is a slow process and it occurs on a time scale of seconds to minutes ⁴¹. After the resealing process has been completed, the microorganism treated with electroporation returns to its original, viable state. Above a critical applied field, electrocompressive forces cause a dielectric

rupture leading to an increase in permeability along with irreversible pore formation. This permanent pore formation finally causes irreversible cell membrane disruption.

Engineering design parameters specific to electroporation are important variables that affect the degree of membrane manipulation. These parameters include: (i) field strength, (ii) type of electrical pulses (e.g. rectangular, exponential decay), (iii) pulse duration, and (iv) number of pulses. Electrical field strength represents the primary parameter, determining the degree of membrane electroporation. This degree in membrane permeability enhancement will translate into transient or irreversible electroporation, which can have multiple global effects to the system of study. Global changes can be as simple as temporary induction of a stress response, or as complicated as improvement of mass transfer. Figure 1.10 illustrates multiple end-results from the application of high pulsed electric field and later permeation of membranes.

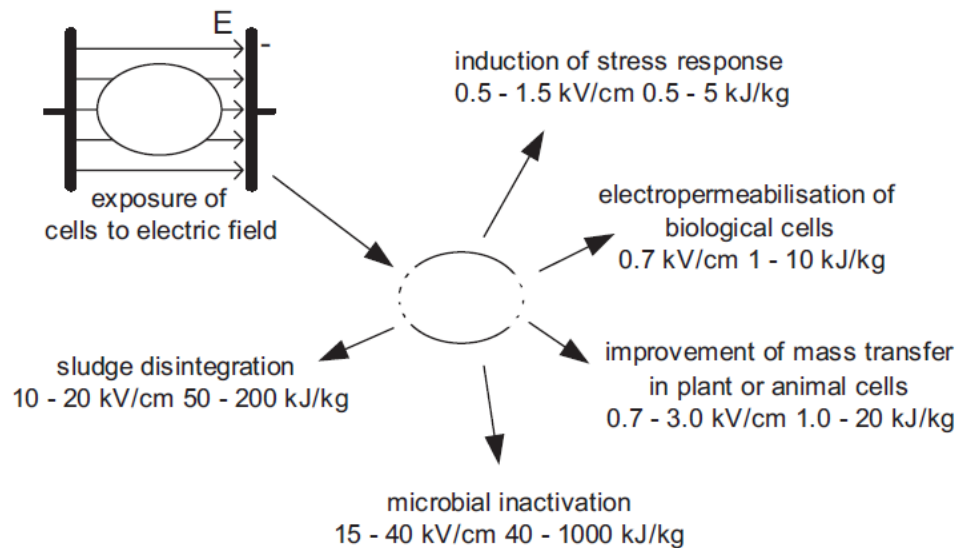


Figure 1.10: Graph obtained from Toepfl et al.⁴², illustrating the permeabilization of cells after exposure to electric field and actual applications with typical electric field strength and energy input requirements.

As imagined, the possible end-effects that the electroporation phenomena provide (e.g. access into/out of cells' cytoplasm, deactivation of pathogenic microorganism, cell disruption) have found multiple potential applications in industry.

Table 1.3 illustrates the vast spectrum of applications for electroporation; significant research efforts are being conducted in these areas. It is extremely important to mention that the concept of electroporation has been proven to work in multiple systems: systems with high cell density with low liquid content, as well as liquid systems with extremely low cell density.

Table 1.3: Electroporation phenomenon has found many possible industrial applications, where significant research efforts are being spent. However, utilization of PEF as algal cell disruption for lipid solvent extraction intensification is a novel application.

Electroporation Applied to Different Systems	Application Goal	Scale	Cont. or Batch	Elec. Field
PEF to Apple Juice (liquid System) ⁴³	PEF as an alternative to thermal pasteurization for microorganism deactivation	Lab & Pilot Plant	C	30KV/cm 100KJ/Kg
PEF to Skim milk (liquid System) ⁴⁴	Inactivation of endogenous enzymes and gram-negative bacteria, which are predominal spoilage organism in milk	Lab	C	25- 37KV/cm
PEF combined with pressing to sugar beet cossettes (solid – liquid system) ⁴⁵	Improve juice extraction by membrane cell disruption, following pressing	Lab	B	1- 0.5KV/cm
PEF to maize plant, grass, and alfalfa (solid system) ⁴⁶	Investigate PEF as part of energy-efficient drying process of plant material for bio-fuel production	Lab	B	7KV/cm
PEF combined with pressing to apples cossettes (solid-liquid system) ⁴⁷	Improve juice extraction by membrane cell disruption, following pressing	Lab	B	1KV/cm
PEF to eukaryote cells. (liquid system) ⁴⁸	Transfer improvement of foreign information into Chinese hamster ovary (CHO)	Lab	B	Up to 1.5KV/cm
PEF to assist extraction of soluble matter from grape skins (solid-liquid system) ⁴⁹	Improvement of extraction rate and total quantity of polyphenols from grape skin	Lab	B	1.5KV/cm

To date, the most frequent application of electroporation has been in the fields of biology, biotechnology, and medicine. All these applications are of small scale and intend

to gain access into the microorganism. A contrasting application of PEF is the inactivation of microbial organism in products like milk ⁴⁴, apple juice ⁵⁰, and other liquid products for human consumption. For this type of application the fundamental intent is to irreversibly permeate cell membranes to produce microorganism death. The application of PEF with this purpose has been proven to be feasible on an industrial scale, and it leads to the potential for PEF to be applied for the intensification of algal lipid extraction.

PEF as a technique to intensify algal lipid extraction

Even though the idea of biodiesel production from microalgae was conceived in the late 1980's, up to this date no commercial technology has been successfully developed due to the high cost associated with current processes. Of the total biodiesel cost, 40-60% has been attributed to the energy intensive downstream processing operations ⁷. The oil extraction process is a specific area recognized as high-energy demanding due to the use of mechanical energy in every step of the cell disruption operation and due to the evaporation of solvents. Any reduction in the downstream cost would be a significant step toward algal biofuel production.

The utilization of PEF during the cell disruption process has all the required characteristics to be a competitive pre-treatment: it is quick and has low-energy requirement. Figure 1.11 illustrates the encouraging features of PEF when utilized to disintegrate multicellular tissue, specifically potato tissue. When compared with other pre-treatment techniques, it is evident that PEF could significantly intensify the solvent extraction of intercellular algal lipids with minimal time and energy requirements.

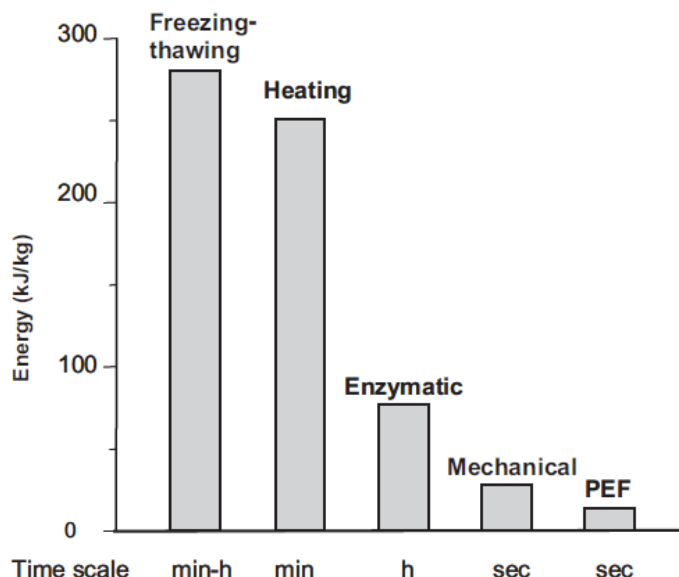


Figure 1.11: Graph obtained from Toepfl et al., comparing the energy required for cell disintegration of multicellular tissue (potato tissue) with different techniques. PEF requires the shortest time as well as the lowest energy to pre-treat the cells. This important characteristics suggest that PEF could be an excellent candidate for algal cell disruption prior to lipid extraction ⁴².

The utilization of electroporation phenomena to intensify the solvent extraction of algal lipids has not been explored in literature. This novel application will be the focus of this Master's Thesis.

1.7 Summary of goals

For successful development of an industrial scale lipid extraction process, a green substitute for the common chloroform-based solvent is required. Furthermore, the requirement of a cell disrupting treatment with low energy requirements and quick application is emphasized, if this solvent extraction process is to be effective and economically feasible.

In this contribution, a greener ethyl acetate-modified B&D method is compared to the chloroform B&D method, and the application of PEF technology as a pretreatment for algal lipid extraction is tested.

References Cited in CHAPTER 1

1. Madigan, M.; Martinko, J.; Dunlap, P.; Clark, D., Brock biology of microorganisms (2009). San Francisco: Pearson Benjamin Cummings.
2. Posten, C.; Schaub, G., Microalgae and terrestrial biomass as source for fuels--A process view. *Journal of Biotechnology* **2009**, *142* (1), 64-69.
3. Chisti, Y.; Moo-Young, M., Disruption of microbial cells for intracellular products. *Enzyme and Microbial Technology* **1986**, *8* (4), 194-204.
4. Chisti, Y., Biodiesel from microalgae. *Biotechnol. Adv.* **2007**, *25* (3), 294-306.
5. Rosegrant, M., *Biofuels and grain prices: impacts and policy responses*. International Food Policy Research Institute: 2008.
6. Schenk, P.; Thomas-Hall, S.; Stephens, E.; Marx, U.; Mussgnug, J.; Posten, C.; Kruse, O.; Hankamer, B., Second generation biofuels: high-efficiency microalgae for biodiesel production. *Bioenergy Research* **2008**, *1* (1), 20-43.
7. Sheehan, J., *A look back at the US Department of Energy's Aquatic Species Program: Biodiesel from algae*. National Renewable Energy Laboratory: 1998; Vol. 328.
8. Capello, C.; Fischer, U.; Hungerbühler, K., What is a green solvent? A comprehensive framework for the environmental assessment of solvents. *Green Chemistry* **2007**, *9* (9), 927-934.
9. Demirbas, A.; Demirbas, M. F., *Algae Energy: Algae as a New Source of Biodiesel (Green Energy and Technology)*. First ed.; Springer: London, 2010.
10. Barclay, W.; Johansen, J.; Chelf, P.; Nagle, N.; Roessler, P.; Lemke, P. *Microalgae culture collection, 1986-1987*; Solar Energy Research Inst., Golden, CO (USA): 1986.

11. Feinberg, D. *Fuel options from microalgae with representative chemical compositions*; Solar Energy Research Inst., Golden, CO (USA): 1984.
12. Griffiths, M.; Harrison, S., Lipid productivity as a key characteristic for choosing algal species for biodiesel production. *Journal of Applied Phycology* **2009**, *21* (5), 493-507.
13. Kilham, S.; Kreeger, D.; Goulden, C.; Lynn, S., Effects of nutrient limitation on biochemical constituents of *Ankistrodesmus falcatus*. *Freshwater Biology* **1997**, *38* (3), 591-596.
14. Sponsler, O.; Bath, J., Electron Microscope Studies of Submicroscopic Structures of *Ankistrodesmus falcatus*. *American Journal of Botany* **1949**, *36* (10), 756-758.
15. Barsanti, L.; Gualtieri, P., *Algae: anatomy, biochemistry, and biotechnology*. CRC press: 2006.
16. Yamaberi, K.; Takagi, M.; Yoshida, T., Nitrogen depletion for intracellular triglyceride accumulation to enhance liquefaction yield of marine microalgal cells into a fuel oil. *Journal of Marine Biotechnology* **1998**, *6* (1), 44-48.
17. Solomon, J.; Hand Jr, R.; Mann, R. *Ultrastructural and flow cytometric analyses of lipid accumulation in microalgae*; Oak Ridge National Lab., TN (USA); Solar Energy Research Inst., Golden, CO (USA): 1986.
18. Shelef, G.; Sukenik, A.; Green, M. *Microalgae harvesting and processing: a literature review*; Technion Research and Development Foundation Ltd., Haifa (Israel): 1984.
19. Molina Grima, E.; Belarbi, E.; Acien Fernandez, F.; Robles Medina, A.; Chisti, Y., Recovery of microalgal biomass and metabolites: process options and economics. *Biotechnol. Adv.* **2003**, *20* (7-8), 491-515.
20. Grima, E.; Medina, A.; Giménez, A.; Sánchez Pérez, J.; Camacho, F.; García Sánchez, J., Comparison between extraction of lipids and fatty acids from microalgal biomass. *Journal of the American Oil Chemists' Society* **1994**, *71* (9), 955-959.
21. Herrero, M.; Cifuentes, A.; Iba ez, E., Sub-and supercritical fluid extraction of functional ingredients from different natural sources: Plants, food-by-products, algae and microalgae:: A review. *Food chemistry* **2006**, *98* (1), 136-148.
22. Ranjan, A.; Patil, C.; Moholkar, V., Mechanistic Assessment of Microalgal Lipid Extraction. *Industrial & Engineering Chemistry Research* **2010**, *49* (6), 2979-2985.

23. Aresta, M.; Dibenedetto, A.; Carone, M.; Colonna, T.; Fragale, C., Production of biodiesel from macroalgae by supercritical CO₂ extraction and thermochemical liquefaction. *Environmental Chemistry Letters* **2005**, 3 (3), 136-139.
24. Minowa, T.; Yokoyama, S.; Kishimoto, M.; Okakura, T., Oil production from algal cells of *Dunaliella tertiolecta* by direct thermochemical liquefaction. *Fuel* **1995**, 74 (12), 1735-1738.
25. Bligh, E.; Dyer, W., A rapid method of total lipid extraction and purification. *Canadian Journal of Physiology and Pharmacology* **1959**, 37 (8), 911-917.
26. Lovern, J., *The chemistry of lipids of biochemical significance*. Methuen London: 1955.
27. Smedes, F.; Thomasen, T., Evaluation of the Bligh & Dyer lipid determination method. *Marine Pollution Bulletin* **1996**, 32 (8-9), 681-688.
28. Molina Grima, E.; Robles Medina, A.; Gimenez Gimenez, A.; Sanchez Perez, J. A.; Garcia Camacho, F.; Garcia Sanchez, J. L., Comparison between extraction of lipids and fatty acids from microalgal biomass. *Journal of the American Oil Chemists' Society* **1994**, 71 (9), 955-959.
29. Kerton, F., *Alternative solvents for green chemistry*. Royal Society of Chemistry: 2009.
30. Anastas, P.; Warner, J., *Green Chemistry Theory and Practice*, 1998. Oxford University Press, New York: p 30.
31. Koller, G.; Fischer, U.; Hungerbuhler, K., Assessing safety, health, and environmental impact early during process development. *Ind. Eng. Chem. Res* **2000**, 39 (4), 960-972.
32. Lee, J.; Yoo, C.; Jun, S.; Ahn, C.; Oh, H., Comparison of several methods for effective lipid extraction from microalgae. *Bioresource Technology* **2010**, 101 (1), S75-S77.
33. Hughes, D.; Wimpenny, J.; Lloyd, D., The disintegration of microorganisms. *Methods in microbiology* **1971**, 5, 1-54.
34. Geciova, J.; Bury, D.; Jelen, P., Methods for disruption of microbial cells for potential use in the dairy industry-a review. *Int. Dairy J.* **2002**, 12 (6), 541-553.
35. Moo-Young, M., *Comprehensive biotechnology: the principles, applications and regulations of biotechnology in industry, agriculture and medicine*. 1985.

36. Neumann, E.; Kakorin, S.; Toensing, K., Principles of membrane electroporation and transport of macromolecules. *Methods Mol. Med.* **2000**, *37*, 1-35.
37. Beattie, J.; Lewis, F., The Electric Current (Apart from the Heat Generated). A Bacteriological Agent in the Sterilization of Milk and Other Fluids. *Epidemiology and Infection* **1925**, *24* (02), 123-137.
38. Stampfli, R., Reversible electrical breakdown of the excitable membrane of a Ranvier node. *An. Acad. Bras. Cienc* **1958**, *30*, 57-63.
39. Gossling, B. S. *United Kingdom Patent UK 845743*. 1960.
40. Teissie, J., Cell membrane electroporabilization. *Bioelectrochemistry of Membranes* **2004**, 205.
41. Teissie, J.; Golzio, M.; Rols, M., Mechanisms of cell membrane electroporabilization: a minireview of our present (lack of?) knowledge. *Biochimica et Biophysica Acta (BBA)-General Subjects* **2005**, *1724* (3), 270-280.
42. Toepfl, S.; Mathys, A.; Heinz, V.; Knorr, D., Review: Potential of high hydrostatic pressure and pulsed electric fields for energy efficient and environmentally friendly food processing. *Food Reviews International* **2006**, *22* (4), 405-423.
43. Schilling, S.; Schmid, S.; Ja ger, H.; Ludwig, M.; Dietrich, H.; Toepfl, S.; Knorr, D.; Neidhart, S.; Schieber, A.; Carle, R., Comparative study of pulsed electric field and thermal processing of apple juice with particular consideration of juice quality and enzyme deactivation. *Journal of agricultural and food chemistry* **2008**, *56* (12), 4545-4554.
44. Shamsi, K.; Versteeg, C.; Sherkat, F.; Wan, J., Alkaline phosphatase and microbial inactivation by pulsed electric field in bovine milk. *Innovative Food Science & Emerging Technologies* **2008**, *9* (2), 217-223.
45. Bouzrara, H.; Vorobiev, E., Beet juice extraction by pressing and pulsed electric fields. *International Sugar Journal* **2000**, *102* (1216).
46. Sack, M.; Eing, C.; Berghofe, T.; Buth, L.; Stangle, R.; Frey, W.; Bluhm, H., Electroporation-Assisted Dewatering as an Alternative Method for Drying Plants. *Plasma Science, IEEE Transactions on* **2008**, *36* (5), 2577-2585.
47. Bazhal, M.; Vorobiev, E., Electrical treatment of apple cosettes for intensifying juice pressing. *Journal of the Science of Food and Agriculture* **2000**, *80* (11), 1668-1674.
48. Wolf, H.; Rols, M.; Boldt, E.; Neumann, E.; Teissie, J., Control by pulse parameters of electric field-mediated gene transfer in mammalian cells. *Biophysical Journal* **1994**, *66* (2), 524-531.

49. Boussetta, N.; Lebovka, N.; Vorobiev, E.; Adenier, H.; Bedel-Cloutour, C.; Lanoiselle, J., Electrically Assisted Extraction of Soluble Matter from Chardonnay Grape Skins for Polyphenol Recovery. *Journal of agricultural and food chemistry* **2009**, 57 (4), 1491-1497.
50. Schilling, S.; Schmid, S.; Jager, H.; Ludwig, M.; Dietrich, H.; Toepfl, S.; Knorr, D.; Neidhart, S.; Schieber, A.; Carle, R., Comparative study of pulsed electric field and thermal processing of apple juice with particular consideration of juice quality and enzyme deactivation. *J Agric Food Chem* **2008**, 56 (12), 4545-54.

CHAPTER 2

EXPERIMENTAL SETUP, METHODS, AND PROCEDURES

2.1 EXPERIMENTAL SETUP

2.1.1 Reactor Setup for Algae Growth

All extraction experiments illustrated throughout this thesis are focused on the utilization of a single algal strain as a lipid source; *Ankistrodesmus Falcatus*. This section describes the reactor setup utilized to grow this single strain.

Figure 2.12, shown below, presents the conceptual diagram of the chemostat operated to grow *Ankistrodesmus falcatus*. The reactor had a nominal size of ~ 4L (C-3000mL, Bellco Glass Inc., New Jersey). It was always operated with a liquid level kept at 3L, with an approximate headspace of 1L. All the streams going into – and out of – the chemostat were $\frac{3}{4}$ inch OD tubing (R-3603, Tygon, Akron OH). Peristaltic pumps (MasterFlex, ColePalmer, Saint Louis, MO) operated the media influent, as well as the chemostat effluent.

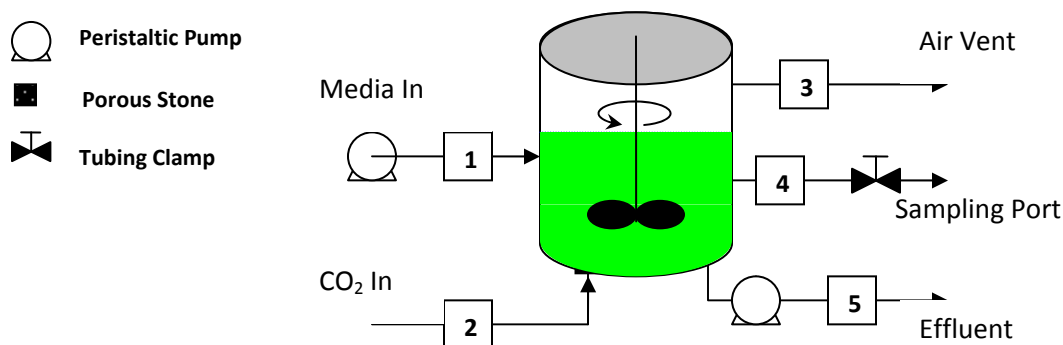


Figure 2.12: Conceptual diagram of the 4L chemostat utilized to cultivate the algal biomass.

As described by Figure 2.12, the *Ankistrodesmus falcatus* chemostat had a combined total of 5 streams feeding and leaving the system. Stream 1 supplied all nutrients to the reactor at a rate of 0.24 mL min^{-1} . In order to keep the reactor at a constant level of 3L, Stream 5 removed algae and media suspension at a similar rate (0.24 mL min^{-1}). With this specific influent/effluent rates the chemostat operated at a hydraulic residence time of 8.7 days. The main carbon source for this biological system was carbon dioxide. Stream 2 fed 1% (v/v) CO_2 and air into the reactor at a rate of 0.5 L min^{-1} , controlled by a flow controller (YO-32460-42, Cole Palmer). The reservoir for this gas was a compressed cylinder of 99.999% purity (UN1013, MathesonGas). Stream 3 represented the reactor's air vent, which had a 0.22 micron filter installed at its exit. Finally, all algae biomass was harvested through Stream 4, which represented the reactor's sample port. The sampling through this stream was enabled by the manipulation of a plastic clamp.

The daily operation of the chemostat was under ambient temperatures. The liquid agitation within the reactor was obtained by magnetic baffles, driven by a magnetic stand (5 Pos Dig, Bellco Glass Inc., New Jersey). The reactor was exposed to 12hr cycles of fluorescent light with irradiance exposure of $120 \mu\text{mol m}^{-2} \text{ sec}^{-1}$, and 12 hrs of darkness. These cycles were controlled by residential light timers obtained from a hardware store. Figure 2.13 presents an image of the actual chemostat setup.

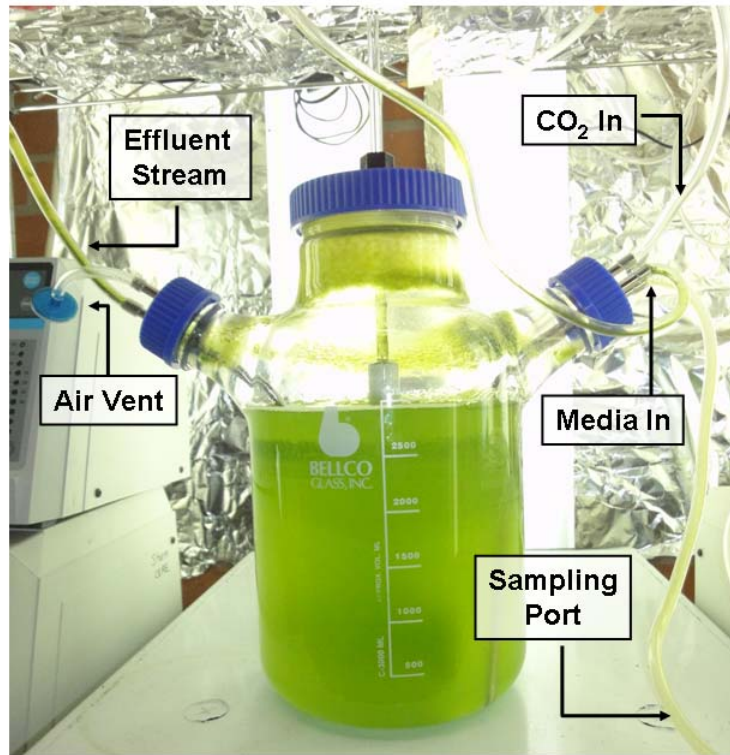


Figure 2.13: Actual image of Ankistrodesmus chemostat operated to obtain the algal biomass.

2.1.2 Feed Preparation & Reactor Maintenance

A synthetic media solution, with N:P molar ratio of 50, was prepared and introduced to the chemostat as a source of important nutrients. This feed solution was prepared by following the procedure explained by Guillard¹. The main components of the media solution are presented on

Table **2.4**, as well as their concentrations.

Table 2.4: List of main chemical components that make up the algal media, which delivered the necessary nutrients and trace metals.

Component	Symbol	Working Concentrations [μM]
Calcium Chloride Dihydrate	$\text{CaCl}_2 \cdot 2\text{H}_2\text{O}$	250
Magnesium Sulfate Heptahydrate	$\text{MgSO}_4 \cdot 7\text{H}_2\text{O}$	150
Sodium Bicarbonate	NaHCO_3	150
Potassium Phosphate Dibasic	K_2HPO_4	50
Sodium Nitrate	NaNO_3	1000
Sodium meta-Silicate Nonahydrate	$\text{Na}_2\text{SiO}_3 \cdot 9\text{H}_2\text{O}$	100
Boric Acid (0.6% W/V)	H_3BO_3	97
Trace Element solution [†]		

[†] Trace element solution consisted in the following components on their respective working media solution concentrations (μM): Cupric (II) Sulfate Pentahydrate (0.039 μM), Zinc Sulfate Heptahydrate (0.077 μM), Cobalt Chloride Hexahydrate (0.042 μM), Manganese (II) Chloride Tetrachloride (0.910 μM), Sodium Molybdate Dihydrate (0.026 μM), and Iron (III) Chloride Hexahydrate (0.999 μM).

The algae media was prepared in a 2L volumetric flask. First, 1.9 liters of Millipore water was placed into the flask. Then, all chemical components were added one at a time in their required volumes to reach the desired concentrations. Afterwards, the volume was brought up to the 2L mark. The solution was mixed, and placed into a 2L media bottle. The solution was sterilized by autoclaving the media bottle. After the solution was allowed to reach room temperature, the filter-sterilized trace metal solution was added. The media bottles were placed in a refrigerated room until they were needed.

The algal media was introduced into the reactor utilizing peristaltic pumps. The pumps controlling the addition of feed solution were calibrated at the initial stages of the reactor inoculation. Further calibrations were performed as needed, when liquid level in the chemostat indicated a significant variation from the normal 3L mark. The $\frac{3}{4}$ inch OD tubing connecting all streams were replaced on a need-basis, when biomass build-up was observed.

2.1.3 Pulsed Electric Field (PEF): Circuit and Pretreatment Chamber

The PEF technique required an apparatus capable of delivering the high voltage and high energy in a pulsing fashion. Therefore, an in-house system was developed at the School of Engineering. This apparatus is made up from 3 main components:

1. **High Frequency (HF) Generator:** This unit represents the first component, requiring a 120V power supply. At this stage, the alternating current from the power supply gets magnified up to 10,000V.
2. **Marx Generator:** This unit receives the alternating current output from the HF Generator and converts it into direct current (DC), in addition to increasing the voltage up to 28,000V. The Marx Generator also achieves the required pulsing effect by utilizing spark gaps. Figure 2.15 describes the electrical circuit that represents the above mentioned units.
3. **Electroporation Chamber:** This chamber holds the algae-water suspension to be treated with the discharges from the HF Generator and Marx Generator. This chamber consists of a modified 4mL UV cuvette, to which two stainless steel electrodes were installed to facilitate the electrical potential. Figure 2.3 describes the dimensions of the electroporation chamber.

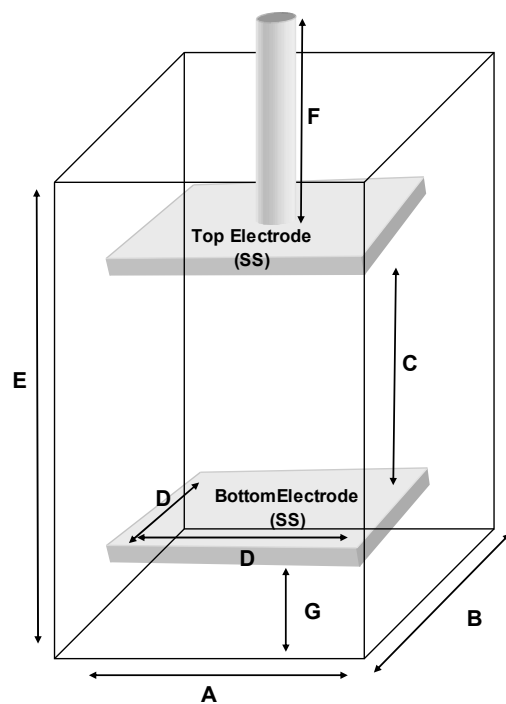


Figure 2.14: Electroporation chamber utilized to treat the algae-water suspension prior to solvent contact. The chamber dimensions are the following: (A) 10.4 mm, (B) 10.4 mm, (C) Top electrode can be adjust as desired, (D) 8 mm, (E) 44.6 mm, and (G) 6 mm.

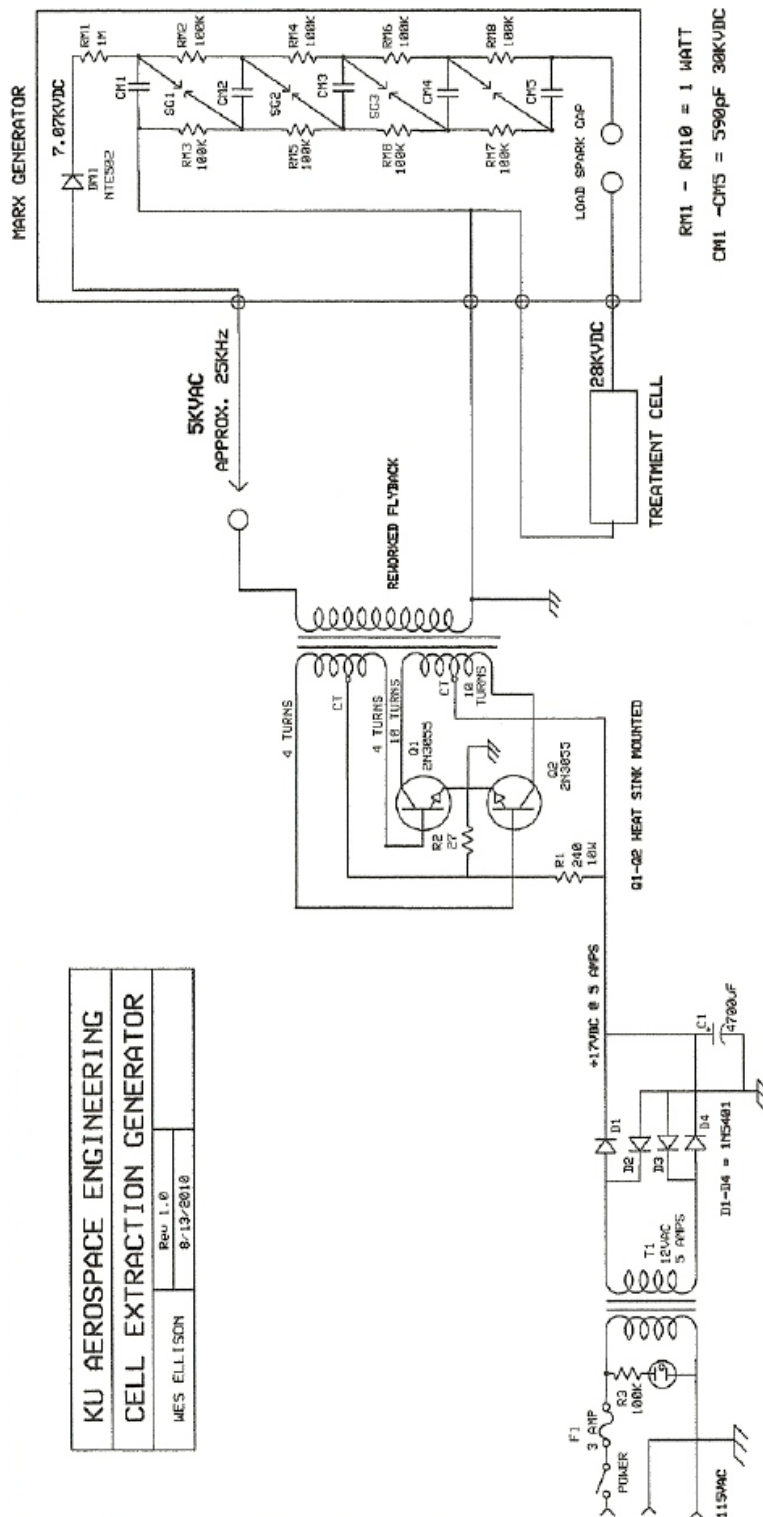


Figure 2.15: Electrical diagram describing the main components of the Pulsed Electric Field apparatus; HF Generator, Marx Generator, and Electroporation Chamber.

2.2 EXPERIMENTAL METHODS & PROCEDURES

The typical data gathered to compare lipid concentrations obtained from extractions using different solvents and PEF pretreatment included several step: (i) algal growth, (ii) algal harvesting, (iii) algal dewatering, (iv) algal pretreatment, (v) solvent extraction and solvent-product separation, (vi) chemical transformation, and finally (vii) product quantification. In addition, fluorescent microscopy in conjunction with molecular probes was another technique utilized to visually inspect the effect of PEF on algae, and it will also be described and explained. Figure 2.5 illustrates the Block Flow Diagram generally followed to gather experimental data throughout this Thesis.

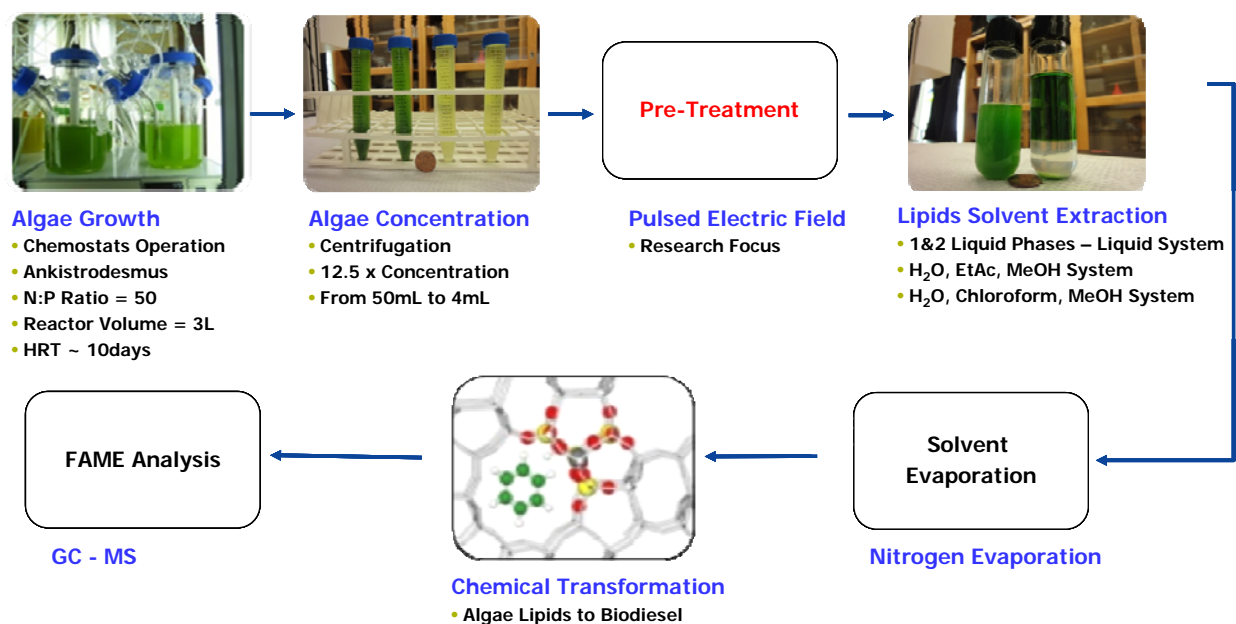


Figure 2.16: Flow Diagram describing the main experimental steps to obtain algal lipid extraction data, incorporating PEF as a pretreatment to intensify this lipid extraction.

2.2.1 Algal Growth

The algae chemostat described in Section 2.1.1 and Section 2.1.2 served as the single source of algae to perform extraction experiments. All algal batches harvested from this chemostat were allowed to freely grow in the reactor for at least 7 days prior to performing any extractions. This time interval between batches allowed enough cell growth to obtain significant amount of lipids for extraction and quantification..

2.2.2 Algal Harvesting

Algae were harvested from the chemostat through the sampling port into a glass container. Enough volume for the necessary number of samples was collected. This initial volume served as the starting source of algae, therefore the suspension needed to be well mixed to avoid experimental error. A magnetic stir bar was introduced into the glass container to achieve homogeneity for all samples.

2.2.3 Algal Dewatering

The dewatering of algae was achieved thru two centrifugation steps at 3500 rpm for 10 minutes (5810R, Eppendorf). For further details regarding this procedure please read Section 2.2.5 – Solvent Extraction.

2.2.4 Algae Pretreatment with PEF

The experimental setup associated with the PEF apparatus was already presented in Section 2.1.3. The strength of the electric field created between the top and bottom electrode has an inverse proportionality with respect to the gap between the electrodes, i.e., the smaller the distance between top and bottom electrodes, the higher the electric

field strength. After performing multiple experiments, it was determined that our electroporation apparatus delivered enough electric field to permeate the algae membrane when the distance between electrodes was set at 1cm. Figure 2.6 describes the approximate distribution of volume in the 4mL chamber when operated at an electrode distance of 1cm.

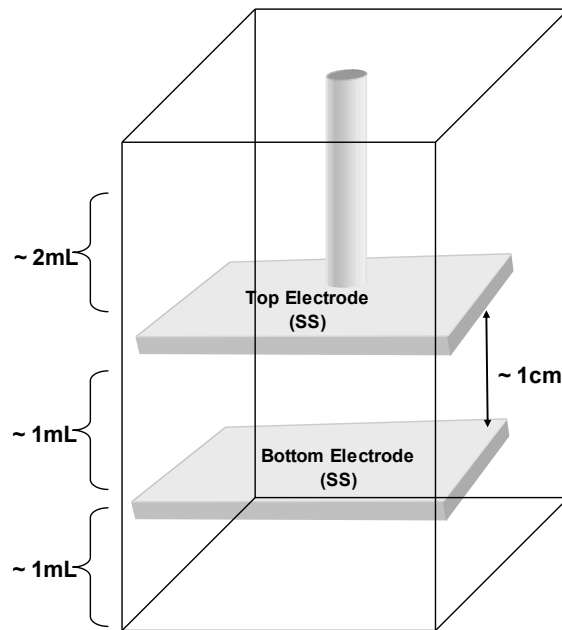


Figure 2.17: A 1cm-gap between both electrodes proved to create the required potential to permeate the algal membrane due to electroporation. Since the original procedure asked for 4mL to be introduced into the chamber, this 1cm spacing between electrodes translated into only treating 25% ~(1mL) of the total volume, since the other 3mL were outside the active volume.

Pulsed Electric Field as a pretreatment

The four main parameters that affect the electroporation efficiency are the electric field strength, electrical pulse duration, type of pulses, and number of pulses.

- **Electric Field Strength:** The PEF system, presented in Figure 2.15, delivers 28,000 Volts to the electroporation chamber.
- **Pulse Duration:** The treatment pulse duration is estimated to be 22.66 *msec*. This value was calculated based on the RC time constant of the chamber by the following equation:

$$t = R \times C = 22.66 \text{ msec}$$

Equation 2.1

where t represents each pulse duration, R is the resistance of the solution measured at 10,000 ohms, and C is the capacitance of the chamber measured with a capacitance meter (Model 810C, BK Precision) and found to be:

$$C = 2.266 \mu F$$

Equation 2.2

The resistance of the chamber filled with algae suspension was measured with the following physical characteristics: Area of each electrode (64mm²), and distance separating each electrode (1cm).

- **Type of pulses:** Exponential decay
- **Number of pulses:** The number of pulses is dependent on the amount of time that the apparatus is delivering potential to the chamber, also referred as “Treatment Regime”. The treatment regime selected for all experiments on this thesis is illustrated by Figure 2.7, which consisted of turning on the apparatus for 10 sec, then turning it off during 10 secs, then turning it on for 10 sec, followed by 10 sec off, and finally turning it on for the last 10 sec. Based on this regime, and the previously calculated pulse duration of 22.66 *msec*, the algal solution is pulsed 1,323 times during the effective 30 sec treatment.

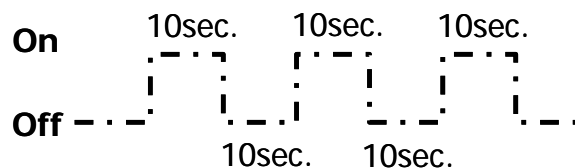


Figure 2.18: “Treatment Regime” utilized for all experiments performed during this research study. The PEF was activated during 3 intervals of 10sec, turning the apparatus off during 10sec between intervals. The apparatus needed to be turned off, since there were concerns about electrical components overheating.

The algae pretreated in the electroporation chamber were previously concentrated following the procedure explained on Section 2.2.3. Once in the chamber, the “treatment regime” described above was utilized to permeate the algae membrane. After the desired electric field was delivered, the pretreated algae were transferred to a glass vial utilizing an Eppendorf pipette to be contacted with solvent, following the procedure explained in Section 2.2.5.

After each pretreatment batch, the electroporation chamber was rinsed with deionized water 5 times to ensure cleanliness of the chamber. The excess water left in the chamber was ejected utilizing pressurized service air.

PEF without Cooling:

The pretreatment obtained from PEF introduces a significant amount of electrical energy into the system. Following the treatment regime described on Figure 2.7, the algae-water suspension reached a final temperature of approximately 70°C (from an initial temperature of ~ 22°C). Temperature was measured utilizing a thermocouple (-200°C to 1,300°C, Fisher Scientific). In order to uncouple the effects of electric pulsing and high temperatures on cell membrane disruption and lipid extraction, a cooling mechanism was created to avoid the final temperature of 70°C.

PEF with Cooling:

After applying PEF, dry ice (solid carbon dioxide) was utilized as a cooling media. The dry ice was pulverized into small particles utilizing a hammer. The small particles of dry ice were arranged in such a way to create a cooling jacket for the electroporation chamber. Prior to initiating the PEF, the algae-water suspension was allowed to cool down until it reached a low temperature of 5°C. At this point the electrical pretreatment was started, following the treatment regime of three 10 sec pulses. The system's temperature was monitored during multiple steps. With the cooling effect of the dry ice jacket, the algae-water suspension reached a final temperature of about 50°C. Figure 2.8 describes the temperature swing to which the algae were exposed to due to the electrical energy input.

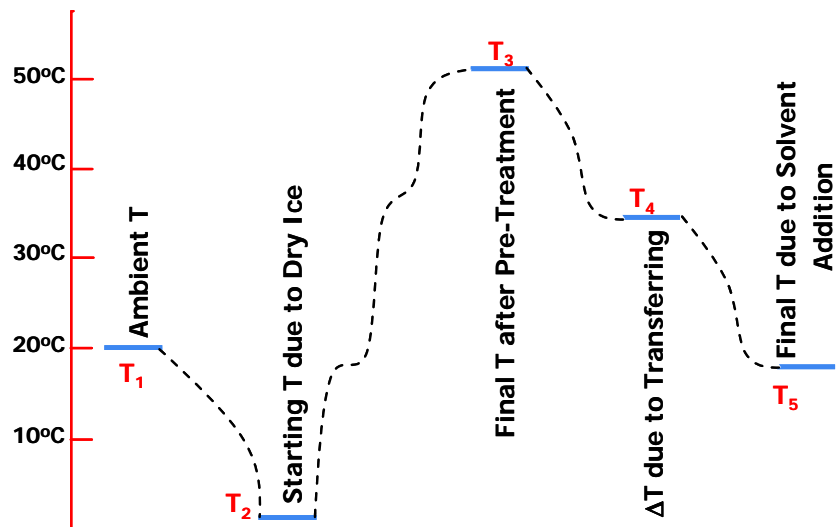


Figure 2.19: Algae-Water suspension was exposed to the above illustrated temperature swing. The lowest temperature T₂ was achieved by utilizing pulverized dry-ice as a “cooling jacket”, such that a final temperature of 70°C would be avoided. The highest temperature achieved, T₃=50°C, proved not the represent a significant temperature stress to permeate the algae membrane. Any membrane damage observed under this temperature swing would have come from the electric field.

2.2.5 Solvent Extraction & Solvent-Product Separation

The main idea throughout this Master's Thesis was to compare the algal lipids extraction efficiency of two solvents: (A) Chloroform, and (B) Ethyl Acetate (EtOAc). The extraction procedures associated with each different solvent are very similar, and a summary for each extraction can be found below. (This Standard Operating Procedure can be found on Appendix A)

Lipid Extraction Procedure with Chloroform

Algal lipid extraction was performed using a method adapted from B&D. The lipid extraction was obtained by utilizing a mixture of chloroform, methanol, and water. A 50 mL sample obtained from the algae chemostat was collected in a 50 mL test tube, then centrifuged at 3,500 rpm for 10 minutes, forming an algal cell pellet at the bottom of the tube. The sample's supernatant was removed from the test tube by carefully pouring off the excess liquid, without disturbing the algal pellet, until reaching a total volume below 15mL. The pelleted cells along with the left supernatant were mixed and transferred to a new plastic test tube (15mL). Enough DI H₂O was added to reach a total volume of 15mL, to later be re-centrifuged at 3,500 rpm for 10 minutes. The supernatant was again removed by pouring off the excess, without disturbing the pellet, until the total new volume was below 4mL. The media-cell pellet solution was mixed and additional DI H₂O was added until the total suspension volume reached 4mL, which was added to a glass tube for solvent extraction.

Solvent extraction began with the addition of 5 mL of chloroform and 10 mL of methanol, resulting in a CHCl₃/MeOH/H₂O ratio of 5:10:4 by volume. At this ratio, all solvents are miscible and form one layer. The one-phase liquid extraction was contacted

for zero to 24 hrs, as noted in the results section, on a vortex mixer (for zero time exposure) or a shaker table (for longer exposures). Then, 5mL of H₂O and 5mL CHCl₃ were added, which results in a 10:10:9 ratio of CHCl₃/MeOH/H₂O. The glass tube was centrifuged for 10 minutes at 3,500 rpm. At this solvent ratio, a two phase liquid-liquid system is formed- a water-methanol top layer and a chloroform lower layer. The chloroform layer, which contained the extracted lipids, was removed by a Pasteur pipette and placed into a smaller glass tube. After the first extraction, 10 mL of additional chloroform was added to perform a second extraction. This chloroform addition again resulted in a CHCl₃/MeOH/H₂O ratio of 10:10:9 forming a two liquid layer system. The tube was again centrifuged at 3,500 rpm for 10 minutes, and the lower chloroform layer was recovered and placed in the same previous glass tube where the first extraction was collected. The chloroform was completely evaporated by heating in a 37°C water bath with a constant overhead flow of nitrogen. At this point the dry algal lipids rested at the bottom on the glass vial, and were resuspended in 1 mL of chloroform to be stored at - 20°C for future chemical transformation into FAMES.

Lipid Extraction Procedure with Ethyl Acetate

The overall procedure for ethyl acetate extraction is the same as the previously presented chloroform extraction, with the only difference that ethyl acetate was utilized as the main solvent. Different ratios were required to form the one phase liquid system and subsequent two phase liquid-liquid system. To obtain the initial miscible solution of all solvents, 10 mL of ethyl acetate and 5 mL of methanol was added to the original 4 mL of media-algae suspension, resulting in a EtOAc/MeOH/H₂O ratio of 10:5:4 by volume. Afterwards, in order to obtain the two phase liquid-liquid system, 5 mL of EtOAc and 5

mL of H₂O were added to reach a final ratio of 15:5:9 of EtOAc/MeOH/H₂O. In this two-layer liquid system, the bottom layer represented the water-methanol rich system and the top layer constituted the ethyl acetate, lipid-rich layer. Besides the above mentioned modifications, the exact same procedure was followed to perform the ethyl acetate lipid extraction. The Standard Operational Procedure for lipid extraction can be found in Appendix A.

Algal Lipids Rate of Extraction – 24hr Kinetics of Extraction

A particular research interest of this Thesis was the investigation of the kinetics of extraction of algal lipids utilizing multiple solvent mixtures. To obtain this information, the time of single liquid phase between all solvent was precisely timed, and after the desired time period (between zero and 24 hours), the single phase system was modified to the two phase system to stop the liquid extraction. The rest of the procedure was followed as usual.

Lipid Extraction at $t = 0, t_0$

Lipid extraction at t_0 was part of the Kinetics of Extraction experiments, as well as more detailed analysis performed later. To obtain the t_0 extraction information, the general procedure stated on Section 2.2.5 was followed, with the only exception that as soon as the single liquid phase contact between the algal biomass and solvents was formed, a quick vortex was provided to the sample and immediately modified to the two liquid phase system to stop the lipid extraction. The rest of the procedure was followed as usual. At the end of the procedure, this sample represented the t_0 extraction data.

2.2.6 Chemical Transformation of Algal Lipids into Fatty Acid Methyl Esters (FAMES)

Independent of the solvent utilized to extract the algal lipids (chloroform or ethyl acetate), the chemical transformation of extracted lipids into FAMES is identical. Lipids were reacted into FAMES via a transesterification reaction, utilizing methanol as a reactant and KOH as a base catalyst. The extracted lipids suspended in chloroform (or ethyl acetate) solvent were dried under constant nitrogen gas. Then, lipids were dissolved in 500 μ L of 1:1 methanol:toluene solution. Catalyst was introduced by adding 500 μ L of 0.2N KOH in methanol solution. Samples were then submerged in a 37°C water bath allowing the reaction to proceed during 15 minutes and then cooled down to ambient temperature. At this point, 500 μ L of 0.2 N acetic acid, 2 mL of chloroform, and 2 mL of DI H₂O was quickly added sequentially, mixing in between each addition. Sample was centrifuged for 5 minutes at 1,500 rpm. At this solvent ratio, a two phase liquid-liquid system was formed, a water-methanol top layer and a chloroform lower layer. The chloroform layer that contained the reacted FAMES was removed by a Pasteur pipette and placed into a new glass tube, which concluded the first extraction. After this initial extraction, 1 mL of additional chloroform was added and the centrifugation-separation steps were repeated twice more for a total of three extractions. All lower chloroform layers were recovered, and placed in the same previous glass tube where the first, and second extractions were collected. Then, the chloroform was completely evaporated, and the dried FAMES were re-suspended in 1 mL of chloroform. At this point the 10 μ L of the 200 μ g/mL internal standard was added, mixed, and the entire sample was placed in a GC vial, ready for GC-MS analysis. The Standard Operational Procedure for FAME production can be found in Appendix A.

2.2.7 Product Quantification

FAMEs were analyzed by Gas Chromatography-Mass Spectrometry (6890 Series-5973N, Agilent, Santa Clara, CA). Details regarding the procedure are in the next section.

2.3 ANALYTICAL PROCEDURES

2.3.1 Gas Chromatography – Mass Spectrometry

Gas Chromatography-Mass Spectrometry (CG-MS) was utilized to quantify the amount of FAMEs recovered. It is important to notice that even though the analytical procedure detects the FAMEs present in the final injected sample, originally the solvents extract triglycerides and multiple other cellular materials. However, since this method only monitors certain types of FAMEs, then the solvent extraction efficiency is represented by the total amount of those FAMEs being detected.

Table 2.5 represents all the FAMEs being monitored by the method. The lipid extraction efficiency of a particular solvent is determined by summation of individual FAMEs found in the particular sample.

Table 2.5: List of main FAMES being monitored by this procedure in order to determine the total lipid extraction of the solvents in question.

Name	Common Name	Formula	Synonym
Decanoic acid, methyl ester	Methyl Decanoate	C ₁₁ H ₂₂ O ₂	C10:0
Dodecanoic acid, methyl ester	Methyl Laurate	C ₁₃ H ₂₆ O ₂	C12:0
Methyl tetradecanoate	Methyl Myristate	C ₁₅ H ₃₀ O ₂	C14:0
Hexadecanoic acid, methyl ester	Methyl Palmitate	C ₁₇ H ₃₄ O ₂	C16:0
9-Hexadecenoic acid, methyl ester, (Z)-	Methyl Palmitoleate	C ₁₇ H ₃₂ O ₂	C16:1
9,12-hexadecadienoic acid, methyl ester		C ₁₇ H ₃₀ O ₂	C16:2
7,10,13-hexadecatrienoic acid, methyl ester		C ₁₇ H ₂₈ O ₂	C16:3
Octadecanoic acid, methyl ester	Methyl Stearate	C ₁₉ H ₃₈ O ₂	C18:0
9-Octadecenoic acid (Z)-, methyl ester	Cis-9-Oleic Methyl Ester	C ₁₉ H ₃₆ O ₂	C18:1
Octadecanoic acid, ethyl ester (I.S.)	Ethyl Stearate		
9,12-Octadecadienoic acid, methyl ester	Methyl Linoleate	C ₁₉ H ₃₄ O ₂	C18:2
9,12,15-Octadecatrienoic acid, methyl ester	Methyl Linolenate	C ₁₉ H ₃₂ O ₂	C18:3
Eicosanoic acid, methyl ester	Methyl Arachidate	C ₂₁ H ₄₂ O ₂	C20:0
Docosanoic acid, methyl ester	Methyl Behenate	C ₂₃ H ₄₆ O ₂	C22:0
13-Docosanoic acid, methyl ester	Methyl Erucate	C ₂₃ H ₄₄ O ₂	C22:1
Tetracosanoic acid, methyl ester	Methyl Lignocerate	C ₂₅ H ₅₀ O ₂	C24:0

The concentration of each FAME was calculated following the following equation:

$$Conc[\mu g / L] = \frac{(A_s)(C_{is})(D)(V_i)}{(A_{is})(\overline{RF})(V_s)(1000)}$$

Equation 2.3

Conc = Resulting concentration of the analyte of interest, µg/L

A_s = Area of peak for the analyte in the sample

C_{is} = Concentration of the internal standard in the concentrated sample extract, 2000 mg/L

D = Dilution factor, if sample was diluted prior to analysis

V_i = Volume of extract injected to column, 1 µL

A_{is} = Area of peak for the internal standard

RF = Average response factor from the initial calibration

V_s = Volume of sample extracted (in mL; multiply by 1000 if L), usually 50mL unless otherwise noted.

The chemical compound chosen to work as the internal standard for this procedure was ethyl stearate (S8269-5G, Sigma Aldrich, Saint Louis-USA)

Apparatus calibration – Determination of Response Factors (RF)

A mixture of FAMES with known concentrations for each component was utilized as the external standard (FAME Mix C8-C24, Supelco, Bellefonte-PA). This calibration sample was dissolved into chloroform solvent, and multiple external standards of progressively higher nominal concentrations were created. These external samples were injected into the GC-MS, and for each FAME for each different nominal concentration, a response factor (RF) was calculated. As expected, the RF for each FAME component did not significantly vary across the concentration spectrum, and

Table 2.6 below presents the average RF utilized in Equation 2.3 to calculate each compound concentration.

Table 2.6: Average Response Factors calculated from GC-MS calibration, utilized to determine each FAME concentration.

Compound Name	Synonym	Average RF
Decanoic acid, methyl ester	C10:0	0.8220
Dodecanoic acid, methyl ester	C12:0	0.7769
Methyl tetradecanoate	C14:0	0.9312
Hexadecanoic acid, methyl ester	C16:0	0.9872
9-Hexadecenoic acid, methyl ester, (Z)-	C16:1	0.9109
Octadecanoic acid, methyl ester	C18:0	0.9649
9-Octadecenoic acid (Z)-, methyl ester	C18:1	0.9261
Octadecanoic acid, ethyl ester (Internal Standard)		1
9,12-Octadecadienoic acid, methyl ester	C18:2	0.7349
9,12,15-Octadecatrienoic acid, methyl ester	C18:3	0.6559
Eicosanoic acid, methyl ester	C20:0	0.9090
Docosanoic acid, methyl ester	C22:0	0.8319
13-Docosanoic acid, methyl ester	C22:1	0.7880
Tetracosanoic acid, methyl ester	C24:0	0.7495

External standards were also used to monitor the GC-MS performance over time by injecting an external standard for each run of the GC-MS. Significant variations in RF for one run, compared with initial calibration values, announced that maintenance on the GC-MS was needed.

Sample Calculation:

The following sample calculation indicates the procedure utilized to calculate each FAME concentration after the sample had been analyzed in the GC-MS. Table 2.7 illustrates the resulting individual FAME concentrations, as well as the calculated “Total FAME” concentration found in a particular sample. The “Total FAME” extraction concentration is calculated by simple addition of all individual FAMES.

Table 2.7: Example of GC-MS results obtained from a particular sample, following by the calculated concentrations of each FAME.

Synonym	Retention T	Peak Area	Average RF	Calc. Conc. [µg FAME/L algal culture]
C14:0	9.34	591,293	0.9312	14.26
C16:0	12.49	103,630,295	0.9872	2357.19
C16:1	12.80	23,624,917	0.9109	582.39
C16:1	12.91	5,434,965	0.9109	133.98
C16:1	13.13	586,054	0.9109	14.45
C16:1	13.39	6,326,734	0.9109	155.96
C16:2	13.60	10,899,833	0.7442	328.88
C16:3	14.17	15,312,022	0.6720	511.65
C18:0	16.46	1,900,557	0.9649	44.23
C18:1	16.95	143,609,134	0.9261	3482.07
C18:1	17.10	3,640,645	0.9261	88.27
Int. Standard	17.29	7,125,349	1	-
C18:2	18.12	83,956,550	0.7349	2565.31
C18:3	18.94	15,991,238	0.6559	547.47
C18:3	19.92	58,296,380	0.6559	1995.80
C22:0	27.75	1,528,629	0.8319	41.26
			Total FAME Σ	12,863

Individual FAME concentrations were calculated utilizing Equation 2.3. As an example, C16:0 concentration present on the above table is calculated using the following parameters:

$V_s = 0.0125$ L; $A_s = 103,630,295$; $A_{is} = 7,125,349$; $\overline{RF} = 0.9872$; $D = 1$; $V_i = 1\mu\text{L}$;
 $C_{is} = 2,000$ mg/L. So

$$\text{Conc}[\mu\text{g} / \text{L}] = \frac{(A_s)(C_{is})(D)(V_i)}{(A_{is})(\overline{RF})(V_s)(1000)}$$

$$\text{Conc}[\mu\text{g} / \text{L}] = \frac{103,630,295}{7,125,349} \times \frac{2,000 \frac{\text{mg}}{\text{L}}}{0.9872} \times \frac{1}{0.0125\text{L}} \times 1\mu\text{L} \times \frac{1\text{L}}{10^6 \mu\text{L}} \times \frac{10^3 \mu\text{g}}{1\text{mg}}$$

$$\text{Conc}[\mu\text{g} / \text{L}] = 2,357 \frac{\mu\text{g}}{\text{L}}$$

GCMS Hardware and Temperature Program:

Analysis of methyl esters was performed on a GCMS with a H.P.-Innowax 15m polyethylene glycol column of 0.25 mm i.d., 0.50 film thickness, with an injection volume of $1\mu\text{l}$. The carrier gas (He_2) flow rate was 1.4ml min^{-1} with initial temperature of 120°C held 2 min, then increased 6°C min^{-1} to 180°C , $1.5^\circ\text{C min}^{-1}$ to 198°C , 5°C min^{-1} to 240°C , remaining constant for 8 minutes. Injection and transfer line temperatures were 250°C , while the Mass Spectrometry (MS) source temperature was 230°C , and MS quadrupole temperature was 150°C .

2.4 MICROSCOPIC INVESTIGATION

Calcein Acetoxymethyl (AM) and Propidium iodide (PI) (Invitrogen, Carlsbad, California) fluorescent molecular probes were utilized to confirm that the cytoplasmic membrane of algae was permeated by PEF treatment. The utilization of this microscopic

technique required the determination of *Ankistrodesmus falcatus* auto-fluorescence (to ensure that auto-fluorescence did not interfere with fluorescent probes), the effective development of a procedure to apply the molecular probes, and the final quantification of the resulting microscopic images. The following sections explain each of these areas.

2.4.1 Determination of Ankistrodesmus Auto-Fluorescence

Ankistrodesmus falcatus was found to possess two distinct fluorescent emissions. This specific strain of algae has auto-fluorescence emission at about 470 nm and 680 nm, which corresponds to the blue and red fluorescence of the visible light spectrum. Figure 2.20 illustrates these findings. Prior to explaining the methodology followed to obtain this result, a brief introduction to epifluorescence microscopy will be presented.

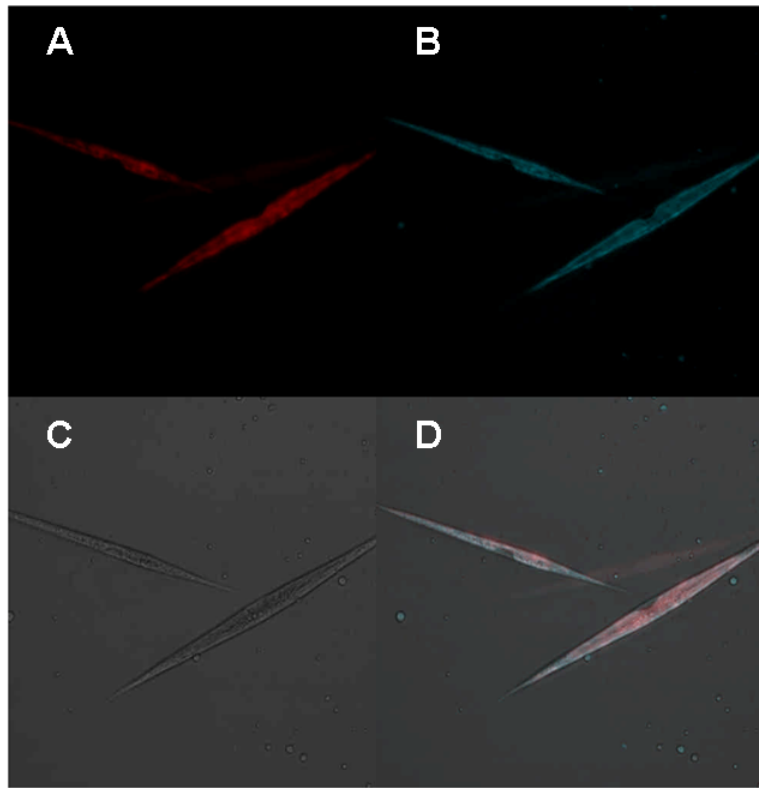


Figure 2.20: *Ankistrodesmus* has two auto-fluorescence regions at 470 nm and 680 nm, which corresponds to the blue and red fluorescence of the visible light spectrum, respectively. (A) illustrates *Ankistrodesmus* red fluorescence, (B) blue fluorescence, (C) illustrates a transmission image of this alga, and (D) illustrates an image of all channels combined.

Epifluorescence microscopy, colloquially synonymous to fluorescence microscopy, utilizes the capability of some molecules to become excited by absorption of light energy (excitation energy), emitting light of a lower energy and different color (emission energy). Some specimens contain molecules that will auto-fluoresce when irradiated, which is typically the case for chlorophyll-containing algae including *Ankistrodesmus*. The basic function of a fluorescence microscope is to irradiate the specimen with a desired and specific band of wavelengths, and then to separate the much weaker emitted fluorescence from the excitation light. In a properly configured microscope, only the emission light should reach the eye or detector, so that the resulting

fluorescent structures are superimposed with high contrast against a very dark (or black) background. Figure 2.21 shows the schematic of an epifluorescence microscope. The first key component of this apparatus is the light source. The light energy produced by the source goes through a wavelength selective excitation filter. Wavelengths passed by the excitation filter reflect from the surface of a dichromatic (also termed a dichroic) mirror through the microscope objective to cover the specimen with intense light. If the specimen fluoresces, the emission light gathered by the objective passes back through the dichromatic mirror and is subsequently filtered by a barrier (or emission) filter, which blocks the unwanted excitation wavelengths. All microscopic images and fluorescence information was obtained utilizing two main apparatus: (1) Confocal Microscope (Meta 510 Spectral Imaging, Zeiss, Germany) or (2) Spinning Disk Confocal and Epifluorescence Microscope (Olympus IX-71, Olympus).

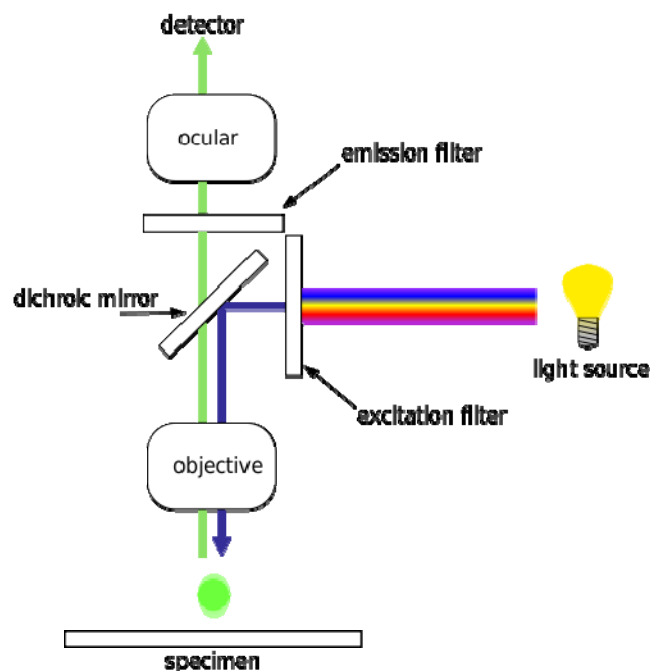


Figure 2.21: Schematic diagram explaining the fundamental component of an epifluorescence microscope.

The two auto-fluorescence emissions from *Ankistrodesmus* were found by systematically varying the excitation light source to which the algae was exposed to, and acquiring the emission signal at incrementally higher wavelengths. The excitation wavelengths allowed to contact the algae were: 458 nm, 477 nm, 488 nm, 514 nm, 543 nm, and finally 633 nm. Figure 2.22 exemplifies the signal acquisition for the 477 nm excitation experiment. This figure represents a montage of 29 images, each one recording emissions at a higher wavelength. It can be observed that the algae present on the images show a clear signal of algae on images 1 through 2 and 17 through 21, indicating two auto-fluorescence regions for *Ankistrodesmus*.

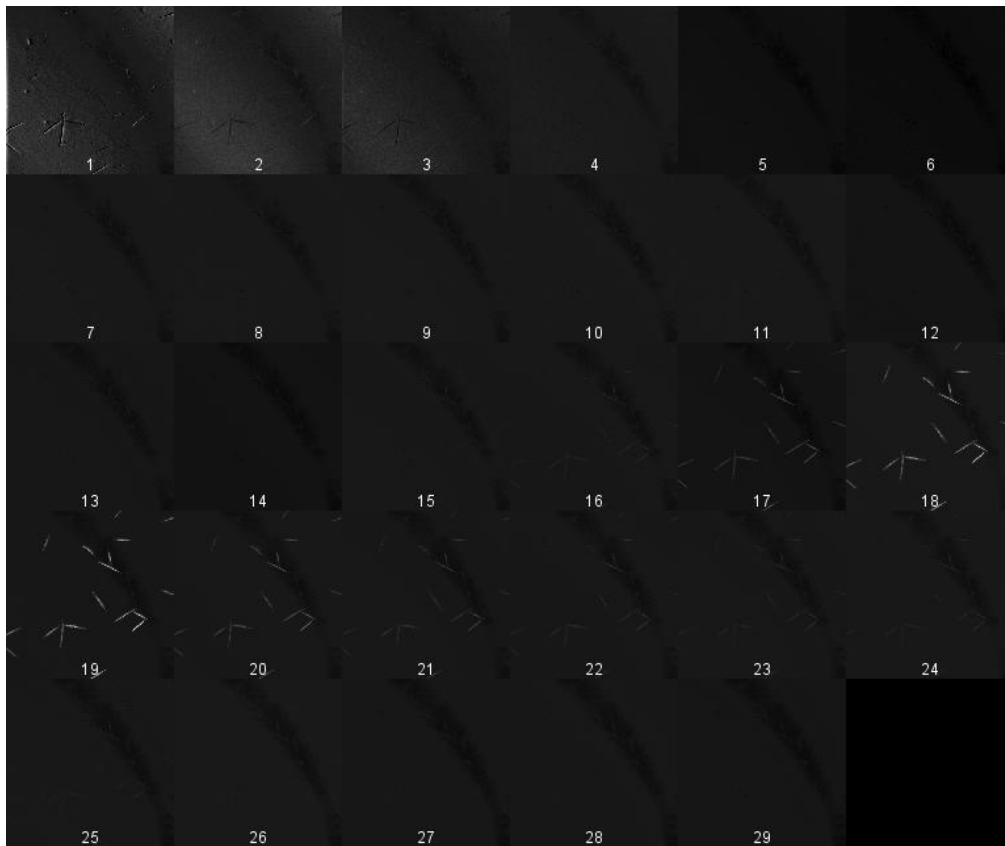


Figure 2.22: Montage of images emitting a signal at higher wavelengths. The excitation wavelength utilized for this montage was of 477 nm. This montage illustrates the regions of auto-fluorescence for *Ankistrodesmus*: images 1-2 (470-490 nm emission) and 17-21 (660-700 nm emission).

Figure 2.22 presents results obtained when utilizing a single excitation wavelength, i.e., 477nm. The other excitation wavelengths available - 458nm, 488nm, 514nm, 543nm, and finally 633nm – were utilized to generate similar montage results. Utilizing computer software, all resulting images were analyzed in order to locate the emission regions generated from each excitation wavelength. The intensity of the fluorescent signals obtained were normalized by assigning a value of 1 to the highest signal generated by the cell and compared against a low value of 0, which corresponded to the background of the image with no signal. Values ranging from 1 (max) to 0 (min) were obtained throughout the entire emission spectrum. All these values were collected and plotted. Figure 2.23 illustrates the information obtained, which shows the presence of two auto-fluorescence regions for this specific strain of algae. These auto-fluorescence regions needed to be effectively determined prior to the utilization of molecular probes.

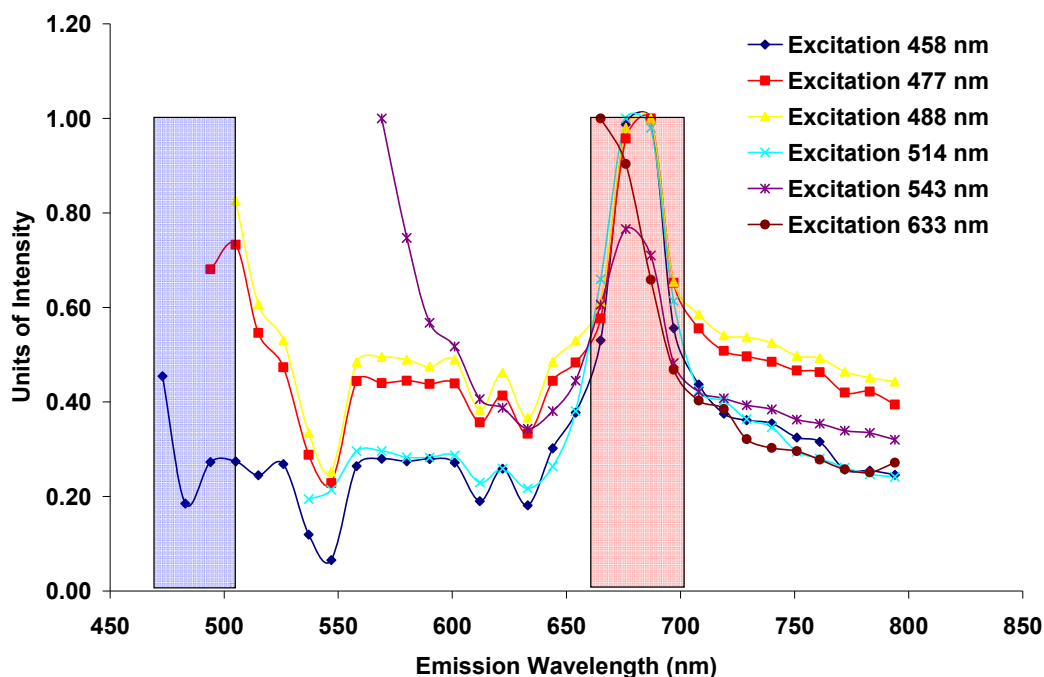


Figure 2.23: The systematic collection of emission wavelength signals associated with multiple excitation wavelengths (458 nm, 477 nm, 488 nm, 514 nm, 543 nm, and 633 nm) produces the above spectrum, proper of *Ankistrodesmus* algae strain. These spectrums indicate the presence of two (2) auto-fluorescence regions. The first region emits its fluorescence approximately 475-500 nm (light blue region), while the second region emits its energy approximately in the 675-700 nm (red region).

2.4.2 Molecular Probes: Live/Dead Assay

Calcein AM, also referred to as the live stain, is a membrane-permeable dye that is used to determine cell viability. This molecule is originally in an uncharged state, so it migrates thru the lipid bilayer membrane without damaging it. Once inside the cell, Calcein AM is converted into Calcein, by cleaving of the lipophilic blocking group by nonspecific esterases and at this point it displays a green fluorescence when excited (excitation 496, emission 510-530). This molecular probe labels a healthy microorganism, where “healthy” is strictly associated with the integrity of the cellular membrane. Cells with a compromised membrane are not able to retain the Calcein stain in the cytoplasm and do not fluoresce.

PI labels dead organisms. PI emits fluorescence on the red spectrum (excitation 533, emission 605-635), if and only if, it has been able to bind with intercellular DNA and RNA. Opposite from Calcein AM, PI is a membrane-impermeable dye. PI fluoresces only in the presence of a compromised membrane thru which it can diffuse and bind to the cell's nucleic acids. In this study, Calcein AM and PI were utilized simultaneously in order to label the healthy population, as well as the dead population.

After having successfully characterized *Ankistrodesmus* auto-fluorescence, the different emission regions of this strain of algae are known. With this information, it was possible to confirm that Calcein AM and PI would not significantly overlap with any auto-fluorescence signal. Table 2.8 summarizes the excitation and emission regions of the live/dead assay, as well as the algal auto-fluorescence.

Table 2.8: Excitation and Emission regions proper of *Ankistrodesmus*' auto-fluorescence, PI molecular stain, and Calcein molecular stain.

Fluorescence Source	Excitation [nm]	Emission [nm]
Blue Auto-Fluorescence	Any wavelength lower than the Emission	470 - 490
Red Auto-Fluorescence	Any wavelength lower than the Emission	680 - 700
PI	533	605 – 635
Calcein	496	510 - 530

Specific Procedure to loading the probes

Multiple experiments were performed in order to obtain optimal imaging quality of the molecular probes. Factors that were tested were Calcein AM concentration, PI concentration, loading time, loading temperature, etc. Table 2.9 summarizes the parameters yielding best results.

Table 2.9: Loading of Calcein AM and PI into Ankistrodesmus was effectively achieved by following this parameters.

Algae Staining Parameter	Parameter Specification
Calcein AM loading concentration	80 μ L calcein per mL algal suspension
Calcein AM loading time	2 hrs
Calcein AM incubation temperature	29°C
Washing step to eliminate excess Calcein AM from background	3 times washing with fresh media
PI loading concentration	2 μ L PI per mL algal suspension
PI loading time	10 minutes

The final live/dead staining procedure is included in the next section.

2.4.3 Algae Staining Procedure Calcein AM and Propidium Iodide (PI) Staining of Algae - Procedure

Calcein AM (1 mg/mL solution in anhydrous DMSO) and PI (1 mg/mL solution in H₂O) were purchased from Invitrogen and utilized to determine if the algal membrane was permeated by PEF treatment. Chemostats were sampled, and 50 mL was concentrated by two centrifugation steps at 3500 rpm for 10 minutes to a final volume of 4mL in a 15mL test tube. At this cell density, 320 μ L of Calcein AM was added to reach a concentration of 8×10^{-5} mmoles/mL of algal suspension. Then the test tube was wrapped with aluminum foil to avoid light degradation, and it was incubated 2 hours at 29°C in a water bath. Afterwards, the excess stain was washed away by performing the following steps three times: resuspending the stained cells with new media up to the 15mL mark, centrifuging the sample for 10 minutes at 4,000 rpm, and pouring off the supernatant to a final volume of 4mL. 10 minutes prior to the desired pretreatment test, add 2 μ L of PI per mL of algal suspension. At this point, the stained algae cells were

ready for pretreatment and subsequent fluorescence imaging. The Standard Operational Procedure for fluorescence staining can be found in Appendix A.

Exemplification of desired results

The following figures exemplify the desired fluorescent images to be obtained when: (i) live, healthy algae possess an intact membrane, (ii) algae have a compromised membrane.

Figure 2.24 shows five different channels, describing healthy algal cells: (A) represents Calcein AM channel, where the live dye has diffused into the microorganism's cytoplasm; (B) shows the transmission channel, indicating the morphological shape of *Ankistrodesmus*; (C) represents the PI channel, which shows no signal (as expected); (D) describes the blue auto-fluorescence' (470-490 nm emission); and finally (E) illustrates a superimposition of all previously mentioned channels (Channels A-D).

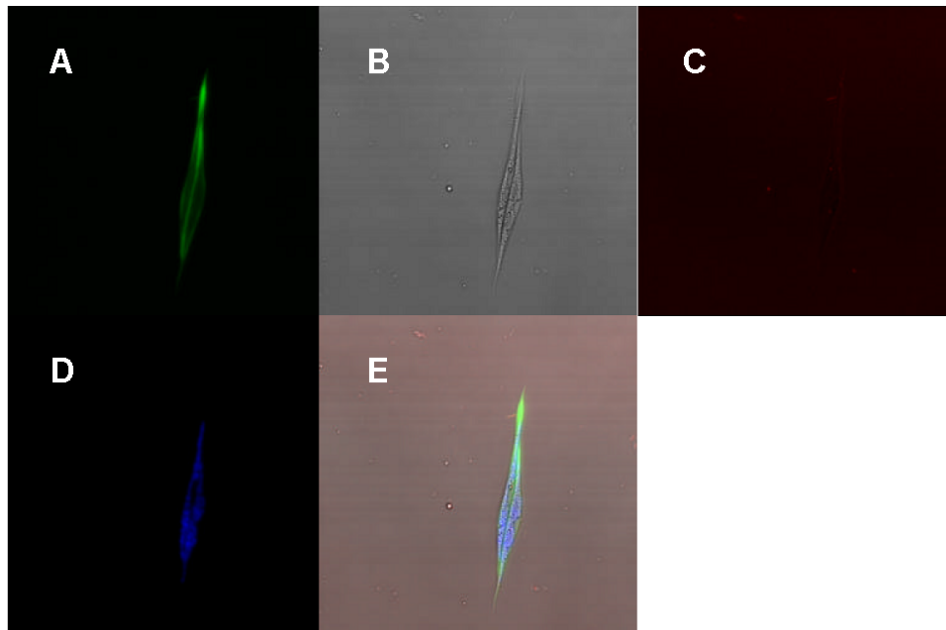


Figure 2.24: Multiple images of two healthy algal cells, describing the desired results of Calcein AM and PI when exposed to microorganisms, whose membranes have not been compromised. (A) Calcein channel, (B) transmission image, (C) PI channel, (D) auto-fluorescence channel, and (E) a superposition of all previously mentioned channels.

Figure 2.25 illustrates the resulting images obtained after live and dead molecular probes have been loaded into solution, and the microalgae's membrane has been permeated. For this example, ethanol was added to the labeled microorganisms. Ethanol is commonly known to disrupt the cellular membrane. Channel (A) shows no Calcein AM present, since this dye was able to leach out of the cell thru the permeated membrane; (B) indicates the transmission obtained from this image; (C) shows PI bounded to DNA and/or RNA inside the cytoplasm; channel (D) shows the blue auto-fluorescence of *Ankistrodesmus*; and finally (E) illustrates all previous channels being superimposed.

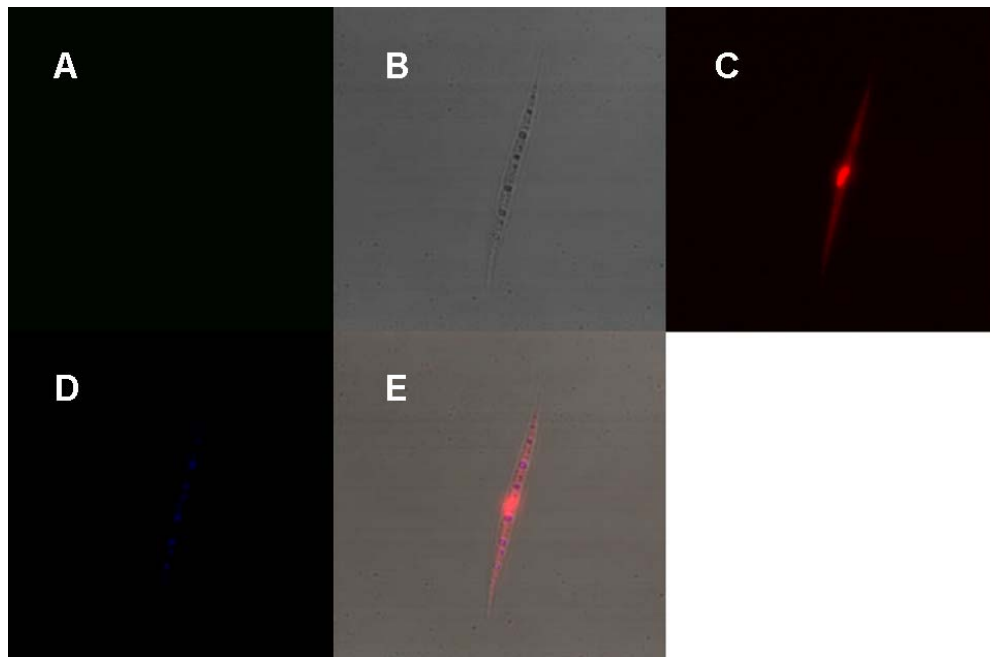


Figure 2.25: Multiple images of a single healthy algal cell, describing the desired results of Calcein AM and PI when exposed to a microorganism, whose membrane have been compromised. (A) Calcein channel, (B) transmission image, (C) PI channel, (D) auto-fluorescence channel, and (E) a superposition of all previously mentioned channels.

2.4.4 Determination of Population Viability after PEF Treatment

The live/dead fluorescent assay provided the capability of determining the effect of PEF pretreatment on the algal membrane. If PEF was effective at permeating the lipid bilayer, the algal population would clearly show PI presence in their nuclei. In case the voltage potential was not capable of damaging the membrane, then the live stain would still be present throughout the population.

Multiple algal samples were concentrated and stained following the procedure described in Section 2.4.3. Samples were divided into controls and treatments, and the different pretreatments were performed. Each experimental group to be analyzed was repeated in triplicate. In order to visually monitor the pretreatment's effect and efficiency, the fluorescent channels presented in Figure 2.25 were recorded. Each sample was analyzed by preparing three 10 μ L-slides. Three random areas in each slide were chosen, and twenty five (25) adjacent images were recorded per area. After all images associated with each different sample were recorded, the population viability was determined by visually counting the number of dead and live cells on each image.

References Cited in CHAPTER 2

1. Bazhal, M.; Vorobiev, E., Electrical treatment of apple cossettes for intensifying juice pressing. *Journal of the Science of Food and Agriculture* 2000, 80 (11), 1668-1674.

CHAPTER 3

RESULTS & DISCUSSION

3.1 Comparison of solvent extraction efficiency and kinetics with chloroform-based and ethyl acetate-based solvent systems

Bligh & Dyer is the most widely cited lipid extraction method, and its CHCl_3 -MeOH solvent mixture has long been known to be extremely efficient at extracting lipids from biological systems ¹. However, its inherent toxicity has prompted significant research efforts to develop a green alternative for industrial scale process application ²⁻⁴. We suggest the utilization of EtOAc as a greener alternative to CHCl_3 due to its lower environmental impact, and the significantly lower health risk associated with it ⁵. The results of this section compare the extraction efficiency of these two solvents with respect to their total lipid extraction and rate of extraction.

Total Algal Lipids Extraction Efficiency

Total algal lipid extractions were performed by contacting the CHCl_3 -based and EtOAc-based solvents to wet biomass for 24hrs while mixing was being applied (see Chapter 2, Section 2.2.5 for procedure). The extraction results represent each system's ability to recover lipids and are compared to establish an efficiency reference point.

Figure 3.26 compares the total lipid extraction efficiency of the chloroform-modified B&D method, where CHCl_3 is the main solvent, versus the ethyl acetate-modified B&D method, where EtOAc is the main solvent. Multiple experimental runs similar to the results presented in Figure 3.26 confirmed that EtOAc-based system has a lower efficiency for extracting algal lipids from *Ankistrodesmus falcatus* after 24 hrs compared to the CHCl_3 -based system. The EtOAc procedure had an 83-88% efficiency in

all replicates, compared to the CHCl_3 procedure which for this experiment obtained an average lipid extraction of 3,700 $\mu\text{g/L}$.

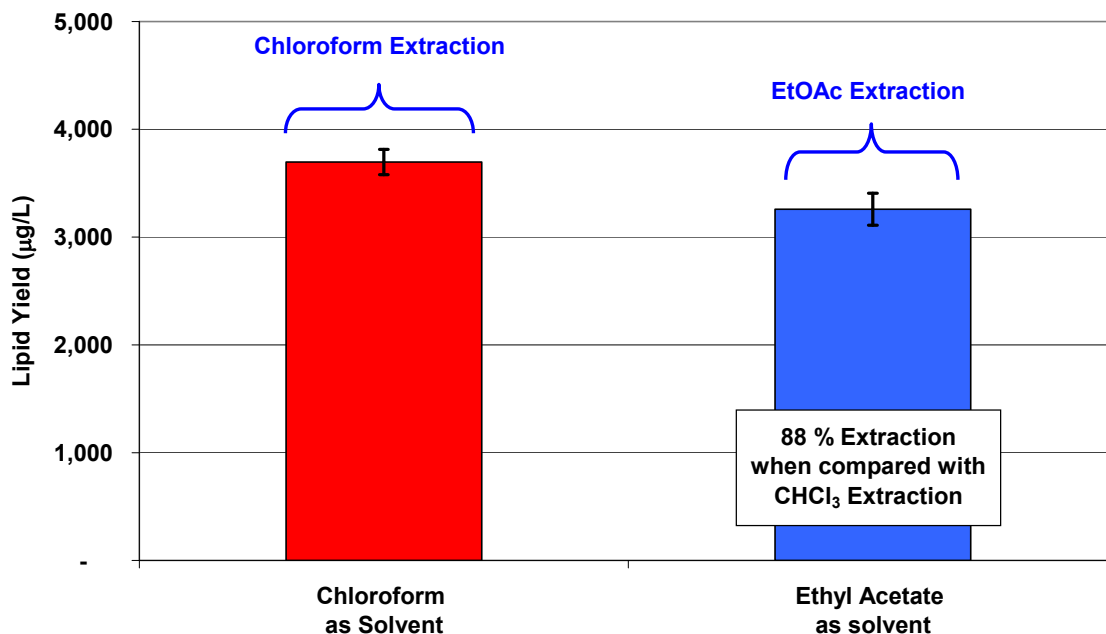


Figure 3.26: The utilization of EtOAc as a green solvent to extract algal lipids from *Ankistrodesmus falcatus* after 24-hr contact proved to perform 83-88% as efficient when compared to CHCl_3 . Results corresponds to average of triplicate samples \pm 90% Confidence Interval (CI).

The lower extraction efficiency compared to chloroform has been observed with many other suggested alternative solvents. Table 3.10 puts into perspective our substitution attempt with respect to other recent ones. Some of the alternative solvents investigate include ethanol, hexane, isopropanol, acetone, and multiple combinations. Their extraction efficiencies when compared against chloroform have broadly ranged between 90-15%. Our suggested EtOAc-based extraction ranks as one of the most efficient alternatives.

There are two possible explanations that have been explored for solvent having a lower efficiency than chloroform: (i) thermodynamics of lipid extraction, and (ii) ineffective contact between solvent-lipid to produce desired mass transfer.

Table 3.10: B&D (CHCl₃/MeOH/H₂O 1:2:0.8 v/v/v) is the most widely cited lipid extraction method. Due to chloroform's health and environmental concerns, multiple solvent mixtures have been investigated as alternatives. Most of the known alternatives do not perform as efficiently as chloroform-based solvent.

Solvent System	Type of Biomass	% Efficiency compared to B&D method	Ref.
Ethanol/H ₂ O, 96:4 v/v	<i>Isochrysis Galbana</i>	90%	3
EtOAc/MeOH/H ₂ O, 2:1:0.8 v/v/v	<i>Ankistrodesmus falcatus</i>	83-88%	*
Hexane/ethanol, 1:2.5 v/v	<i>Isochrysis Galbana</i>	85%	3
Ethanol/H ₂ O, 96:4 v/v	<i>Synechocystis</i>	76%	4
Hexane/isopropanol, 3:2 v/v	<i>Botryococcus braunii</i>	69%	2
Dichloroethane/EtOH, 1:1 v/v	<i>Botryococcus braunii</i>	65%	2
Acetone/dichloromethane, 1:1 v/v	<i>Botryococcus braunii</i>	65%	2
Dichloroethane/MeOH, 1:1 v/v	<i>Botryococcus braunii</i>	62%	2
Hexane/ethanol, 1:2.5 v/v	<i>Synechocystis</i>	62%	4
Hexane/isopropanol, 3:2 v/v	<i>Synechocystis</i>	17%	4
Isopropanol only	<i>Synechocystis</i>	15%	4

* Results presented in this thesis.

One possible thermodynamic explanation for the extraction inefficiency of EtOAc-based system could be the solubility limit. Had extracted lipids reached the maximum solubility in EtOAc-MeOH, no enhancement in lipid recovery to CHCl₃-levels could be achieved. Literature solubility limits of three model TAGs in multiple solvents, including CHCl₃ and MeOH, are presented in Table 3.11. Combined, these model TAGs represent 40% of the total lipids recovered from *Ankistrodesmus falcatus*, making them important compounds of reference in terms of solubility. The lipid extractions that we have observed in EtOAc-MeOH are 0.011-0.059 µg Lipid/mL_{solvent mixture}, while in CHCl₃-MeOH they have been 0.013-0.067 µg Lipid/mL_{solvent mixture}. Even though the literature solvent systems presented in Table 3.11 are not exactly identical to our experimental systems, they also represent important reference points regarding saturation

limits. For instance, solubility of trimyristin, and tripalmitin in CHCl_3 -MeOH (2:1) is greater than 40mg/mL for each lipid model, while our experimental system of CHCl_3 -MeOH (1:2) only achieves concentrations as high as 0.067mg/mL. This significant difference in concentration suggests that extractions in our system are not near solubility limits, and that other factors are determining the limits of extraction. Similarly, our lipid extraction in EtOAc-MeOH system (2:1) is significantly lower than tristearin's solubility in pure EtOAc. Thus for EtOAc extraction, the inability to perform as effectively as CHCl_3 cannot be explained by solubility limits. Further confirmation of this can be done by performing laboratory solubility experiments in solvent systems identical as the ones described in this contribution.

Table 3.11: Maximum solubility of selected lipids in organic solvents (mg/mL). TAG concentrations are reported in an attempt to understand if solubility limits have been reached, possibly explaining the observed extraction inefficiencies of the EtOAc-based system.

TAGs solubility limits reported in literature							
TAGs	Synonym	C_6H_{14}	CHCl_3	CHCl_3 - MeOH 2:1	EtOAc	Acetone	MeOH
Trimyristin	3*C14:0	>40.0	>40.0	>40.0	n/a	4.01	0.04
Tripalmitin	3*C16:0	5.84	>40.0	>40.0	n/a	0.22	0.01
Tristearin	3*C18:0	1.04	>40.0	12.89	36.7 [£]	<0.001	0.11
Total TAG extracted concentrations found in our extractions							
TAGs	Synonym	C_6H_{14}	CHCl_3	CHCl_3 - MeOH 1:2	EtOAc- MeOH 2:1	Acetone	MeOH
Total from <i>Ankistrodesmus</i>	n/a	n/a	n/a	0.013- 0.067	0.011- 0.059	n/a	n/a

All solubility values were obtained from Schmid et al.⁶, unless otherwise noted.

[£] Solubility value obtained from Hoerr et al.⁷ at approximately 35 °C.

Another possible thermodynamic explanation for the inefficiency of EtOAc-based system observed in Figure 3.26 could be drawn by comparing the solvation power of both systems. This qualitative approach, also exemplified by the like-dissolve-like rule,

essentially tries to describe the polarity and molecular attractive forces of solvents and/or solutes. The polarity of a solvent can be characterized by its *dipole moment* and *dielelectric constant*, while the molecular attractive forces are described by the *Hildebrand's solubility parameter* (δ), and *H-Bonding*⁸. In evaluating these parameters a significant difference between the EtOAc-MeOH and CHCl₃-MeOH systems could help explain the lipid extraction discrepancy observed.

Table 3.12 presents these chemical properties of solvents, solvent mixtures, and a model TAG⁴. A general rule of thumb for the δ *Parameters* estimates that compounds more than 3.4 units apart will not be miscible. The presented model TAG ($\delta=17.44$) and chloroform-based solvent ($\delta=25.80$) are more than 8 units apart. It would be expected to find immiscible characteristics between two compounds. However, as presented earlier (Table 3.11), these two systems are highly soluble, contradicting the δ *Parameter* thermodynamic approach. Also, in regards to *dipole moment*, it was shown that CHCl₃, with a value of 1.155, is favorable dissolving TAGs, while MeOH (1.623) does not. The small difference between the two extremes in solubility makes it impossible to draw significant conclusions about observed solubility inefficiencies, specifically when all solvents' *dipole moments* are so close to each other (1.155 – 1.85). Consequently, based on the properties evaluated in

Table 3.12, it is doubtful that these properties represent a reliable trend at explaining the inefficiency of ethyl acetate to recover higher algal lipids when compared to CHCl₃-MeOH system.

Table 3.12: Chemical properties of solvents, solvent mixtures, and TAG. Original obtained from Sheng et al.⁴

	Dipole moment (Debye)	Solubility Parameter* (J/cm ³) ^{0.5}	H-Bonding (J/cm ³) ^{0.5}
Solvents			
Hexane	0	14.71	Poor
Isopropanol	1.615	22.81	Poor
Butanol	1.521	21.95	Poor
Chloroform	1.155	18.79	NA
Ethyl Acetate	1.831	18.06	Moderate
Methanol	1.621	30.23	Strong
Ethanol	1.55	26.12	Strong
Water	1.85	23.5	Strong
Solvents Combinations ‡			
CHCl ₃ -MeOH 2:1		22.56 ‡	
CHCl ₃ -MeOH-H ₂ O 1:2:0.8		25.80 ‡	
EtOAc-MeOH-H ₂ O 2:1:0.8		22.48 ‡	
TAG			
3*C16:0	1.71	17.44	4.90

‡ *Hilderbrand's solubility parameters* for multiple solvents is calculated by using the volume fraction of each component as follows: $\delta(\text{mixture}) = \varphi_1\delta_1 + \varphi_2\delta_2 + \dots$ φ is the volume fraction of a mixture component 1 or 2, is the Hinderbrand solubility parameter for each compound.

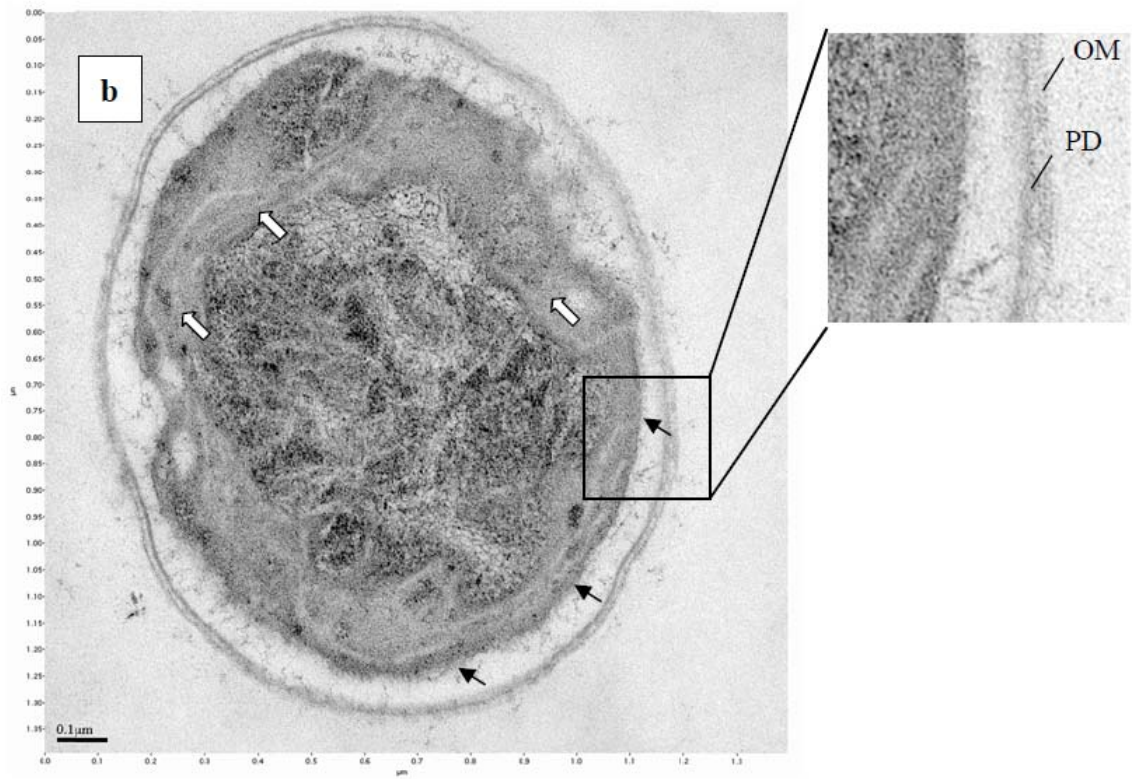
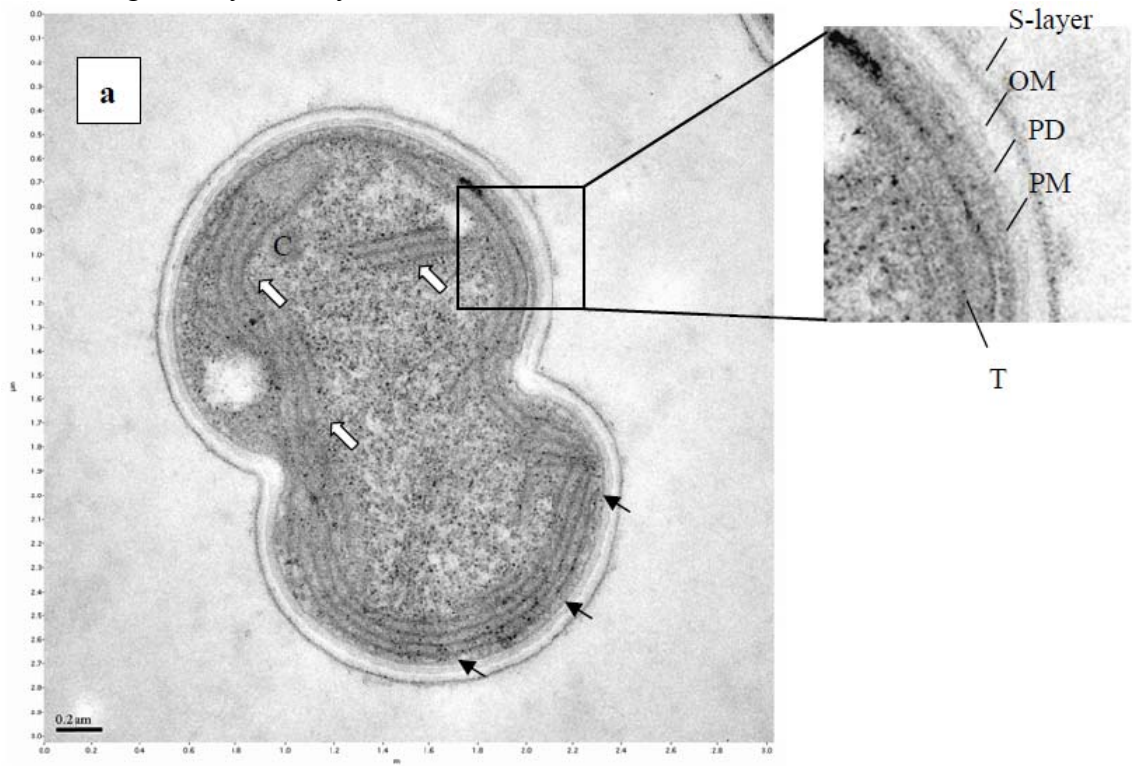
Another possible explanation for the higher lipid recovery with the CHCl₃-based system (Figure 3.26) could be related to a more successful penetration and destruction of intracellular membranes by this chlorinated solvent. Recently, Sheng et al.⁴ investigated this hypothesis by obtaining TEM images of the Cyanobacteria *Synechocystis PCC 6803* before and after several extractions with different solvents. Chloroform-Methanol and

isopropanol-only were two of the solvent mixtures investigated in their research. Figure 3.27a, b, and c, taken by Sheng et al.⁴, show the images of the microorganism before the extraction, after Chloroform-Methanol extraction, and after isopropanol extraction, respectively.

Figure 3.27a presents a TEM image of a healthy Cyanobacteria cell, detailing the different layers that make up its wall and membrane. Similar to *Ankistrodesmus falcatus*, *Synechocystis* cells possess a thick cell wall and cell membrane, through which solvents are required to permeate in order to reach the storing lipid bodies. Figure 3.27b demonstrates the effects of Chloroform-Methanol extraction, which has completely dissolved the outer S-layer. Sheng et al. stated that even though the outer membrane and the Peptidoglycan layer were still identifiable, other inner layers (thylakoid membranes) were severely disrupted, indicating an efficient penetration of Chloroform-Methanol inside the cell. This effective penetration was hypothesized to be a main factor at obtaining the highest lipid extraction among multiple solvents, which also included isopropanol. On the other hand, isopropanol-only extraction obtained a 17% efficiency at recovering lipids when compared to chloroform (Table 3.10). Figure 3.27c shows the corresponding *Synechocystis*' structure after contact with this solvent. This image indicates that the cell membrane layer has been only mildly damaged, while inner membranes (intracellular thylakoid membranes) were still well aligned, thus indicating the inefficiency of isopropanol to penetrate inside the cell and extract the lipids. The results of Sheng et al. show that the macroscopic lipid extraction discrepancy correlated with the degree of wall damage, membrane damage, and intracellular organelles disruption. These microscopic observations indicate that the solvent penetration

capabilities, which create a better lipid-solvent contact, directly affect the extraction efficiency. The differences in the ability of the solvents to facilitate membrane destruction could also be the reason for the inefficiencies observed in the suggested ethyl acetate-based system. Although more efficient than isopropanol at extracting algal lipid, it is possible that EtOAc shows the same poor cell penetration ability as isopropanol. Further confirmation of this should be obtained by comparing TEM images of *Ankistrodesmus falcatus* pre and post extraction with the suggested EtOAc-based solvents, specifically looking for incomplete cytoplasmic and intracellular membrane disruption.

TEM Images of Synechocystis:



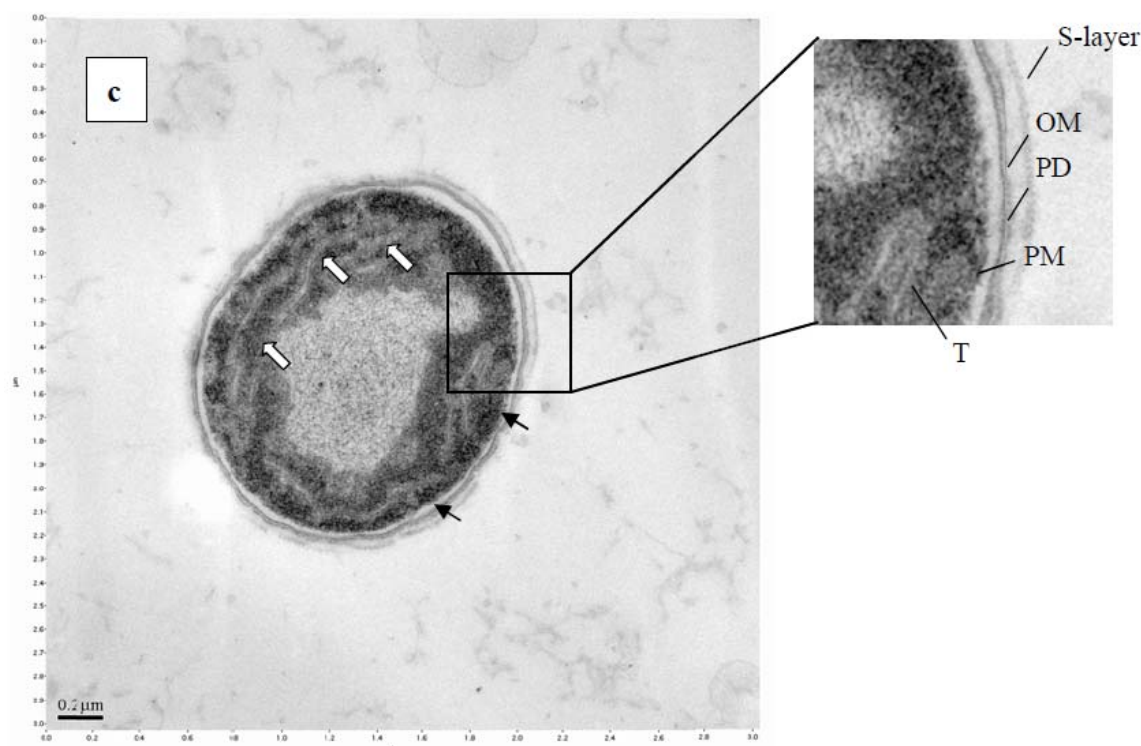


Figure 3.27: Original image obtained from Sheng et al. ⁴. TEM image of *Cyanobacteria Synechocystis* cells before, and after, solvent contact in order to compare the different effects of these solvents to the microorganism's structure. Comparison between an intact healthy cell with no solvent contact (a), cell residual after CHCl_3 -Methanol extraction (b), and isopropanol extraction (c). Black arrows indicate the cytoplasm membrane. White arrows show disruption and loss of thylakoid membrane. OM: Outer membrane; PD: Peptidoglycan layer; PM: plasma membrane; T: thylakoid membranes; C: carboxysome.

Kinetics of Extraction

In order to effectively characterize the extraction behavior of EtOAc as a greener solvent, it was critical to determine how fast EtOAc could reach its highest lipid removal, and also to determine how it compared to the traditional CHCl_3 extraction. Thus, 24-hr kinetics of extraction experiments were performed for both solvent systems. For these experiments, the solvent-biomass contact time was closely monitored and timed, and extraction samples of progressively longer exposures (up to 24-hrs) were collected and analyzed (See Chapter 2, Section 2, 2, 5 for procedures).

Figure 3.28 represents the 24-hr kinetics of extraction for the chloroform-based system (B&D). Even though the contact between solvent and biomass is progressively increased, no strong signs of additional extraction are obtained after the 10th hour of biomass-solvent contact. Algal lipid extraction from *Ankistrodesmus falcatus* utilizing CHCl₃-MeOH as the main solvents does not show any time dependency during the final period. While making a closer analysis at this figure, it could be argued that CHCl₃ shows an increasing extraction between the 2-6 hr period, followed by an extraction decrease. In order to address this possible trend, a reduced 6-hr kinetics of extraction study was repeated and the results are illustrated in Figure 3.29.

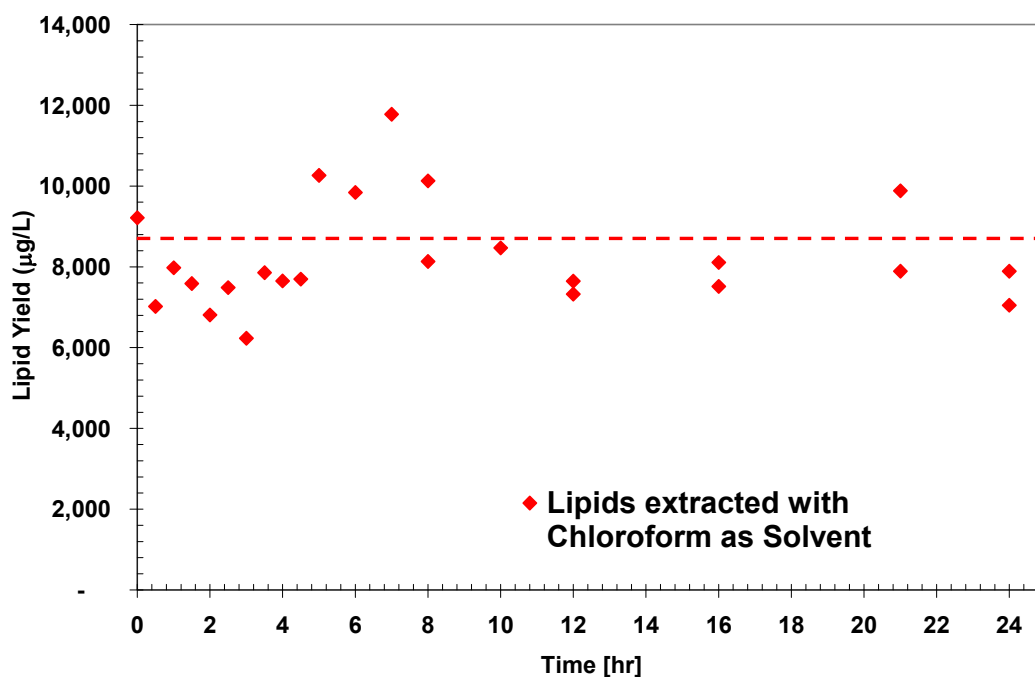


Figure 3.28: 24-hr kinetics study analyzing the extraction rate of the chloroform-modified B&D method, where CHCl₃ acts as the main solvent. This technique showed no time dependency at recovering the algal lipids from the wet-biomass. Figure 3.29 shows a simplified experiment, where only the first 6hrs were investigated.

Figure 3.29 confirms that during the initial 6-hr kinetics of extraction experiment, CHCl₃ does not have any time dependency for extracting the algal lipids. Chloroform-

based extractions obtained after short biomass-solvent contact time displayed the same lipid recovery as extraction after 6 or 24 hrs of solvent-biomass exposure.

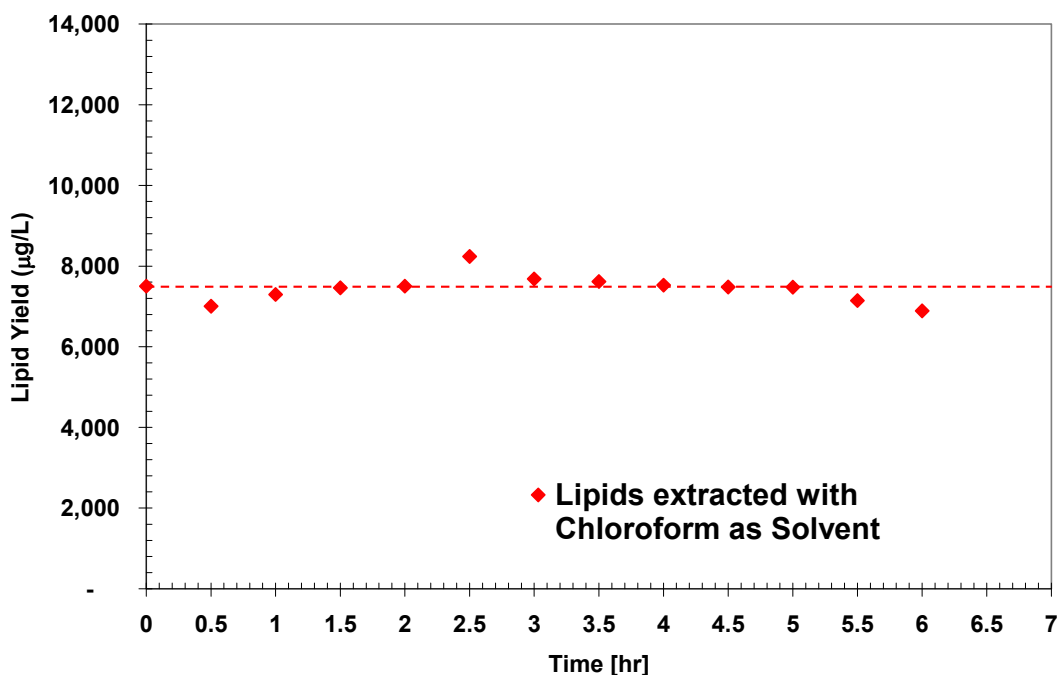


Figure 3.29: 6-hr kinetics study analyzing the extraction rate of the “chloroform-modified” B&D method, where CHCl_3 acts as the main solvent. This experiment, in conjunction with Figure 3.28 confirms that this system shows no time dependency at recovering the algal lipids from wet-biomass.

The lack of time dependency for extracting lipids demonstrated by these results, in conjunction with the observed efficiency of CHCl_3 -MeOH at penetrating the cytoplasm and intracellular membranes, implies that this solvent system breaks up these membranes with great ease, speed, and efficiency.

In regards to the suggested EtOAc-modified B&D method, Figure 3.30 illustrates the 24-hr kinetics of extraction for this greener system. The lipid extraction observed with brief solvent-biomass contact time is significantly lower than with extended exposure to the solvent. The time dependence for lipid recovery occurs during the initial 4 hours of

exposure, with a plateau for the remainder of the 24hr period, suggesting that a maximum recovery has been reached.

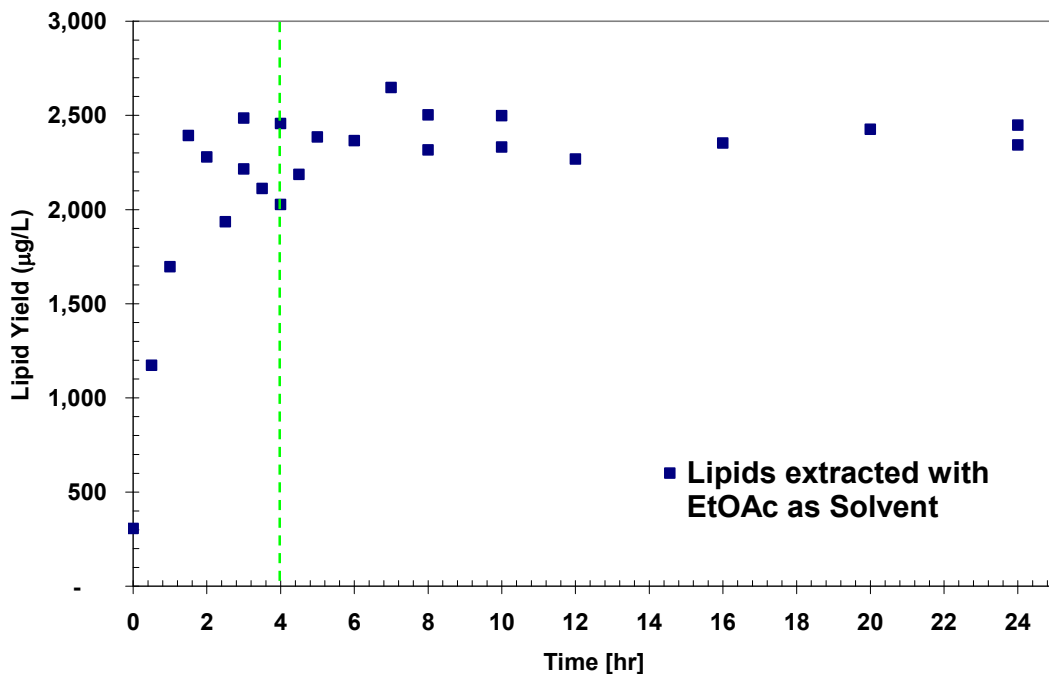


Figure 3.30: 24-hr kinetics study analyzing the extraction rate of the ethyl acetate-modified B&D method, where EtOAc acts as the main solvent. This technique showed that a minimum of 4 hours are required to recover the algal lipids from the wet-biomass.

A shortened 6-hr kinetics of extraction experiment with EtOAc was also performed. This reproduction confirmed the increase of lipid extracted at longer biomass-solvent exposure. This time, approximately 2 hours were needed to reach maximum recovery (data not shown).

In contrast to fast acting CHCl_3 , EtOAc-modified B&D method shows a significant time dependency for extracting lipids from wet biomass. Similar to EtOAc's inefficient extraction of total lipids, poor cell membrane disintegration could also be the reason for this slow extraction rate. It could be possible that EtOAc not only penetrates the cell membrane ineffectively, but it also dissolves the cell membrane slowly,

generating this distinct time dependency. With this in mind, it is hypothesized that EtOAc's extraction efficiency and/or time to maximum algal lipid extraction could be enhanced by more successful cell membrane permeation.

To definitely determine if EtOAc is not capable of quickly penetrating the cell wall and cytoplasmic membrane of *Ankistrodesmus falcatus*, collection of TEM images would again be needed. In addition to comparing the structure prior and post extraction, the relationship between degree of membrane/organelle penetration and time of contact should be studied.

Recent applications of cell disrupting treatments prior to solvent contact have demonstrated extraction efficiencies higher than those obtained by CHCl₃-only^{9, 10}. In general, selection and application of any cell disrupting pretreatment will be based on its efficiency at enhancing solvent-lipid contact, as well as the resulting lipid recovery enhancement. Furthermore, energy requirements related to any pretreatment will be a critical parameter to minimize if the production of algal fuel is to have a feasible industrial scale application. This next section explores the utilization of PEF technology as a cell-membrane disrupting pretreatment to intensify solvent-lipid contact and extraction.

3.2 PEF Application to Ankistrodesmus falcatus: Increase in Membrane Permeability validated with Fluorescent Microscopy

This contribution suggests the novel application of PEF as an algal membrane disrupting pretreatment to intensify solvent lipid extraction. Due to the novelty of this application, an electrical circuit capable of delivering the high voltage electric field in a pulsed mode needed to be developed in house. The results of this section utilize molecular probes and fluorescent microscopy to determine if the in-house-built apparatus successfully compromises *Ankistrodesmus falcatus* cell membrane.

Calcein AM (green fluorescence) and Propidium Iodide (PI) (red fluorescence) are the two molecular probes utilized to ascertain if the in-house-built apparatus successfully permeates the cell membranes. Calcein AM is a membrane permeable stain that labels all healthy cells, while PI is a membrane impermeable dye that labels cells, whose membranes have somehow been ruptured. The images presented below represent the different treatments and controls analyzed to determine if the apparatus is successfully working (see Chapter 2, Sections 2.4 for procedures)

Figure 3.31 shows a sample epifluorescence image of pre-stained *Ankistrodesmus falcatus* population taken out of the chemostat. This sample represents the negative control state. The Calcein fluorescing cells (green channel) illustrate that the vast majority of the algal population is healthy, with completely intact cytoplasmic membranes. The PI fluorescing cells (red channel) signify the naturally dead algae present in chemostats. These compromised cells have experienced degradation of their membrane which allowed contact of the cytoplasmic interior with the bulk media. The fraction of dead cells in Figure 3.31 is extremely low, representing only 3% of the entire

population. This low percentage characterizes a normal population viability of algal growth.

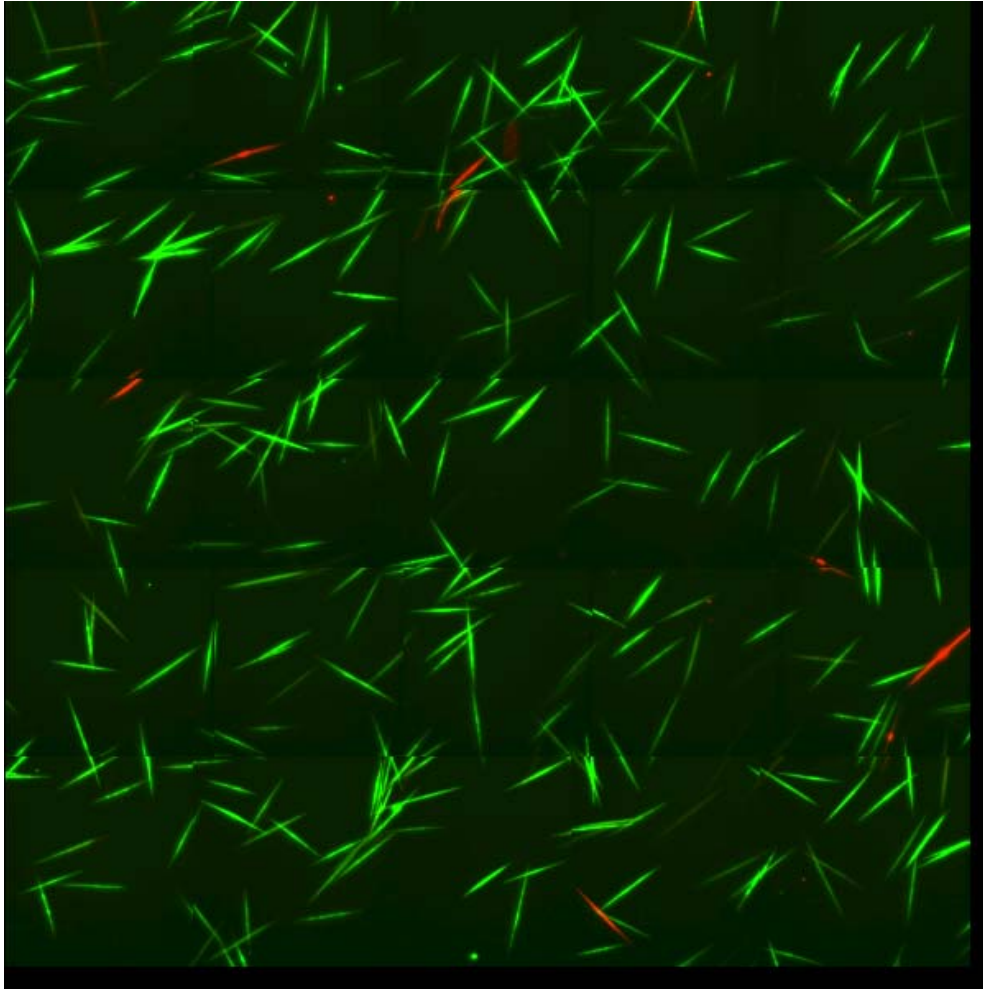


Figure 3.31: Epifluorescence microscopy images of *Ankistrodesmus falcatus* population prior to any pretreatment (Negative Control) indicate the healthy state of most of the algal cells. Calcein fluorescing cells (green channel) signify that their cytoplasmic membranes are intact. On the other hand, PI fluorescing cells (red channel) indicate that these cells are dead. The red fluorescing strictly indicates that the cytoplasmic membranes of these cells have been permeated, allowing bulk fluid to penetrate into the cells.

The PEF apparatus always treated wet algal biomass in a batch mode. The introduction of electrical energy into the algal suspension created a significant temperature increase up to 70°C. This high temperature alone is known to produce

significant heat stresses to the cell, causing the disruption of the cytoplasmic membrane¹¹. In order to avoid this high final temperature, a heat sink was utilized to absorb some of the heat produced by the electrical energy. This removal of heat translated into a reduced high temperature of 50°C (see Chapter 2, Section 2.2.4, Figure 2.8 for more details). In order to decouple the effects of this new temperature profile and the effects produced by the electric field, two separate sample sets were acquired and analyzed. The first set was exposed to only the temperature profile associated with PEF by mimicking its temperature swing, while the second sample was treated with the actual PEF (and associated temperature increase).

Figure 3.32 shows the results obtained from *Ankistrodesmus falcatus* when the batch sample was exposed only to the temperature profile (no electric field applied). The fraction of dead cells in Figure 3.32 represents only 4% of the entire population, strongly resembling the results obtained in the negative control. These observations demonstrate that the temperature stresses associated with the PEF treatment (50°C max temperature) are not significant to produce cell lyses.

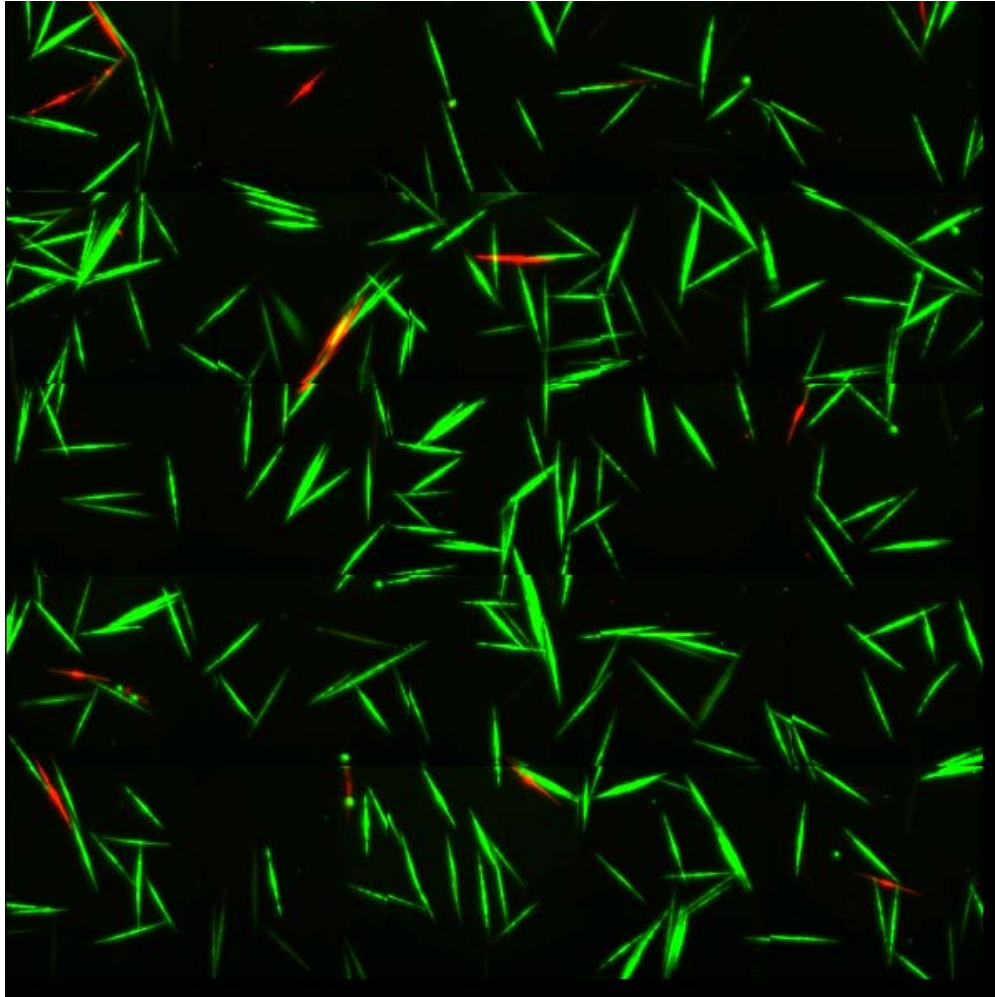


Figure 3.32: An experimental artifact of PEF treatment in a batch system is a temperature increase of the treated media. This *Ankistrodesmus* population has only been exposed to the temperature swing associated with PEF pretreatment (no electric field was applied). This image indicates that the temperature stresses have not induced any cytoplasmic membrane permeation. This algae population exposed to temperature stresses is as healthy as the negative control population shown on Figure 3.31.

In contrast to the previous images, Figure 3.33 represents an algal suspension treated with PEF. The vast majority of the population has been labeled with PI. Since PI is a membrane impermeable molecular probe, which only becomes fluorescent if bounded to cells' DNA and RNA, it can be concluded that the PEF pretreatment causes an effective increase in membrane permeability.

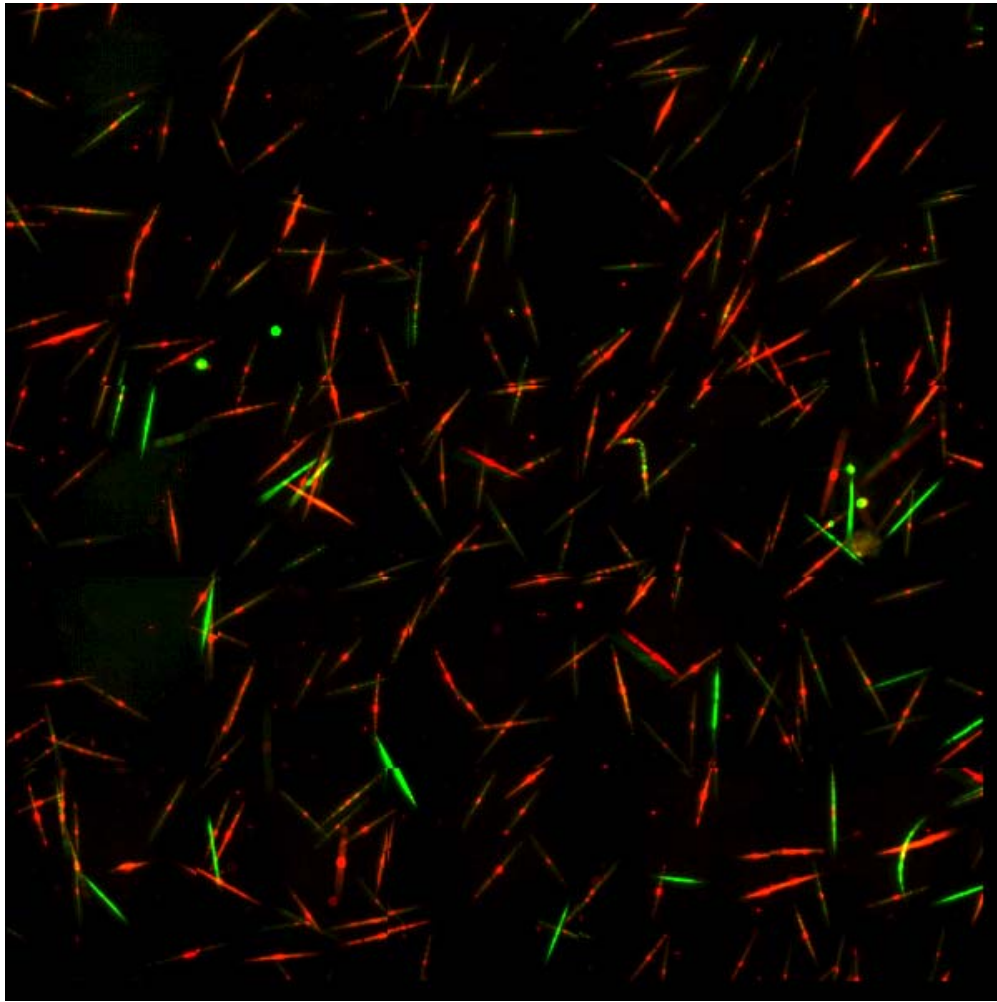


Figure 3.33: This *Ankistrodesmus* population was exposed to PEF treatment. The epifluorescence image clearly indicates that the vast majority of the algal population has had their cytoplasmic membranes irreversibly permeabilized due to the electrical pulses. The PI fluorescing cells (red channel) have seen bulk media fluid freely penetrate inside the cells.

In order to quantify the efficiency delivered by the electroporation unit disrupting algal membranes and lysing the wet biomass, an eye-count of the microscopy images was performed. Figure 3.34 provides the population viability of the three samples presented earlier, showing the distinct degree of effectiveness obtained by the PEF treatment at permeating the algal membrane in wet samples. The exposure to the electric field delivered by the in-house-built unit disrupted the cell membrane of 90% of the entire

population, while the associated exposure to temperature stresses and the negative control only showed a population with 4% and 3% disrupted membranes, respectively.

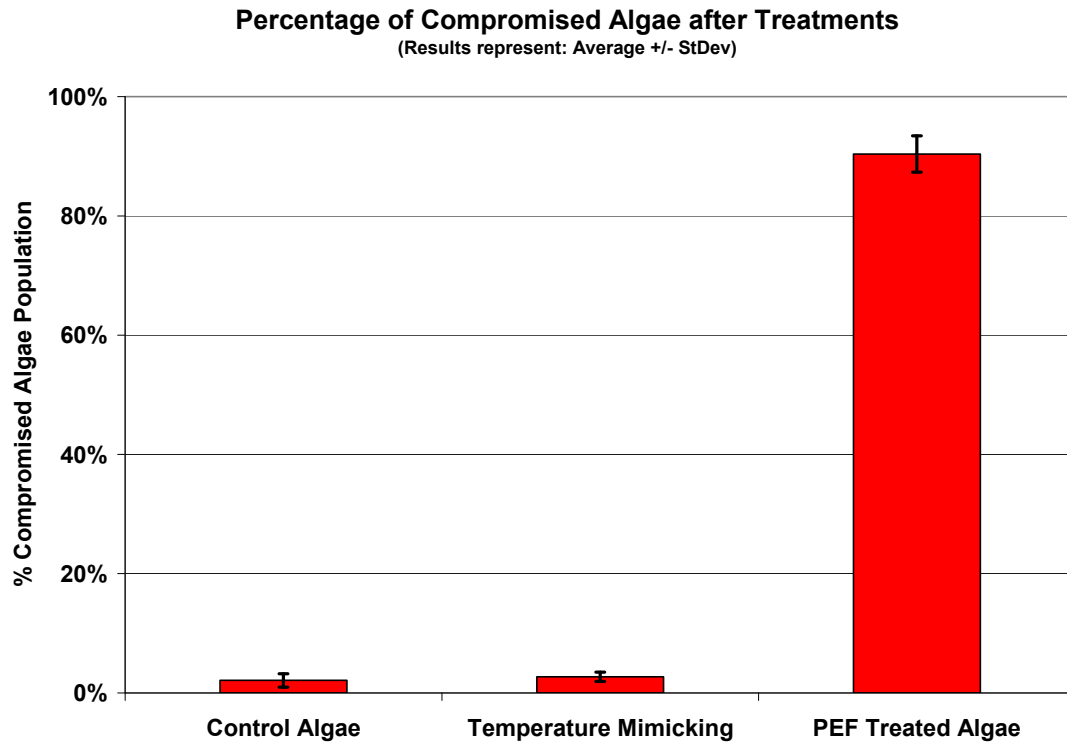


Figure 3.34: Cell viability of the previously shown images (Figure 3.31, Figure 3.32, and Figure 3.33) was determined by eye-count. The PEF pretreatment resulted into an extremely effective technique to permeate the algal membranes, allowing fluid to rush inside the cell. These results clearly show that the electric field associated with our PEF treatment is the reason behind membrane permeation; not temperature stresses.

By utilizing fluorescent microscopy, it has been demonstrated that the in-house-built PEF apparatus effectively increases membrane permeability of *Ankistrodesmus falcatus*. This successful application of electroporation to wet algal biomass allows non-denaturalizing media to permeate through the cell wall and cytoplasmic membrane to finally obtain access to intracellular organelles that before were not accessible with a healthy cell. In this sense, application of PEF pretreatment might enhance the lipid

recovery of solvents with apparent membrane penetrating limitations, as appeared to be the case for isopropanol⁴ and our own suggested ethyl acetate-modified B&D method.

3.3 Application of PEF as an intensification treatment for solvent lipid extraction

Once the concept of wet algal biomass treatment with PEF had been effectively demonstrated with our in-house-built apparatus, the research focus turned into the application of this technique to intensify solvent extraction of lipids. This section explores the utilization of PEF as a possible intensification pretreatment, capable of increasing membrane permeability. This increase in permeability could translate into an enhancement in solvent-lipid contact, resulting in higher and/or faster recovery of lipids.

To evaluate the effect of PEF as a pretreatment, kinetics of extraction studies with EtOAc-based solvents were repeated (see Chapter 2, Section 2.2.5). This time, non-treated samples were compared against electroporated samples. Figure 3.35 presents a 12-hr kinetics of extraction for the ethyl acetate-based system, with and without prior PEF treatment. It must be noted that this pretreatment consisted of an application of PEF to only a fraction of the total volume (25%). As previously observed for this system, the extracted lipids gradually increased as the solvent-biomass contact time increased. This was the case observed for both sets of data, showing similar time dependency.

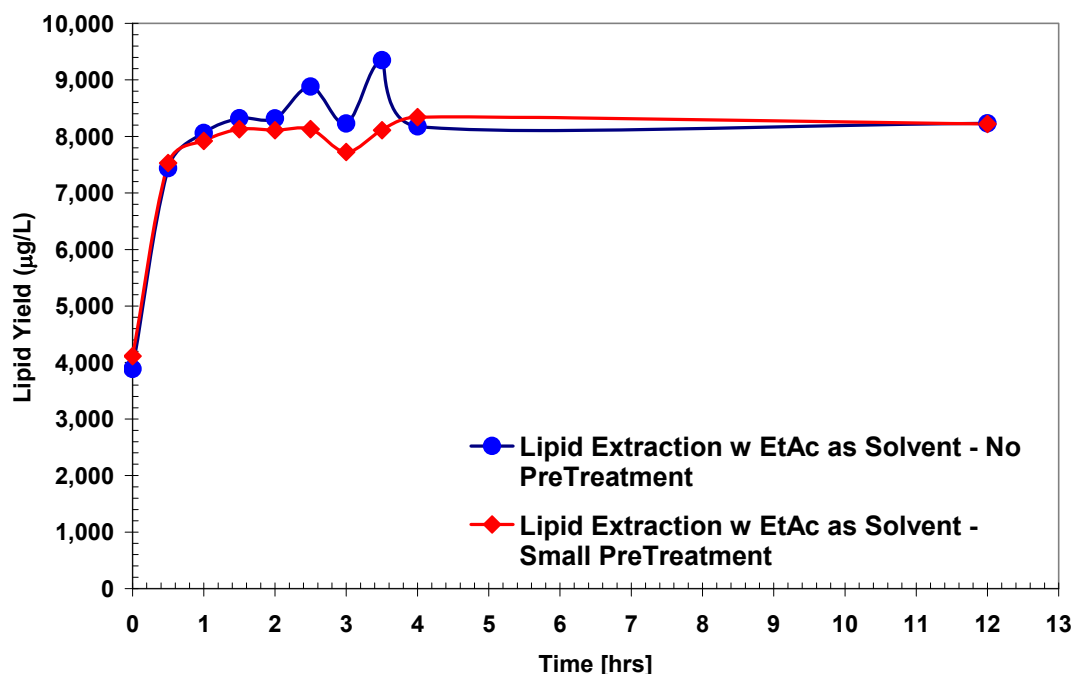


Figure 3.35: Application of PEF to a fraction of the wet biomass attempted to intensify the extraction. The small electroporation pretreatment did not show any indication of lipid recovery intensification.

The application of PEF treatment to a fraction of the algal suspension did not translate into any extraction intensification. Both experiments showed the same initial extraction level, the same gradual extraction gain at longer contact time, and the same final total extraction. While application of PEF was demonstrated to increase membrane permeability of treated cells, it is possible that the intensification obtained in the reduced volume was not enough to deliver macroscopic intensification results. Therefore, treatment of the complete volume prior to solvent extraction needed to be performed.

Figure 3.36 shows the results of a kinetics of extraction study in which the entire volume of algal suspension was exposed to PEF prior to solvent extraction. Two main observations regarding these new results are: (i) PEF did not enhance the recovery of total lipids, however (ii) a significant extraction increase was observed at $t = 0$ (t_0).

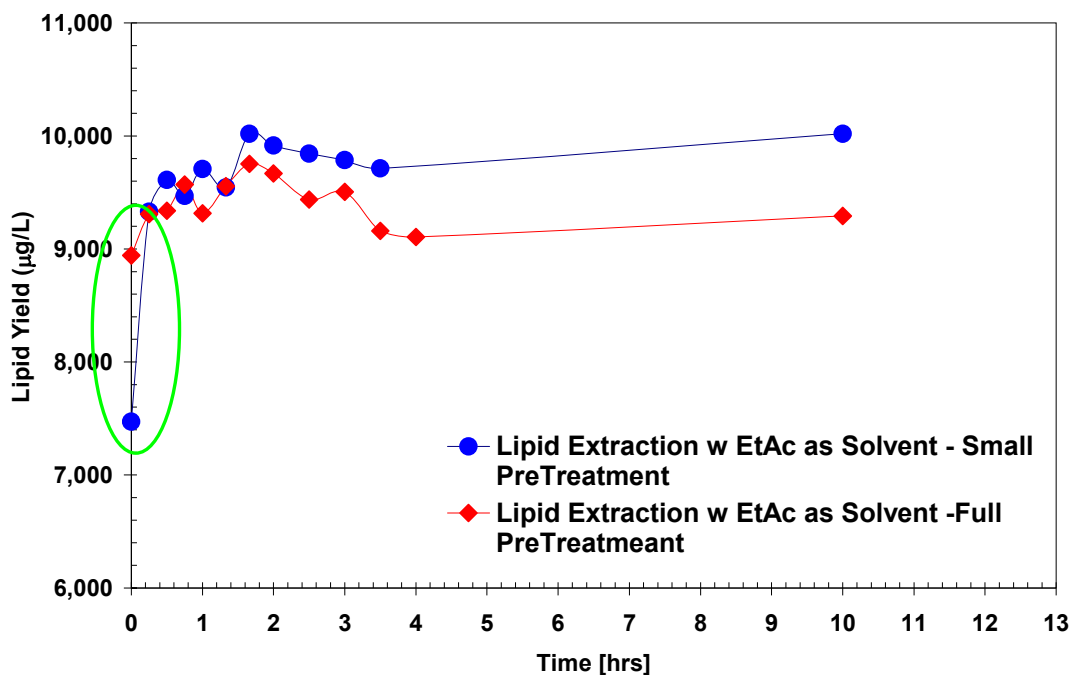


Figure 3.36: This time, the entire volume of wet algal biomass was exposed to the PEF treatment prior to solvent extraction (Full PreTreatment). Even though the total lipid extraction did not show indications of recovery improvement, the rate of extraction of the fully pretreated system did indicate faster recovery at time $t = 0$ (t_0).

Despite the application of PEF to the entire algal suspension prior to solvent contact, no increase in total extraction was achieved. This observation puts into questions the degree and depth of cell disruption obtained by PEF treatment. Even though microscopy demonstrated that PEF allows external bulk fluid to penetrate inside the cytoplasm, it is possible that this treatment is only limited to superficial deterioration of the cytoplasmic membrane. In this sense, physical barriers located deeper inside the cell, such as membranes enclosing lipid bodies, might not be affected by this pretreatment.

The other important observation from Figure 3.36 indicated a significant lipid extraction increase at t_0 associated with the fully pretreated sample. The sample exposed to PEF obtained close to 25% gain in lipid extraction at t_0 . This trend suggests that an accelerated extraction rate was obtained due to the increase in membrane permeability.

To further investigate this intensification, several t_0 -extractions were performed and compared. The experiments included CHCl_3 -based extractions at t_0 , and EtOAc-based extractions at t_0 with and without PEF pretreatment. The chloroform extraction data represented a point of reference in terms of global efficiency, while the non-pretreated extraction was considered as the negative control. An important point that must be taken into account is the temperature of contact between the algal biomass and the solvent. As it was previously mentioned, the introduction of electrical energy as part of the PEF pretreatment generated significant temperature rise in the algal suspension. In terms of mass transfer, the system temperature plays a critical role, since the lipid mass transfers rate is directly related to the system's temperature. Moreover, to truly determine any possible intensification of solvent lipid extraction due to membrane permeability produced by PEF pretreatment, it was imperative that the treated sample and its corresponding negative control share the same biomass-solvent contact temperature. This requirement guarantees that if any intensification of lipid recovery is obtained, it will be due to the exposure to the electric field, and not due to the associated increase in temperature.

Figure 3.37 shows the effect of PEF pretreatment on the extraction of lipids with EtOAc-based solvent (biomass-solvent contact temperature of 35°C) at t_0 . Application of a PEF pretreatment resulted in a significant increase of lipid extraction for the EtOAc-based solvent when compared against the negative control, effectively reproducing the results observed in Figure 3.36.

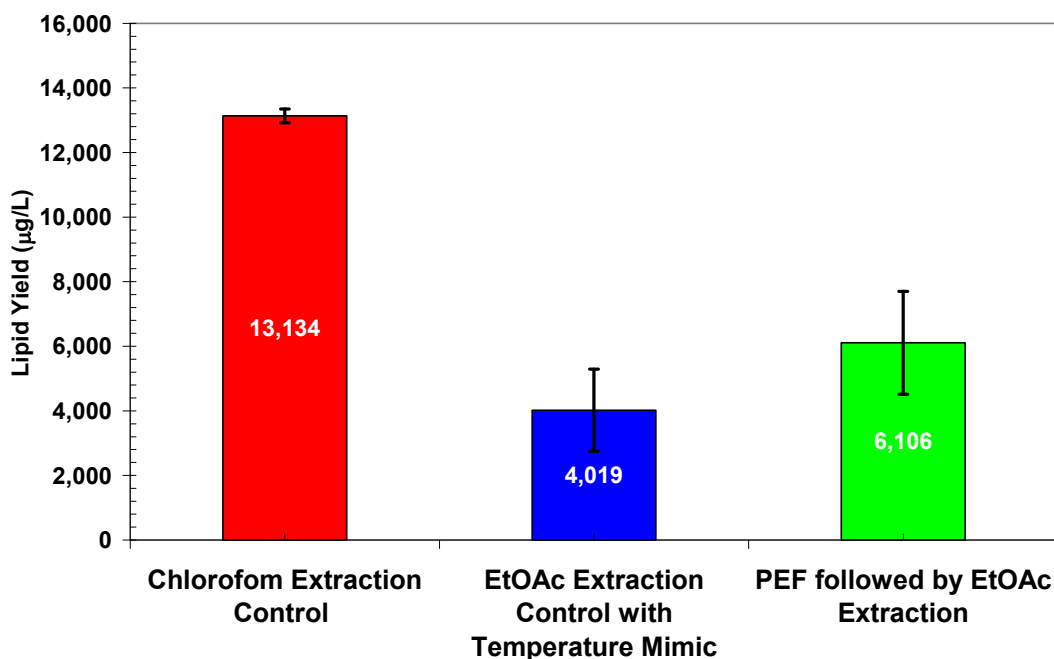


Figure 3.37: Research efforts were focused at investigating the apparent extraction intensification observed at time t_0 due to PEF pretreatment. All these results were obtained at t_0 . Wet biomass contacted the solvents at the same elevated temperatures (35°C) observed after electroporation to obtain temperature consistency. Ethyl acetate extractions with prior PEF pretreatment (green column) did indicate significant extraction rate intensification, when compared to the ethyl acetate control (blue column). Chloroform extraction was plotted for total extraction reference. Results correspond to average of triplicate $\pm 90\%$ confidence interval.

Similar to Figure 3.37, the results presented in Figure 3.38 confirm the t_0 enhancement of lipid extraction after PEF application, this time with a solvent-media contact at 20°C . The similarities between Figure 3.37 and Figure 3.38 prove that the solvent-biomass contact temperature is not the cause for this improvement.

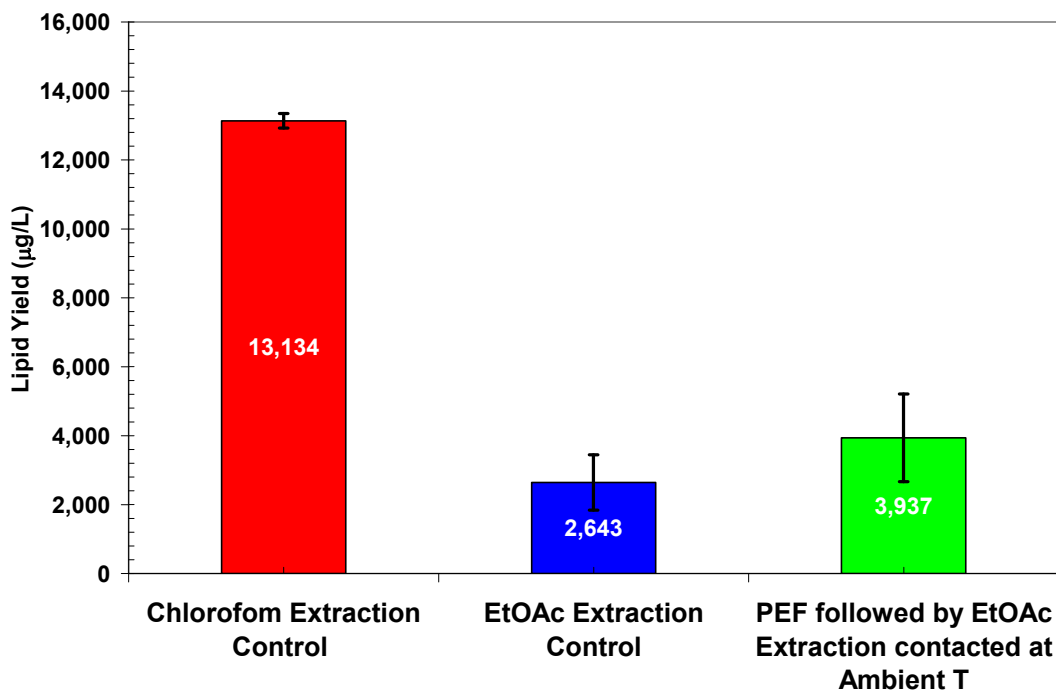


Figure 3.38: Was the temperature increase associated with the electrical pretreatment the reason behind the observed extraction intensification? For this set of results the all wet biomass contacted the solvents at ambient temperature. Wet biomass exposed to PEF pretreatment did indicate consistent extraction intensification at t_0 . Chloroform extraction was plotted for total extraction reference. Results correspond to average of triplicate \pm 90% confidence interval.

The results shown in Figure 3.37 and Figure 3.38 provide support to the already suggested hypothesis that an increase in membrane permeability facilitates an easier and therefore faster solvent-lipid contact. In the specific case of EtOAc, the permeation of the cytoplasmic membrane by the PEF, allows EtOAc to reach the lipid bodies faster. This is why its original time dependency is reduced at t_0 .

Furthermore, the increase in lipid extraction at t_0 obtained by PEF application supports the idea that EtOAc's time dependency is in fact driven by its slow dissolving capabilities of the cell cytoplasmic membrane, and with PEF assistance it can be shortened.

References Cited in CHAPTER 3

1. Schmid, P., Extraction and purification of lipids: II. Why is chloroform-methanol such a good lipid solvent. *Physiol. Chem. Phys* 1973, 5, 141-150.

2. Lee, S.; Yoon, B.; Oh, H., Rapid method for the determination of lipid from the green alga *Botryococcus braunii*. *Biotechnology Techniques* 1998, 12 (7), 553-556.
3. Molina Grima, E.; Robles Medina, A.; Gimenez Gimenez, A.; Sanchez Perez, J. A.; Garcia Camacho, F.; Garcia Sanchez, J. L., Comparison between extraction of lipids and fatty acids from microalgal biomass. *Journal of the American Oil Chemists' Society* 1994, 71 (9), 955-959.
4. Sheng, J.; Vannela, R.; Rittmann, B., Evaluation of Methods to Extract and Quantify Lipids from *Synechocystis* PCC 6803. *Bioresource Technology* 2010.
5. Koller, G.; Fischer, U.; Hungerbuhler, K., Assessing safety, health, and environmental impact early during process development. *Ind. Eng. Chem. Res* 2000, 39 (4), 960-972.
6. Schmid, P.; Hunter, E., Extraction and purification of lipids. I. Solubility of lipids in biologically important solvents. *Physiol. Chem. Phys* 1971, 3, 98-102.
7. Hoerr, C.; Harwood, H., The Solubility of Tristearin in Organic Solvents. *The Journal of Physical Chemistry* 1956, 60 (9), 1265-1269.
8. Kerton, F., *Alternative solvents for green chemistry*. Royal Society of Chemistry: 2009.
9. Ranjan, A.; Patil, C.; Moholkar, V., Mechanistic Assessment of Microalgal Lipid Extraction. *Industrial & Engineering Chemistry Research* 2010, 49 (6), 2979-2985.
10. Lee, J.; Yoo, C.; Jun, S.; Ahn, C.; Oh, H., Comparison of several methods for effective lipid extraction from microalgae. *Bioresource Technology* 2010, 101 (1), S75-S77.
11. Madigan, M.; Martinko, J.; Dunlap, P.; Clark, D., *Brock biology of microorganisms* (2009). San Francisco: Pearson Benjamin Cummings.

CHAPTER 4

CONCLUSIONS & RECOMMENDATIONS FOR FUTURE WORK

4.1 Conclusions

The main two objectives of this work were: (i) the evaluation of EtOAc as a greener substitute for chloroform for algal lipid extraction and (ii) the preliminary investigation of PEF as a cell-membrane permeating pretreatment to intensify the solvent-lipid contacting and therefore extraction of these lipids.

To effectively benchmark EtOAc as an alternative solvent, it, together with chloroform, was evaluated and compared. In contrast to CHCl_3 , EtOAc was found to be a less efficient and also a slower solvent for extracting algal lipids from *Ankistrodesmus falcatus* wet biomass. A possible explanation for these inefficiencies was hypothesized to be its poor membrane disintegrating capabilities, resulting in a limited solvent penetration inside the cell.

Utilization of PEF as a membrane disrupting pretreatment to enhance solvent recovery of lipids was investigated, focusing on the inefficiencies presented by the EtOAc-based system. The novel application of PEF to *Ankistrodesmus falcatus* wet biomass suspension resulted in mixed conclusions. Although no increase in total lipid extraction was achieved, a significant enhancement in the rate of lipid recovery was demonstrated. This crucial intensification shows the PEF application to be a valid enhancement treatment that warrants further investigation. These and other conclusions are outlined below:

- Chloroform-based B&D method was shown to perform better than our suggested ethyl acetate-based B&D at extracting lipids. EtOAc-based system only performed 83-88% as efficient when compared to CHCl₃-based system.
- CHCl₃-based extraction proved to be an extremely fast acting solvent, recovering the algal lipids instantly once in contact with the wet biomass. No time dependency was observed during 24 hour kinetic studies using *Ankistrodesmus falcatus*.
- In contrast to CHCl₃, the suggested EtOAc-based lipid extraction exhibits a distinct time dependency at extracting algal lipid from *Ankistrodesmus falcatus*. Multiple replicates of kinetics of extraction experiments showed that EtOAc can take up to 4 hours before reaching maximum lipid recovery.
- Through the use of molecular labeling dyes in conjunction with epifluorescence microscopy, the utilization of the in-house-built Pulsed Electric Field (PEF) apparatus was shown to effectively increase the membrane permeability of *Ankistrodesmus falcatus*. The PEF apparatus was able to effectively permeate up to 90% of the algal population. This gain in cytoplasmic membrane permeability facilitated the penetration of previously excluded bulk media into the cells' cytoplasm gaining access to intracellular organelles.
- The utilization of PEF as a novel cell membrane disrupting pretreatment followed by contact with EtOAc-based solvent intensified the rate at which algal lipids were extracted from *Ankistrodesmus falcatus*. PEF application significantly accelerated the extraction of lipids at t_0 . This finding suggests that EtOAc's time dependency is generated by slow cell membrane disintegration. With the increase in membrane permeability, EtOAc is allowed to penetrate inside the cell more rapidly and obtain faster lipid extraction. However, even with this strong indication of better solvent penetration

associated after PEF pretreatment, no signs of total lipid extraction intensification were observed.

4.2 Recommendations for future Work

The results obtained in this investigation encourage additional work in developing PEF technology as a cell disrupting pretreatment and in the utilization of EtOAc as an alternative substitute of lab-scale CHCl_3 -based extraction. Although this investigation focused mainly in preliminary feasibility studies with experimental emphasis, future research must also converge on the fundamental reasons behind EtOAc inefficiencies at obtaining CHCl_3 -level extractions, as well as exploring specific enhancement produced by PEF as a pretreatment. These and other recommendations for future work are included below:

- Lipid solubility studies in CHCl_3 -based systems as well as EtOAc-based systems should be performed to conclusively determine that lipid solubility limits in the solvents have not been reached, and that solubility limits are not the reasons for inadequate lipid extraction.
- Poor ability of EtOAc at disintegrating the cytoplasmic membrane and other layers could negatively affect the solvent-lipid contact, and consequently lipid extraction. TEM images should be obtained to determine the actual efficiency of EtOAc at disintegrating *Ankistrodesmus falcatus* structural layers. These studies should focus on visually characterizing the different biological barriers (e.g. cytoplasmic membrane, cell wall, others) associated with this algal strain, comparing images prior and post solvent extraction. This information could provide critical insight to understand the causes for EtOAc inefficiency, which could be utilized to effectively design intensification processes.

- Similar to total lipid extraction, poor and slow membrane disintegration could be the cause for EtOAc's time dependency at extracting lipids. Obtaining TEM images to analyze the degree of membrane disruption/disintegration as a function of contact time could provide valuable insight of the microscopic limitations of EtOAc.
- The feasibility of applying electroporation to wet algal systems has been demonstrated. However, optimization of all electroporation parameters was out of the scope of this investigation. A natural progression from this study is the optimization of all multiple variables (i.e. electric field strength, number of pulses, type of pulses, etc) with the global goal of efficient membrane permeabilization with minimal energy requirements.
- Although PEF application was proven to increase membrane permeability, its utilization prior to EtOAc extraction did not improve total lipid recovery. Based on this, it can be hypothesized that internal organelles storing the lipid bodies do not get affected by this treatment and they still remain as physical barriers for adequate extraction. Therefore, TEM imaging focusing on internal organelles could establish the limitations of PEF as a disrupting agent.
- Application of PEF as a disrupting treatment in this investigation was limited to batch operations. Another natural transition of this research would be the application of this technique in a continuous process, mimicking a possible industrial scale model. The development of a continuous electroporation process coupled with solvent extraction will enable meaningful investigation of the different electroporation parameters. Also, the investigation of energy requirements under continuous treatment will be of great importance at benchmarking PEF as a potential membrane disrupting pretreatment.
- Development of an electrical system capable of varying the electrical operating outputs (e.g. electrical field strength, type of pulses, number of pulses) should be

emphasized as critical future work. The current in-house-built apparatus is limited to the current parameters, and modifications of these variables require complex and time consuming alterations to the system. While disrupting membrane effects should be maximized to obtain better lipid extraction, energy requirements associated with the pretreatment should by all means be minimized. Thus, the development of a flexible electrical system would enable the optimization of these results while meeting operational constraints.

Appendix A

A.1 Solvent Extraction & Solvent-Product Separation

The main idea throughout this Master's Thesis was to compare the algal lipids extraction efficiency of two solvents: (A) Chloroform, and (B) Ethyl Acetate (EtOAc). The extraction procedures associated with each different solvent are very similar, and can be found as follows:

Lipid Extraction Procedure with Chloroform

Day #1 – Lipid Sampling

1. Mix each sample & add each to 50 mL centrifuge tube, utilizing a volumetric pipette to ensure accuracy.
2. Centrifuge for 10 min. at 4,000 rpm (Balance Tubes)
3. Pour off until liquid reaches middle of pellet (50 mL to < 4 mL)
4. Vortex and transfer to 15 mL test tube
5. Bring to top mark with Milli-Q-Water
6. Centrifuge 10 min. at 4,000 rpm.
7. Pour off until liquid reaches middle of pellet (15 mL to < 4 mL) and vortex

Note: If there is not enough time to finish complete procedure of “Day #1 – Lipid Sampling”, then stop here and freeze at this point.

8. Bring up to 4 mL with Milli-Q-Water

Note: If required, PEF pretreatment and/or molecular staining is to be performed at this stage

9. Transfer to 35 mL glass bottle (pipette residuals)
10. Add 5 mL chloroform & 10 mL methanol in hood using auto dispenser (ratio is what matter)
11. Cap & place on shaker table at 320 overnight

Day #2 – Lipid Sampling

12. Remove from shaker table and add 5 mL chloroform & 5 mL water
13. Centrifuge for 10 min. at 3,500 rpm
14. Get glass vials and label
15. Remove bottom layer and add to glass vials. (Positive Pressure Displacement)
16. When nearing bottom, add 10 mL chloroform to each sample
17. Centrifuge sample for 10 min. at 3,500 rpm
18. Repeat step (15) for samples
19. Add 1 mL chloroform & vortex

20. Freeze

Lipid Extraction Procedure with Ethyl Acetate

Day #1 – Lipid Sampling

1. Mix each sample & add each to 50 mL centrifuge tube.
2. Centrifuge for 10 min. at 4,000 rpm (Balance Tubes)
3. Pour off until liquid reaches middle of pellet (50 mL to < 4 mL)
4. Vortex and transfer to 15 mL test tube
5. Bring to top mark with Milli-Q-Water
6. Centrifuge 10 min. at 4,000 rpm.
7. Pour off until liquid reaches middle of pellet (15 mL to < 4 mL) and vortex

Note: If there is not enough time to finish complete procedure of “Day #1 – Lipid Sampling”, then stop here and freeze at this point.

8. Bring up to 4 mL with Milli-Q-Water

Note: If required, PEF pretreatment and/or molecular staining is to be performed at this stage

9. Transfer to 35 mL glass bottle (pipette residuals)
10. Add 10 mL ethyl acetate & 5 mL methanol in hood using auto dispenser (ratio is what matter)
11. Cap & place on shaker table at 320 overnight

Day #2 – Lipid Sampling

12. Remove from shaker table and add 5 mL ethyl acetate & 5 mL water
13. Centrifuge for 10 min. at 3,500 rpm
14. Get glass vials and label
15. Remove top layer (EtAc rich phase) and add to glass vials. (Positive Pressure Displacement)
16. When nearing the end of the EtAc rich phase, add 15 mL ethyl acetate to each sample
17. Centrifuge sample for 10 min. at 3,500 rpm
18. Repeat step (15) for samples
19. Add 1 mL chloroform & vortex
20. Freeze

Note: On Step 15, EtAc rich phase is transferred to the new glass vial, and this glass vial is exposed to nitrogen flow to enhance the solvent evaporation (leaving the lipids behind). During this EtAc evaporation (approx when half the volume has been evaporated) a new 2-phase system will form. A small water-rich phase will appear at the bottom of the vial and the EtAc-rich phase will stay on the top. It is advised that this new water-rich phase is removed (with disposable glass pipette) from the glass vial. Otherwise, the water evaporation under nitrogen flow will take significantly more time,

already on a system that does not evaporate as fast as CHCl_3 . It is worth mentioning that extractions performed with the removal of this new water-rich phase did compare with extraction without the removal. In other words, the total lipid extraction stayed the same.

A.2 Chemical Transformation of Algal Lipids into Fatty Acid Methyl Esters (FAME)

Phospholipids are generally composed of a phosphoric ester of glycerol along with two fatty acids residues esterified to the other hydroxyl groups. This procedure causes the transmethylation of these fatty acids but does not catalyze the production of FAMES from free fatty acids.

Procedure of FAMES Production

1. Start evaporating off solvent (chloroform) from stored samples by placing uncapped test tubes in the hood under a nitrogen stream evaporator at 37°C.
2. Turn on the water bath to 37°C.
3. Make 0.2N methanol KOH solution as outlined at the bottom of the page. (25 mL of methanol may be dispensed with the automatic dispensette; a stir bar may be added to the solution to help dissolve on an un-heated stir plate)
4. Use dried samples from previous step 1. Dissolve the dried lipids in 500µL of 1:1 methanol:toluene solution. Vortex the tube once capped.
5. Add 500µL of 0.2N KOH in methanol, seal test tube with a PTFE lined cap, vortex and heat at 37°C for 15 minutes in a water bath.
6. Prior to step 7, flush out automatic dispensettes containing chloroform and water. Place the vortex next to these, so that Step 7 can be performed quickly.
7. Cool to room temperature, then add 500µL of 0.2N acetic acid (see solutions at the bottom of the page), vortex (quickly), add 2mL of chloroform, vortex, and 2mL of deionized water. Place the cap on the vial, and vortex for 30 seconds. See note.
8. Centrifuge at 1500rpm for 5 minutes.
9. Transfer chloroform (bottom layer) to a clean, labeled test tube using a Pasteur pipette. See note.
10. Add 1 mL of chloroform to reaction tube, vortex, repeat steps 8 and 9.
11. Add 1 mL of chloroform, do not vortex or centrifuge. Transfer chloroform layer. At this point, a total of 3 chloroform transfers should have been performed.
12. Evaporate all chloroform from the test tubes under a nitrogen evaporator.

If samples will be stored before GCMS analysis, these samples can be stored at -20°C. Steps 13 through 15 can be performed immediately before GCMS analysis.

13. Resuspend FAMES in 1 mL of chloroform. Vortex for 30 seconds.
14. Transfer the 1 mL of solution to a GC vial.
15. Add 2 µg of an internal ethyl ester standard (ethyl stearate). If the internal standard stock solution is 2000 µg/mL, then add 1 µL to the 1 mL sample. This provides a final concentration of 2 µg/mL in the sample.
16. Add 1 mL of chloroform to three additional GC vials, which will be used as blanks.

Notes

3. Make the methanol KOH fresh daily.
5. This reaction produces the FAMES.
7. **Very Important** – NO DELAY between the addition of the acetic acid and the addition of the chloroform and water. Do all additions to each sample sequentially. FAMES are easily broken down by the presence of water and an acidic or basic catalyst. The chloroform protects the FAMES from degradation.
8. Centrifugation is done to clarify phase boundary, the g force and speed are not critical.
9. Leave behind a drop of chloroform, this is to minimize the chance of transferring any water.
11. A total of 4ml of chloroform will be transferred.
16. The internal standard may be added to the hexane blanks. These samples should be placed at the beginning, middle and end of the GC run to check the cleanliness of the column and its performance.

Solutions

methanol:tolulene- 1:1 (volume/volume)

0.2N acetic acid- 1.15ml glacial acetic acid in 100ml deionized water.

0.2N methanol KOH-0.28g KOH in 25ml methanol.

Ethyl ester standard- 20:0 fatty acid ethyl ester. If the internal standard stock solution is 2000 µg/mL, then add 1 µL to the 1 mL sample. This provides a final concentration of 2 µg/mL in the sample.

A.3 Algae Staining Procedure Calcein AM and Propidium Iodide (PI) Staining of Algae - Procedure

Calcein AM and Propidium Iodide (PI) were utilized as viability staining dyes to help determine if algae membranes were permeated.

Materials

All the different materials utilized in this procedure were purchased from Invitrogen (www.invitrogen.com)

Molecular Dye	Supplier	Concentration	Volume	Catalog #	Prize
Calcein AM	Invitrogen	1 mg/mL solution in anhydrous DMSO	1 mL	Invitrogen C3099	\$199
Propidium Iodide (PI)	Invitrogen	1 mg/mL solution in water	10 mL	Invitroge P3566	\$58

Procedure

1. Collect into a container an initial volume of algae suspension from the chemostat.
2. Ensure that this volume is extremely well mixed, by adding a magnetic bar and mixing its content to reach a uniform cell density.
3. Divide initial volume into multiple samples, by adding the algae suspension into multiple 50mL centrifuge tubes.
4. Centrifuge the 50mL samples for 10 min. at 4,000 rpm.
5. Due to centrifugation, algae biomass falls towards the bottom of the tube. Pour off excess media until liquid reaches middle of pellet (50 mL to <15 mL).
6. Vortex the concentrated algae-media suspension. Transfer this new volume into a 15 mL test tube.
7. Add Milli-Q-Water to top the fluid level until it reaches the 15mL mark.
8. Again, centrifuge 10 min. at 4,000 rpm.
9. Pour off excess media until liquid reaches middle of pellet (15 mL to <4 mL) and vortex.
10. Bring to 4mL mark with Milli-Q-Water.

At this point, algae have been concentrated utilizing centrifugation. Now, the different dyes will be added. It is important to notice that the amount of dyes to be added in this procedure proved to be effective with the cell density obtained after Step #10.

11. CalceinAM and PI are susceptible to light. Avoid any direct exposure of the molecular probes to light by working on a dark room and switching the lights off.
12. Add 80 μ L of CalceinAM stain per mL of algae-media suspension. This volume translates into 8×10^{-5} mmoles of CalceinAM per mL of algae-media suspension. (Calcein AM: MW=994.87). In other words, add 320 μ L (4 x 80 μ L) of CalceinAM into the 4mL of algae-media suspension.
13. Wrap the 15mL test tube with aluminum foil to ensure no contact with light.
14. Incubate the samples during 2hrs at 29°C in order to ensure proper stain loading. The temperature control was achieved on a water-bath.
15. Now it is important to eliminate all excess stain, by washing the algae with new media. Add fresh media to top the fluid level until it reaches the 15mL mark.
16. Vortex sample.
17. Centrifuge sample for 10 min. at 4,000 rpm.
18. Pour off excess media until liquid reaches middle of pellet (15 mL to <4 mL).
19. Repeat Steps 15-18 twice more.
20. Precisely bring to 4mL mark with Milli-Q-Water. This step needs to be performed with extreme precision in order to achieve a contestant cell density in all samples.

It is important to recognize that these samples will be evaluated under the microscope, and cell will be counted. Therefore, maintaining a constant cell density is very important.

At this point, enough time has been allowed for the Calcein AM molecules to diffuse through the cytoplasmic membrane, become fluorescent, and all excess stained has been washed out. If desired, utilize the fluorescent microscope to confirm that the Calcein AM has loaded effectively. Now it is time to add the PI fluorescent dye.

21. Add 2 μ L of PI per mL of algae-media solution. Since at this point we should have 4mL, add a total of 8 μ L PI.
22. Wait for 10 min. and later perform the desired treatment

PI will eventually make its way through the viable membrane and become fluorescent. It is very important to perform the desired treatment, and collect all images as soon as Step 22 has been executed.